Discovering Ecological and Evolutionary Principles Governing Microbial Community Responses to Bacteriophage Infection of a Cross-Feeding Synthetic Coculture and Implications for Phage-based Applications

A DISSERTATION

SUBMITTED TO THE FACULTY OF

THE UNIVERSITY OF MINNESOTA

By Lisa Diane Fazzino

IN PARTIAL FULFILLMENT OF THE REQUIREMENTS

FOR THE DEGREE OF

DOCTOR OF PHILOSOPHY

Advisor: William R. Harcombe

August 2020

Acknowledgements & Dedications

Thanks, Will, for taking a chance on accepting me as your 2nd student and for creating a great lab environment. Your unwavering support and understanding have helped me get to this moment. And thanks to all present and past members of the Harcombe lab for upholding and expanding that great lab environment: Beth Adamowicz, Jeremy Chacón, Sarah Hammarlund, Leno Smith, Brian Smith, Jon Martinson, the numerous undergrads who help keep my cynical self in check and provide endless enthusiasm when all of mine was tapped out. To the MICaB, EEB, and IMV communities at large, thanks for welcoming me into your family. And to my personal champions - Serina, Sarah Lucas, Beth, Kelsey, my parents, Matt, and Mia, your never-ending support, encouragement, and understanding got me through when I would have sat down and watched Harry Potter for the 15th time instead. Also, writing my dissertation during the COVID pandemic was an experience to say the least.

I would like to dedicate this doctoral thesis to the teachers and mentors who nurtured my love of science from 6th grade to now: Mrs. Maley, Alberto Mimo, Dr. Deron Chang, Dr. Antonia Monterio. To Dr. Betsy Kirkpatrick - my mentor and academic advisor in undergrad who gave me the keys to the lab and said - sure go for it, and Dr. Mark Martin for so many cookies. To Dr. Kit Tilly for giving me the opportunity to experiment at Rocky Mountain Labs. And of course, to Will, Dr. Harcombe, for being infinitely patient and ever the optimist. Hopefully, something of what I have presented here has made you proud.

Abstract

Bacterial viruses, called bacteriophage (phage), infect bacteria and alter microbial community structure. Phages are an untapped resource to manipulate agriculture and medically applicable microbial communities. Yet, we cannot predict how phage impact a microbial community. My research aims to uncover ecological and evolutionary principles governing responses of microbial communities that contain cross-feeding interactions, where one species provides nutrients to ('feeds') another, phage. I combine wet-lab experiments on an engineered microbial co-culture with mathematical modeling to explore aspects of phage infection that are difficult to manipulate experimentally.

I use a cross-feeding bacterial co-culture with *Escherichia coli (E. coli)* and *Salmonella enterica* (*S. enterica*) bacterial strains. In this cross-feeding system, *E. coli* cannot produce methionine, but does produce acetate and galactose. *E. coli* is paired with *S. enterica* that over-produces methionine and consumes acetate and galactose that *E. coli* secretes. To this co-culture, I add phage that infect either species.

I have asked how simple cross-feeding co-cultures respond to phage infection. In Chapter 2, I used mathematical modeling and wet-lab experiments to show that single phage infections can break the cross-feeding relationship by liberating nutrients previously sequestered in the infected bacterial cells, ultimately changing community composition, and that partial, not full, resistance was necessary for this effect. In Chapter 3, 'cocktails' made of two different phage suppressed community growth the longest in a novel formulation that targeted both the pathogenic bacterial species and the slowest growing cross-feeder. Mathematical modeling showed that this was a generalizable concept to all cross-feeding systems. In Chapter 4, despite impacting community structure, I found that long term co-evolution between phage and *E. coli* cross-feeding with *S. enterica* only had weak effects on rates of adaptation. Phage treatments tended to increase rates of adaptations, as predicted by the Red Queen hypothesis, and cross-feeding tended to decrease rates of adaptation, as predicted by the Red King hypothesis. Overall, this thesis helps set baseline expectations of how phage influence cross-feeding microbial communities.

Table of Contents

List of Tables

List of Figures

Chapter 1

Introduction

Microbes live in large communities that include fungi, bacteria, and bacterial viruses called bacteriophage, or phage. These organisms interact in complex ways that form a web and perform a variety of functions. Some of these microbial-based functions are leveraged by humans and impact myriad aspects of human life - ranging from human health to agriculture and the food industry. We, as researchers, can manipulate microbial communities to improve application outcomes. For example, purposefully altering the human gut microbial community could improve treatment outcomes for complex human microbiome diseases like Crohn's disease, or carefully choosing the microbial community that a plant seed encounters when in an agricultural field could increase crop yields. Yet, predicting how microbial communities respond to treatments remains difficult. How can we nudge microbial communities in a beneficial direction if we cannot accurately predict how they will respond to outside pressures? One notable pressure on microbial communities is the diverse range of phage that infect community members, and can alter community structure and function.[1–4]

Two core challenges are: 1) accurately predicting ecological consequences of infections by bacteriophage, and 2) knowing how ecological interactions between bacterial species alter community responses to infection. Broadly, my thesis focuses on several ways that phage infection of a microbial community can affect the community's ecology and evolution. I investigate the impact of single phage, multiple phages, and evolving phage on a model bacterial community.

To provide context, this introduction explores a variety of applications for bacteriophage manipulation of microbial communities. I then present background information on bacteriophage lifestyles, molecular interactions with bacterial hosts, and possible

outcomes of phage infection of a population of bacteria. Finally, I place my thesis question of how bacteriophage influence microbial community structure and function in the context of previous research about this question and identify a gap in understanding how cross-feeding interactions impacts phage infection outcomes.

Applications for knowledge of bacteriophage manipulation of microbial communities

Bacteriophage (phage) are viruses that infect bacterial cells and influence outcomes of a variety of human services that rely on bacteria. We now know that bacterial communities impact human health (reviewed in[3]), agricultural and aquacultural production (reviewed in[1]), food safety (reviewed in[4]), and biogeochemical cycling - or how elements move through ecosystems.[2] Typically, we control bacterial replication with antibiotics, but spreading antibiotic resistance is a global crisis that we cannot afford to ignore.[5] The scientific community is returning to phage as an alternative method for killing pathogenic bacteria. In a human health context, this is called phage therapy; in an agricultural or aquacultural context - biocontrol. One of the earliest documented uses of phage to cure a human infection is from Félix d'Hérelle in 1931 where he treated patients with bacillary dysentery, a severe form of shigellosis, with phage.[6] Now, formulations of phage can be purchased for controlling plant diseases (e.g. AgriPhage™ to control *Pseudomonas syringae* and *Xanthomonas campestris* infections of tomato or pepper plants) and the U.S. Food and Drug Administration has approved some formulations to limit contamination of food by bacterial pathogens (e.g. Listshield™ against *Listeria* contamination) (reviewed in[1]). While phage as treatments for a variety of applications is gaining momentum, there are hurdles remaining - preventing the evolution of phage resistance and regulatory considerations particularly for use in humans (reviewed in[7]). My thesis aims to identify

basic ecological and evolutionary principles that govern how phage impact structure and function of bacterial communities in the hopes that leveraging these principles will result in phage applications that are more effective with fewer consequences.

Life histories and molecular interactions between bacteriophage and bacterial hosts

Phage come in several types - lytic, lysogenic, and filamentous. Although phage life histories are varied, they all have several stages of phage infection in common, including bacterial host recognition, genetic material injection, phage replication, phage packaging, and release of phage progeny from hosts (Fig 1.1a). Key differences are in replication timing and mechanism of progeny release. Lytic (or virulent) phage immediately replicate inside the host cell after infection whereas lysogenic (or temperate) and filamentous phage can delay replication. Lytic and lysogenic phage lyse open and kill their bacterial hosts to release phage progeny but filamentous phage are continually exuded from an intact and alive host cell (reviewed in[2]). One key outcome of the lytic phage life cycle, which is the focus of my dissertation, is the need to lyse host cells to release phage progeny. This kills the host cell and can be leveraged to treat pathogenic infections with phage therapy. To accurately predict how phage infection influences the ecology and evolution of microbial communities, like those targeted during phage therapy or biocontrol, we need to understand how phage infect a bacterial host cell and how those molecular interactions can cause community-level responses.

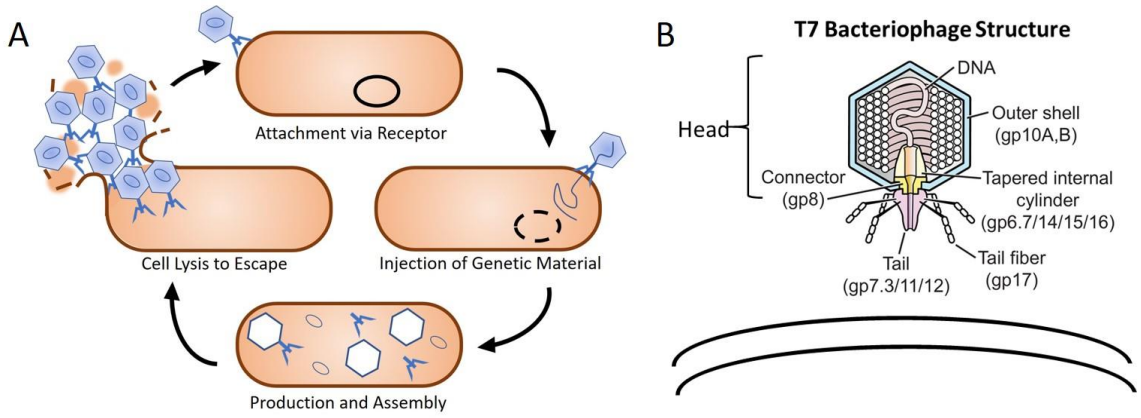

Figure 1.1. Lytic phage life cycle and structure. A) General lytic phage infection cycle. Lytic phage have multiple stages of infection including attachment, injection, production and assembly, and cell lysis to release phage progeny and escape the host cell. Adapted from Labrie *et. al.* 2010. **B)** Representative phage structure. T7 bacteriophage have an icosahedral phage head consisting of an outer protein shell and several proteins that connect the head to the tail. The tail interacts with bacterial host outer surface structures. Phage gene names are indicated in parentheses. Adapted from[8].

Phage tail proteins bind to host receptor proteins to recognize bacterial hosts. The first stage of lytic phage infection is recognition of a viable bacterial host. Phage recognize a potential host bacterium through molecular interactions between phage proteins on the phage tail, called tail fibers, and bacterial proteins or other structures that are on the bacterial outer membrane, called receptors. Receptor proteins are often highly conserved and perform essential functions for bacterial survival such as transporting nutrients into the cell or providing membrane structural integrity. These proteins, or other surface structures, have been coopted by phage for host recognition. The specificity of phage protein - host protein interactions means that, typically, phage infect specific bacterial species, or even strains, although there are many exceptions (reviewed in[2]). Furthermore, mutating bacterial receptor proteins can cause a new phage-resistant strain of the host bacteria to evolve and frequently serves as the mechanism of acquired phage-resistance *in vitro* (Fig. 1.2).[9–11] However, mutations to receptor proteins are often associated with fitness costs - a decrease in competitive ability against susceptible genotypes in the

absence of phage - and are therefore not always stable in a microbial community context.[12–16]

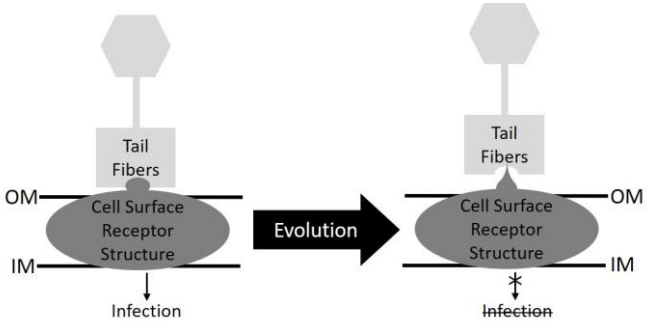

Figure 1.2. Phage-host recognition and evolution of resistance. Phage tail fiber proteins interact with cell surface receptor structures to identify host bacteria. One way bacteria can evolve phage resistance is by changing the shape of surface receptor structures, preventing interactions between phage tail fibers and receptor structures, ultimately preventing infection. OM = outer membrane, IM = inner membrane. Adapted from[9]

Lytic phage lyse host cells to release phage progeny. Once bacterial hosts are identified, phage inject their genetic material - frequently dsDNA but can be ssDNA, ssRNA or dsRNA - into the host cell through the syringe-like phage tail. Phage genetic material is replicated often with host cell transcription and translation machinery, although some phage encode genes for their own replication machinery. Once phage proteins have been translated, phage are assembled inside the bacterial host cell and then must escape the bacterial host cell to infect other cells. They use proteins called holins and/or lysins that make holes in the bacterial cell membranes, causing cells to burst and release phage progeny along with the cellular contents.[17] Released phage from a single lysed cell typically number in the tens to hundreds, and can be modulated by environmental conditions.[18,19] Although the goal, from the phage's perspective, is to release phage progeny and continue the infectious cycle, there is a secondary outcome that is potentially beneficial to humans. In the process of bursting host cells to release phage progeny, lytic phage kill the bacterial host cell.

While phage-mediated bacterial host cell death occurs on a cellular level, rapid phage replication, at a much higher rate than bacterial reproduction, amplifies phage-bacteria interactions generating powerful, population-level effects on the bacterial host population.

Three possible outcomes of phage populations infecting isolated bacterial populations

After phage initiate infection of a susceptible bacterial population, several outcomes are possible depending on how the bacterial population responds to the phage infection. These outcomes range from extinction of bacteria to extinction of phage, and can even include phage-bacteria coexistence (Fig 1.3). Outcomes are influenced by factors including absorption rate, lysis time, burst size, environmental phage degradation, and evolutionary rates. Coexistence of phage and bacterial hosts can occur through rapid evolutionary cycles providing temporary resistance, or through mechanisms that provide partial, not full, resistance to phage infection.

Extinction of bacterial population through phage-mediated death - the basis for phage therapy. If the infected bacterial population does not evolve resistance to phage infection, then it is likely that the bacterial population will go extinct (Fig 1.3).[20,21] In this case, the bacteria 'lost' to the phage in the evolutionary race and did not evolve when it was required for survival. Phage infected and lysed every bacterial host cell successfully. Extinction of the host bacteria has been observed repeatedly in many different phage-bacterial systems,[15,20,22–25] and has been attributed to the faster rate of evolution of viruses compared to bacteria.[26] Others suggest that phage dynamics are density-dependent, meaning that if phage predation drives bacterial host populations to a diffuse-enough level,

then phage are unlikely to encounter susceptible bacteria making extinction difficult, but still possible.[27] It is also possible that both asymmetric rates of evolution and density-dependent growth contribute to extinction rates of phage.

This feature of killing bacterial host cells and decreasing bacterial density or even causing extinction is a natural outcome of the lytic phage life cycle that is leveraged in phage therapy - using phage to treat pathogens infecting humans. If the pathogenic bacteria instead infect a plant, the phage treatment is instead referred to as biocontrol. Even if phage do not drive hosts to extinction, they are still useful for decreasing the density of a host bacterial population which is an alternative goal of phage therapy. Recent research suggests that the human immune system can eradicate pathogenic bacteria once phage therapy significantly decreases the pathogen population.[28–30]

Extinction of phage through evolution of resistance. In contrast, if bacterial hosts evolve resistance to phage infection, then phage can be driven to extinction because they cannot replicate on evolved resistant bacteria (Fig 1.3).[31] While phage are not actively killed by resistant bacteria, they degrade over time and lose infectivity[32] or can be washed out of an environment if they do not coevolve to infect evolved hosts. Furthermore, some phage-host systems will go through several rounds of coevolution before phage are ultimately driven extinct.[31]

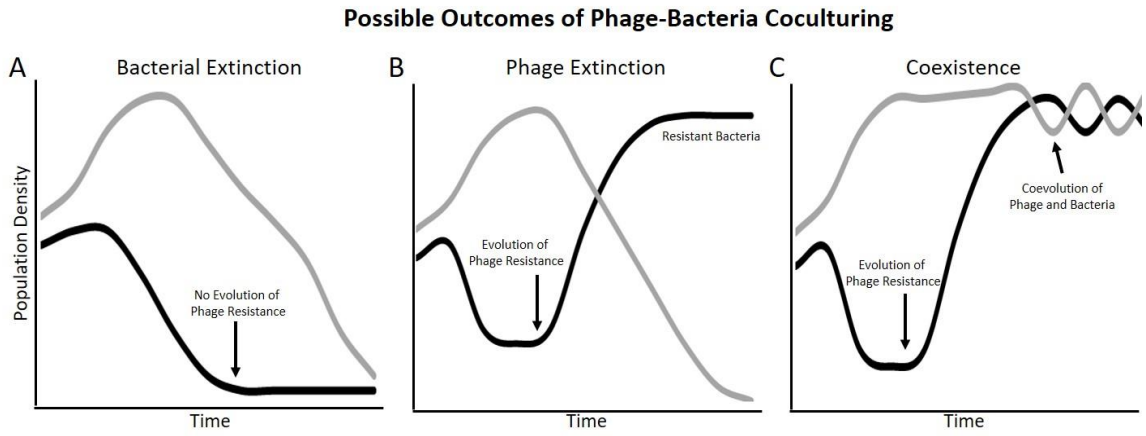

Figure 1.3. Possible outcomes of phage-bacterial coculturing. When bacteria (black line) and phage (grey line) are cocultured, there are three different possible outcomes. **A)** Bacterial extinction when bacteria do not evolve phage resistance. **B)** Phage extinction when bacteria evolve phage resistance and phage subsequently degrade. **C)** Phage and bacteria coexist after bacteria evolve resistance to phage and phage evolve to infect resistant bacteria. Complex growth dynamics, such as the illustrated oscillatory dynamics, can result.

Coexistence of phage and bacteria through multiple mechanisms studied with experimental evolution. A third possible outcome of phage-bacterial interactions is that both bacterial hosts and phage coexist through some additional mechanism. The frequent isolation of phage and sensitive bacteria from the same natural environment necessitate that coexistence is possible. Described coexistence mechanisms include coevolution of phage and bacteria,[33] evolution of incomplete resistance,[25,34] spatial structure that creates refugia for phage and/or bacteria,[16,35] or reversion of hosts back to sensitive, which is likely if resistance confers a strong fitness cost to the bacteria.[36] Any of these mechanisms functionally results in a continual supply of phage and bacteria in an environment.

Coexistence of phage and bacteria is frequently studied with experimental evolution, which uses controlled laboratory environments to explore evolutionary processes.[37] Experimental evolution of a phage-bacterial coculture helps researchers to explore evolutionary processes that facilitate long-term coexistence. These experiments use frequent dilutions into fresh culture media to grow phage and bacteria for many

generations in controlled laboratory environments, and allow interrogation of both phenotypic traits of evolved phage or bacteria with experimental assays and genetic changes using sequencing techniques (Fig 1.4). Combining phenotypic assays and genomic analysis can help identify the genetic basis of functional evolutionary outcomes.

Experimental evolution of phage and bacterial hosts have frequently shown continual reciprocal evolution between the two organisms - called an evolutionary arms race or the Red Queen hypothesis.[15,38–42] In this case, 'tit-for-tat' evolutionary changes accumulate in both the phage and host genomes over time, and can increase the rate of adaptation[42–44]. The phage tail proteins that interact with bacterial hosts, and the bacterial proteins that serve as receptor proteins often evolve, although more complex resistance mechanisms such as evolution of CRISPR (Clustered Regularly Interspaced Short Palindromic Repeats), and anti-CRISPR systems are also observed.[45] Alternatively, partial resistance or frequent reversion from resistant to sensitive can also support a population of replicating phage.[34]

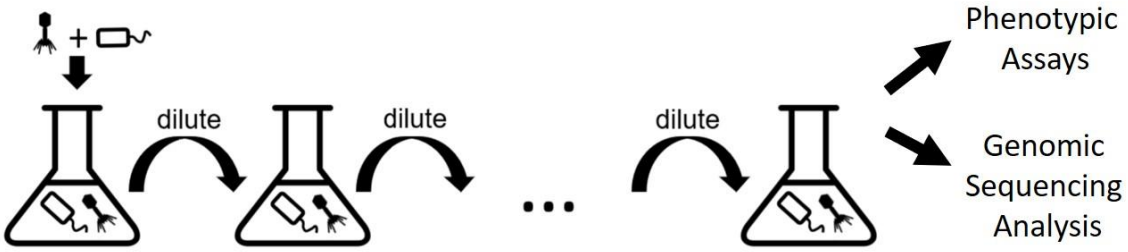

Figure 1.4. Experimental evolution set-up with phage and bacteria. Phage and bacteria are cocultured in a controlled laboratory environment. Dilutions into fresh culture media allow phage and bacteria to grow together from many generations. After evolution, evolved clones of either phage or bacteria can be isolated for phenotypic assays to determine functional changes. Clones or whole populations can be sequenced to identify genetic adaptations. Adapted from[38].

Despite the extensive number of studies about phage-bacteria coevolution and coexistence, it remains difficult to predict *a priori* which of three above outcomes is likely,

and what genetic changes will likely evolve to facilitate such an outcome. Unknown population-level outcomes make predicting dynamics in a complex ecological context, like those of natural microbial communities, even more complicated. In this thesis, I aim to build on some significant advances in this field to uncover guiding ecological and evolutionary principles of consequences of phage-host interactions.

How do ecological contexts of the bacterial host affect outcomes of phage infection?

There is a plethora of factors that affect the outcome of phage infection. Some are internal to the phage-bacterial interaction such as how many phage are there per host cell, called multiplicity of infection.[26] Other factors are external to the phage-bacterial interaction such as nutrients[20] or temperature conditions.[46] A particularly understudied external factor affecting phage infection outcomes is the ecological interactions between the bacterial host and other microbial community members.[47] The influence of complex ecological interactions found in natural microbial communities must be formalized with sound ecological and evolutionary theory in order to leverage phage for human services.

Studying natural ecosystems to explore global effects of phage communities on bacterial communities. Studying viral biogeography with sequencing, while limited by available technology and cost inefficiency, was the first step in addressing how phage affect natural microbial communities. The initial studies typically sequenced a small number of isolated bacterial clones because of prohibitive sequencing costs or time-intensive isolation procedures. These pioneering studies suggested that phage communities are locally adapted to bacterial host populations in terms of physical proximity[48–50] and time.[50,51] Other

early studies found that bacteriophage infections in the marine environment influence global biogeochemical cycles such as the carbon and nutrient cycles.[52–56]

With improvements in sequencing technologies in the past decade, researchers began to take a community-level view of the effects of phage infection in a variety of environments. For example, there are associations between human gut phage communities and gut dysbiosis diseases[57] like Crohn's disease, and alterations to plant microbiome structure when complex phage communities were inoculated on plant leaves.[1,58] Other studies identified changes in non-host bacterial populations when applying a single phage in a high dose, like during a phage therapy treatment.[59–62] Others use techniques such as tracking radiolabeled substrates to show that phage-mediated lysis of bacterial hosts liberates carbon and nutrients from bacterial cells into the open ocean in bioavailable forms - a process called the ‘viral shunt’.[2] Yet, how these liberated resources alter microbial communities is not well understood. These and other studies have illustrated the large and important impacts that bacteriophage infection can elicit on entire natural bacterial communities but predominantly have used techniques that preclude mechanism discovery.

Studying natural ecosystems with tools like sequencing technologies powerfully demonstrates that interesting patterns arise during phage infection, but makes identifying mechanisms and, importantly, generating theory difficult. Phage infection at large is a powerful ecological and evolutionary pressure that can alter microbial community structure in unexpected ways. We need generalizable ecological and evolutionary theory to accurately predict outcomes of phage infection to effectively use phage as microbial community manipulators.

Using synthetic microbial consortia to determine mechanisms and effects of bacterial ecological interactions of phage infection in bacterial communities. While studying bacteriophage communities in natural ecosystems has illustrated the potentially long-reaching influence of phage infection, interrogating mechanisms of phage-host interaction and phage resistance can be technically challenging with these systems. Some researchers have turned to synthetic microbial consortia - manipulatable model microbial communities made up of few isolated bacterial species - to bridge the gap between complex natural systems and the simplicity of monoculture laboratory experiments.[63] The biofilm research field has used microbial consortia ranging from two to five bacterial species to study the community-level effects of single or multiple phage treatments. Generally, the goal of these studies is to treat one or multiple pathogenic bacteria that are part of a multispecies biofilm. Phage treatment outcomes of multispecies biofilms have ranged from increased to decreased lytic efficacy of phage treatments depending on the exact phages and biofilm model used.[63] Several methods for effective destruction of biofilms emerged including the use of multiple phage in a cocktail particularly if the chosen phage facilitated infection by additional phage (e.g.[64]).

Studies using synthetic biofilm microbial consortia have illustrated the power and control that is possible when manipulating microbial communities. Including well-characterized bacterial species as a tool has aided the detailed study of mechanisms of phage. As a result, we are poised to repurpose these types of consortia to discover how ecological interactions among bacterial community members might impact responses to phage infection, and rates of adaptation. In fact, the ecological interactions between bacterial species and their bacterial community members could be one possible explanation for the variety of responses to phage treatment that have been observed.[23,47,63,65]

Responses of competitive microbial communities to phage infection. One common ecological interaction among organisms is competition. Others found with experiments and modeling that when bacterial hosts compete for resources with a bacterial species which is not susceptible to phage, that phage infection decreases host population sizes more than in phage infection of a host monoculture.[23,47,65,66] In the experimental studies phage were added to a coculture of at least two species of bacteria grown on a single carbon source to force competition for a resource.[23,65,67] The combined competitive pressure for the essential resource and predation pressure from phage significantly reduced host abundance in the community, even when phage resistance evolved in the host population.[47] Competition between hosts and other non-host species can amplify phage effects on a bacterial population to a community-level change in structure, but is not the only ecological interaction that can occur between species.

Responses of cooperative cross-feeding microbial communities to abiotic perturbations. Another common type of bacterial interaction is cooperation - or when species rely on others for certain resources or services. One cooperative bacterial interaction of interest is cross-feeding, in which metabolites secreted by one bacterium are used as a nutrient source by another (Fig 1.4a). This is a common interaction in natural systems, but remains understudied.[68–71] While there is almost no information about how phage influence bacterial communities with cooperative cross-feeding interactions, we can make inferences from studies on responses of cross-feeding systems to abiotic disturbances.

The intimate, and occasionally obligate, interactions among cross-feeding community partners generate unique ecological patterns because the fate of partners are intertwined. In the absence of disturbance, obligate cross-feeding communities typically

constrain species ratios and force convergence on an equilibrium ratio from any initial ratio (Fig 1.4b).[72,73] This constraint on final species ratios is governed by the production and consumption rates of cross-fed nutrients. A population of one partner cannot grow if the population of another partner does not produce a sufficient amount of the cross-fed resource. This can elicit initial asymmetric growth patterns while cross-feeding partners reach the equilibrium ratio, ultimately slowing community-level growth. Therefore, limiting the growth of one species indirectly inhibits cross-feeding partners, decreasing total community biomass, but maintaining species ratios.[74] For example, antibiotic treatment of a three-species cross-feeding community that inhibited the most sensitive member - the 'weakest link' - inhibited growth of all members of the community by depriving community partners of cross-fed nutrients.[75]

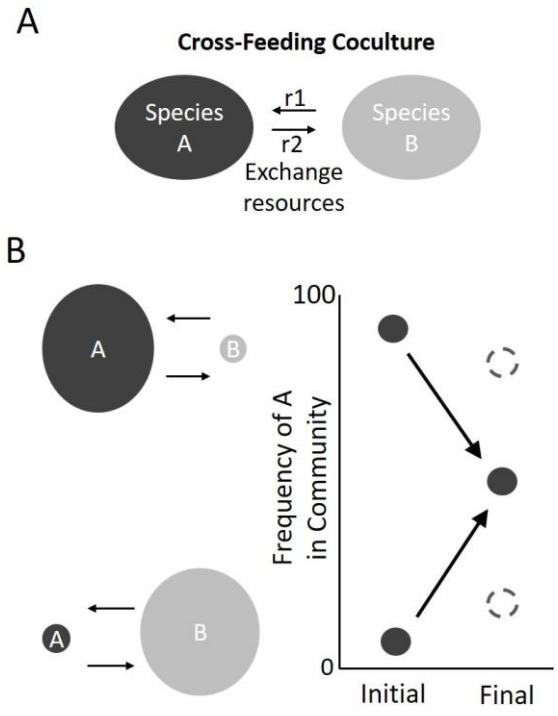

Figure 1.5 Cross-feeding cocultures constrains species ratios. A) An example of a cross-feeding coculture with two different bacterial species (A and B) that exchange resources (r1 and r2). **B)** When cross-feeding cocultures have different starting frequencies, represented by the size of the circles of A and B, they converge on a single final ratio that is determined by production and consumption parameters of cross-fed nutrients. The equilibrium ratio does not need to be 50:50 (final dark grey circle), but could be other ratios as well (dotted circles).

Cross-feeding and phage infection are ecological forces that are both predicted to change the rate of adaptation of a focal bacterium. The Red King hypothesis predicts that cross-feeding interactions slows the rate of adaptation by requiring each partner to wait for the other before evolving to maintain cross-feeding relationships.[76] In comparison, the Red Queen hypothesis predicts in increase in the rate of adaptation by continually pitting the phage and host against one another, piling up evolved mutations in an effort to evolve faster than the other.[15,38–42] An open question is how do both of these evolutionary forces interact with one another, and how does that impact the rate of adaptation of a cross-feeding community during phage infection.

Concluding introductory remarks and thesis summary

Phage have significant impacts on structure and function of microbial communities. Understanding phage impacts requires knowledge at all levels - from molecular interactions between phage and host cells to community-level patterns. Studies about the effects of perturbations on communities with cross-feeding interactions suggest that how cross-feeding microbial communities respond to disturbances are different from communities with predominantly competitive ecological interactions. It is likely that there is also a difference in response to phage infections, a type of perturbation with ecological and evolutionary-scale consequences. In my thesis, I explore the following questions: How does phage infection influence microbial communities with cross-feeding interactions at ecological and evolutionary timescales? And what are some ways to maximize the effect of phage on a pathogenic bacterium involved in cross-feeding?

I leverage a previously-constructed synthetic microbial consortium that has cross-feeding interactions.[77] In this synthetic consortium, two bacterial species obligately exchange metabolites. Specifically, a methionine auxotrophic *Escherichia coli* consumes

lactose and through overflow metabolism produces acetate, which a methionine-producing *Salmonella enterica* consumes. Methionine production was selected for first with resistance to ethionine, and then through passages on lactose agarose plates with the *E. coli* methionine auxotroph. This construction resulted in an obligately cross-feeding two-species consortium that when cocultured is a simplified model cross-feeding community. To this cross-feeding coculture, I added *E. coli*- or *S. enterica*-specific phage to tease apart how targeting different species in a cross-feeding relationship influences outcomes.

In my thesis, I began by asking how phage infection influenced the ecological dynamics of a model cross-feeding bacterial coculture (Chapter 2). Using a combination of wet-lab experiments and mathematical modeling, I found that phage infection of a cross-feeder can alter non-host populations indirectly through metabolic dependencies, and that the released cellular contents during lysis can also facilitate non-host growth. I then extended this framework in two ways. In Chapter 3, a Masters student, Jeremy Anisman, and I collaborated and discovered that combinations of phage were most effective at suppressing a focal bacterial population when the combinations included targeting a slower-growing cross-feeder, rather than simply maximizing death of the focal strain. Finally, in Chapter 4, I asked how phage infection influences the evolutionary dynamics of our *E. coli* - *S. enterica* cross-feeding coculture. Here, I used T7 phage to infect *E. coli* cross-feeding with *S. enterica* in an experimental evolution set-up. I then used phenotypic- and genomic-based measurements of rate of adaptation. Phage infection tended to cause slight increases and cross-feeding slight decreases in rates of adaptation, as hypothesized by the 'Red Queen' and 'Red King' hypotheses. Overall, cross-feeding ecological interactions can modulate community-level responses to phage infection, and growth rates of cross-feeding bacterial species heavily influence effectiveness of phage treatment.

Chapter 2

Lytic bacteriophage have diverse indirect effects in a synthetic cross-feeding community

This chapter is a reprint with minor alterations of *ISME J*. 2020;14(1):123-134. doi:10.1038/s41396-019-0511-z

See Appendix 1 for supplemental figures and methods and Appendix 2 for invited associated Nature Research Microbiology Community Blog Post

Lisa Fazzino[1,2], Jeremy Anisman[2,3], Jeremy M Chacón[2,4], Richard H Heineman[5], William R Harcombe[6,7,8]

[1]Department of Microbiology and Immunology, University of Minnesota, Minneapolis, MN, USA.

[2]BioTechnology Institute, University of Minnesota, Minneapolis, MN, USA.

[3]College of Continuing and Professional Studies, University of Minnesota, Minneapolis, MN, USA.

[4]Ecology, Evolution, and Behavior, University of Minnesota, Minneapolis, MN, USA.

[5]Biology Department, Kutztown University, Kutztown, PA, USA.

[6]Department of Microbiology and Immunology, University of Minnesota, Minneapolis, MN, USA.

[7]BioTechnology Institute, University of Minnesota, Minneapolis, MN, USA. harcombe@umn.edu.

[8]Ecology, Evolution, and Behavior, University of Minnesota, Minneapolis, MN, USA.

Summary

Bacteriophage shape the composition and function of microbial communities. Yet it remains difficult to predict the effect of phage on microbial interactions. Specifically, little is known about how phage influence mutualisms in networks of cross-feeding bacteria. We mathematically modeled the impacts of phage in a synthetic microbial community in which *Escherichia coli* and *Salmonella enterica* exchange essential metabolites. In this model, independent phage attack of either species was sufficient to temporarily inhibit both members of the mutualism; however, the evolution of phage resistance facilitated yields similar to those observed in the absence of phage. In laboratory experiments, attack of *S. enterica* with P22*vir* phage followed these modeling expectations of delayed community growth with little change in the final yield of bacteria. In contrast, when *E. coli* was attacked with T7 phage, *S. enterica*, the non-host species, reached higher yields compared with no-phage controls. T7 infection increased non-host yield by releasing consumable cell debris, and by driving evolution of partially resistant *E. coli* that secreted more carbon. Our results demonstrate that phage can have extensive indirect effects in microbial communities, that the nature of these indirect effects depends on metabolic and evolutionary mechanisms, and that knowing the degree of evolved resistance leads to qualitatively different predictions of bacterial community dynamics in response to phage attack.

Introduction

Bacteriophage significantly influence microbial community structure and function.[78] Phage limit the size of bacterial populations, which can change microbial community composition. For example, phage kill >20% of marine bacteria every day.[79] Viral infection of bacterial populations not only impacts the composition of bacterial communities, but also influences

emergent community functions such as the rate at which nutrients are converted into biomass .[80] As a result, phage critically influence biogeochemical cycling,[2] biotechnology,[81] the food industry,[82] and human health.[83,84] Despite the importance of phage in microbial communities, we cannot reliably predict the impact of phage on the composition or function of communities. As we strive to manage microbial communities, we must improve our understanding of responses to phage infection in multi-species systems.

Phage alter competitive bacterial communities by changing the species abundance. When phage kill dominant competitors, weaker competitors that are resistant to phage can flourish, changing species ratios, which can change community function.[23,47,65,66] Sometimes, species ratios rapidly revert to pre-phage frequencies once a host evolves phage resistance, but costs of resistance can generate persistent changes in competitive community composition following phage addition.[47] However, phage attack of one species often has little impact on total community biomass. In communities of competitors, a reduction in host biomass is typically compensated for by the growth of non-host competitors.[85] Taken together, in competitive systems, phage alter species ratios, but have little impact on total microbial biomass.

Much less is understood about how phage influence cooperative networks in microbial communities. Microbial communities are often organized into cross-feeding webs in which each species relies on metabolites excreted by others.[86,87] Networks of metabolic dependencies have been described in marine, terrestrial, and human-associated microbial communities.[86] While phage are likely present in all of these systems, the impact of phage on the composition and function of cross-feeding microbial communities remains under-studied.

However, the response of cross-feeding communities to abiotic disturbances may inform how cross-feeding communities respond to phage infection. In the absence of disturbance, obligate mutualism typically constrains species ratios such that communities converge on an equilibrium ratio from any initial ratio.[72,73] This constraint on final species ratios means that limiting one species should indirectly inhibit cross-feeding partners, thereby decreasing total community biomass, but maintaining species ratios.[74] For example, antibiotic treatment of a three species cross-feeding community that inhibited the most sensitive member inhibited growth of all members of the community by depriving community partners of cross-fed nutrients.[75] Therefore, our null hypothesis is that phage infection on one member of a cooperative network will limit growth of the entire cross-feeding network but will not change species ratios.

Yet, the null hypothesis that phage infection will alter cooperative community biomass but not composition has several underlying assumptions that may not hold. First, it assumes that bacteria obtain nutrients directly from the secretions of bacterial partners. Yet there is a rich body of literature suggesting that phage-mediated cell lysis releases nutrients into the environment. Indeed, this 'viral shunt' is thought to play a major role in global nutrient cycling,[52,88,89] and may alter species interactions.[90,91] Second, the hypothesis overlooks possible ecological consequences of the evolution of phage resistance. For example, it assumes that phage resistance does not alter the exchange of cross-fed nutrients. If phage resistance causes changes in either nutrient secretion or uptake, it could alter species ratios, potentially changing community function.

In this study, we sought to determine the effects of phage attack on cooperative communities by combining resource-explicit mathematical modeling and wet-lab experiments of a synthetic cross-feeding co-culture of *Escherichia coli* and *Salmonella enterica*.[73,77] An *E. coli* strain auxotrophic for methionine was paired with a *S. enterica*

strain that was evolved to secrete methionine.[77] The pair forms an obligate mutualism in lactose minimal medium, as *S. enterica* cannot consume lactose and instead relies on acetate excreted by *E. coli* during overflow metabolism. Grown under these conditions, these bacteria are a simple two-species cooperative community. To this community, we added either an *E. coli*-specific (T7) or *S. enterica*-specific (P22*vir*) lytic phage and tracked community responses (Fig. 2.1a). As a null hypothesis, we predicted that cross-feeding would constrain species ratios and therefore targeted phage attack would inhibit growth of the entire community. However, we anticipated that phage resistance would evolve, making biomass reduction temporary. We found that both phage delayed community growth, but neither phage reduced final host yields and T7 infection of *E. coli* led to surprising changes in species ratios.

Results

Resource-explicit model suggests phage have little impact on final community composition.

We used a resource-explicit model to predict how a cooperatively growing bipartite bacterial community responds to lytic phage attack during batch growth. We modeled densities of *E. coli* (E), *S. enterica* (S), and phage (T7 or P22*vir*), as well as cross-fed metabolite concentrations (Fig. 2.1a, Appendix 1). Growth of each bacterial species was a function of maximum growth rate (m_x) and Michaelis-Menten saturation parameters (k_m) of essential metabolites. Bacterial death due to phage infection was modeled as a linear interaction between phage and host, and modified by an adsorption (i.e. predation) constant (g). Phage attack generated new phage particles at a rate set by the burst size (b). Phage-resistant hosts (E_R or S_R) were initiated at a frequency of 0.1% in each bacterial

population so that resistance alleles increased in frequency during phage infection. The cost of resistance, if any, was represented by a smaller growth rate (m_x) of resistant bacteria. Parameters were informed by the literature and adjusted to match experimental observations in the absence of phage (Fig. S2.1).

When modeled in the absence of phage, the community converged to 88% *E. coli* regardless of the starting bacterial ratio, consistent with previous wet-lab observations (Fig. 2.1c, Fig. S2.1).[73] In the absence of phage, sensitive and resistant bacterial genotypes increased in density with relative frequencies determined by the cost of resistance (Fig. S2.2).

The model predicted that the presence of phage increases the time required for the community to reach carrying capacity, but has little impact on the final species yields. Both T7 and P22*vir* rapidly killed all sensitive hosts (Fig. 2.1b, Fig. S2.2). The reduction in the host population reduced the amount of cross-feeding, thereby temporarily stalling community growth. However, phage-resistant hosts rapidly increased in abundance, allowing the community to reach carrying capacity. Host species reached 1.03-1.32 fold lower final densities as a result of phage attack (Fig. 2.1d). This reduction is because sensitive host cells consume resources before they are killed by phage, and fewer resources are therefore available for growth of the resistant host. However, sensitive hosts are killed before they consume many resources. No change was observed in the final abundance of the non-host bacteria. Furthermore, reducing maximum growth rates of phage-resistance genotypes as a proxy for the cost of resistance did not change yields, but did cause small delays of community growth (Fig. 2.2a,b).

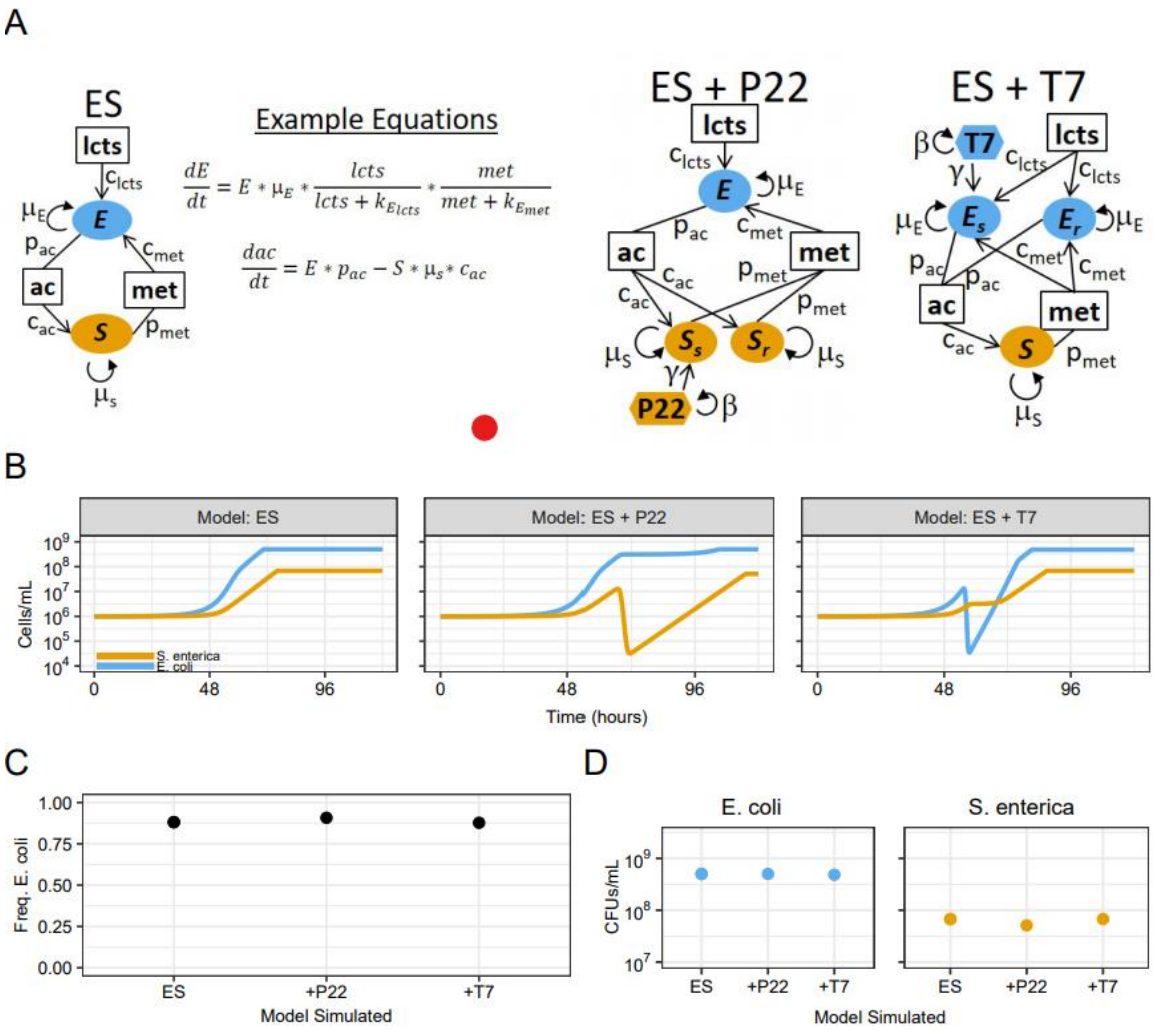

Figure 2.1. Mathematical model predicting consequences of phage infection of cooperative co-cultures. A) Schematic of models for systems with *E. coli* (E), *S. enterica* (S) and phage (T7 or P22). Bacteria are represented by ovals. Phage sensitivity (s) or resistance (r) is indicated by subscripts. Phage are indicated by hexagons and are colored to match their bacterial host. Boxes indicate metabolites (lcts = lactose, ac = acetate, met = methionine). Parameters are next to interaction arrows. c_x = consumption rate of subscript nutrient, p_x= production rate of subscript nutrient, m_x = growth rate (h^{-1}), b = burst size, g = adsorption constant. **B)** Simulated growth curves with and without phage treatment. Yellow = *S. enterica*, blue = *E. coli.* **C)** Species ratios represented with frequency of *E. coli* at time = 125 hours. **D)** Final densities of bacteria (cells/mL) in mathematical models at time = 125 hours.

In wet-lab experiments, T7 infection changed species ratios while P22vir infection did not.

Using our wet-lab experimental cross-feeding system, we tested the mathematical model prediction that phage attack would delay growth but have little impact on the final

community. Communities were started with a multiplicity of infection (MOI) of ~0.01 (Table S2.2). Any resistant host cells arose via mutation during cooperative community growth; they were not intentionally seeded into the host population. Growth of each bacterial species was tracked with a unique fluorescent marker which could be converted to a species-specific OD (Fig. S2.3).[75] After growth, co-cultures were plated for *E. coli* and *S. enterica* colony forming units (CFUs), and T7 or P22*vir* plaque-forming units (PFUs).

When the co-culture was exposed to the *S. enterica* – specific P22*vir* phage, P22*vir* rose to high titers (Fig. S2. 4), caused evolution of resistance in *S. enterica* (Table 2.1), and delayed community growth compared to no phage controls (p=0.0037, Fig 2.2a). However, compared to no-phage controls, P22*vir* significantly affected neither the species densities of *E. coli* (p = 0.35, Fig. 2.2c) or *S. enterica* (p = 0.95, Fig. 2.2c), nor the frequency of *E. coli* (p = 0.51, Fig. 2.2b). Overall, P22*vir* infection of the co-culture delayed growth and did not change final community composition, as predicted by co-culture simulations.

The effects of T7 phage on the cooperative co-culture differed in some ways from the effects of P22*vir* phage. Like P22*vir*, T7 phage rose to high titers (Fig.S2. 4), caused evolution of resistance in *E. coli* (Table 2.1), and delayed community growth compared to no phage controls (p=0.0037, Fig. 2.2a). However, there were changes to the cooperative co-culture composition. T7 infection of *E. coli* in a cooperative community decreased *E. coli* density in the presence of T7 (p = 0.017, Fig. 2.2b). In fact, *E. coli* went extinct in two of the five T7 phage replicate communities. In addition, the final frequency of *E. coli* relative to no-phage controls decreased following T7 phage attack (p=0.008, Fig. 2.2c). Surprisingly, growth of *S. enterica* was not constrained by the phage-mediated death of *E. coli*. Instead, *S. enterica* reached between 8- and 35-fold higher density in the presence of T7 (Fig. 2.2c). In addition, *S. enterica* entered log-phase sooner, despite its dependence on *E. coli* secreted acetate (Fig. S2.3a). This led to a rapid increase in biomass of

communities with T7 phage (Fig. S2.3b). Phage attack on *E. coli* appeared to release *S. enterica* from the constraints typically imposed on cross-feeding community partners – a novel result that we interrogated further.

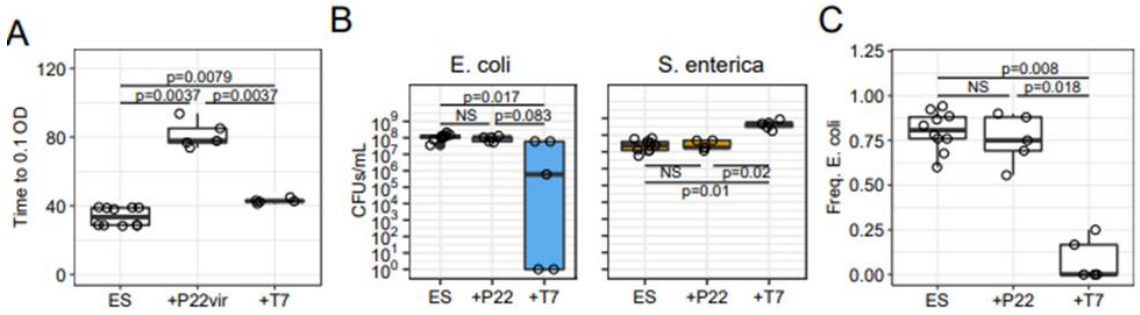

Figure 2.2. Experimental data of cooperative co-culture growth and the effect of adding phage. A) Time to 0.1 OD for each phage treatment. Statistical significance determined with Mann-Whitney-U test with FDR multiple hypothesis correction. **B)** Species ratios represented with frequency of *E. coli* at the end of growth. Ratios were calculated from plated CFUs. **C)** Boxplot depicting measured CFUs/mL of *E. coli* or *S. enterica* at the end of growth. Statistical significance of B) and C) determined with Mann-Whitney-U test with FDR multiple hypothesis correction. ES = no phage controls, +P22*vir* = P22*vir* phage treatment, +T7 = T7 phage treatment.

Table 2.1. Resistance and mucoidy in phage-treated cooperative co-cultures.

Treatment	# communities	resistant[a] / total isolates	mucoid / total isolates
ES	10	0/30	0/30
ES + P22*vir*	5	15/15	0/15
ES + T7	3[b]	9/9	9/9

[a] Resistance assayed with cross-streaks.

[b] Two replicate communities were driven extinct.

T7-resistant E. coli increase S. enterica densities in the absence of phage.

The increase of *S. enterica* during T7 infection of *E. coli* could result from T7-resistance altering *E. coli* secretion of cross-fed metabolites. To test if T7-resistant *E. coli* provide more metabolites than sensitive *E. coli,* we assayed the growth of *S. enterica* when paired with evolved *E. coli* isolates in the absence of phage. *S. enterica* reached an average of

1.43-fold higher density when co-cultured with evolved T7-resistant isolates than with ancestral *E. coli* (Fig. 2.3a, $p = 0.004$). In these co-cultures, the yield of T7-resistant *E. coli* only reached 67% the yield of the ancestor ($p = 0.004$, Fig. 2.3a), suggesting that T7-resistant *E. coli* isolates supported a larger cross-feeding *S. enterica* population. We also paired P22*vir*-resistant *S. enterica* with ancestral *E. coli* and found that P22*vir* resistance led to a ~2% decrease in *E. coli* yield (Fig. 2.3b, $p < 0.0005$), and increased *S. enterica* 5% (Fig. 2.3b, $p = 0.012$). While our data illustrate that *S. enteric* receives more carbon from evolved *E. coli* than ancestral *E. coli*, we cannot differentiate between increased secretion or poor re-uptake. These results suggest that the divergent impact of T7 and P22*vir* on community composition is in part driven by how resistance to each phage influences the abundance of cross-fed metabolites.

An alternative explanation for the asymmetric response to T7 and P22*vir* phage would be differences in the cost of resistance – such as decreased growth rates. However, costs of resistance to either T7 or P22*vir*, measured by isolate monoculture growth rate or species-specific co-culture growth rate were less than 8% (Fig. S2.2c). Furthermore, mathematical modeling suggested that costs of resistance, encoded by decreasing growth rate when phage resistant, do not alter final yields, but causes small delays in community growth (Fig. 2.2a-b).

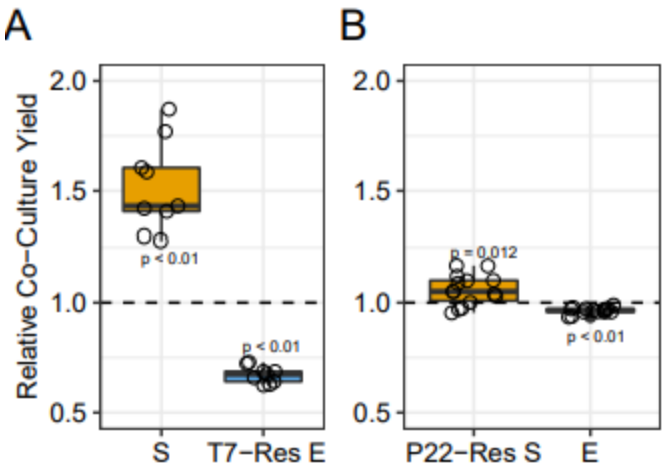

Figure 2.3. Relative yield of co-cultures with resistant isolates in the absence of phage. The relative yield (CFU) for each strain in co-cultures with one resistant partner as compared to the ancestral co-culture. **A)** Relative yields of co-cultured ancestral *S. enterica* (S) and T7-resistant *E. coli* isolates (T7-Res E) (n = 9). **B)** Relative yields of co-cultured P22*vir*-resistant *S. enterica* isolates (P22-Res S) and ancestral *E. coli* (E) (n = 15). Dashed lines represent standardized yields of ancestral *S. enterica* and *E. coli* co-cultures. Points represent averages of triplicate replicates. Statistical significance determined using Wilcox Sign Test with m = 1.

S. enterica grows on cellular debris released by phage lysis.

When lytic phage burst host cells to release phage progeny, intracellular carbon and nutrients are also released into the environment, referred to as the "viral shunt".[89] We tested whether consumption of lysed *E. coli* cellular debris increased the density of *S. enterica* in the presence of T7 by measuring *E. coli* and *S. enterica* monoculture yields on cellular debris without phage. We produced cellular debris by sonicating monocultures of *E. coli* and *S. enterica* grown in minimal medium. We then grew ancestral *E. coli* or *S. enterica* in lysates in lactose minimal medium without methionine supplemented with 25% sonicated supernatant for 48 hours without phage. We plated for CFUs to determine yields after 48 hours of growth. While both *E. coli and S. enterica* were capable of growth in lactose minimal media supplemented with cellular debris, we observed different responses. *S. enterica* reached 100-fold higher densities than *E. coli* when both were grown independently on *E. coli* cellular debris (p = 0.050) and 2-fold higher densities than *E. coli* when both were grown independently on *S. enterica* cellular debris (p = 0.046, Fig.

2.4). These results suggest that *S. enterica* reaches relative higher yields during T7 infection because it more efficiently converts *E. coli* cellular debris to cells compared to *S. enterica* conversion of *E. coli* cellular debris released during P22*vir* phage infection. In fact, in lactose minimal medium supplemented with 25% sonicated cellular debris supernatant, *S. enterica* generated 7.3 new cells per cellular equivalent of *E. coli* cellular debris while *E. coli* generated 0.05 new cells per cellular equivalent of *S. enterica* cellular debris (Table S2.4).

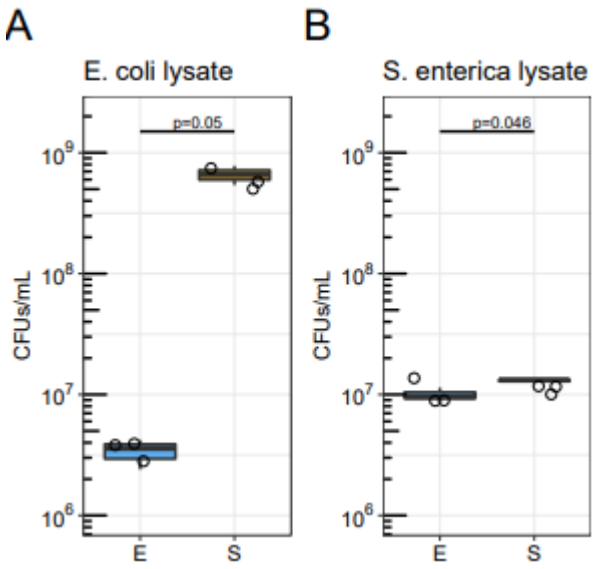

Figure 2.4. Growth of *S. enterica* and *E. coli* on sonicated cellular debris. *E. coli* (E) and *S. enterica* (S) monocultures were each grown in lactose minimal medium + 25% (v/v) sonicated cellular debris lysate. **A)** Monoculture yields on *E. coli* cellular debris lysate. **B)** Monoculture yields on *S. enterica* cellular debris lysate. Cultures were inoculated with 5 x 10^5 cells/mL. Statistical significance was tested with a Kruskal Wallis test.

A modified mathematical model incorporating changes in secretion profiles and cellular debris exchange does not reflect wet-lab experiments.

In wet-lab experiments, we observed that pairing T7-resistant *E. coli* with ancestral *S. enterica* in cooperative co-culture results in ~50% more *S. enterica* than when paired with ancestral *E. coli* (Fig. 2.3). We incorporated this into our model to test how changes in secretion profile changed *S. enterica* yields. We found that the increase in acetate

production by resistant *E coli* increased simulated *S. enterica* yields 1.95-fold compared to the base model (Fig. 2.5).

Wet-lab experiments also showed more efficient *S. enterica* growth on cellular debris than *E. coli* (Fig. 2.4). Therefore, we incorporated non-host consumption of host cellular debris (cd) into our model as well. Cellular debris was included as a metabolite produced when host cells are lysed by phage (Fig. 2.5, Appendix 1). One lysed *E. coli* host cell was set to generate enough nutrients for 7.33 *S. enterica* cells, in agreement with experimental measurements (Table S2.4). Incorporating consumable cellular debris increased simulated *S. enterica* yields by 2.88-fold compared to the base model (Fig. 2.5).

Combining both increased acetate production and consumption of cellular debris mechanisms in the mathematical model increased the final density of *S. enterica* 3.84-fold, still far less than observed experimentally (Fig. 2.5). In fact, we had to increase the production-to-consumption ratio to ~25 *S. enterica* produced per lysed *E. coli* cell, an unrealistic number, to match the observed increases in *S. enterica* yields in wet-lab experiments (Fig. S2.5). Taken together, changes in carbon secretion and consumption of cellular debris partially explain the observed increases in *S. enterica* during T7 infection, but additional mechanisms likely contribute.

Figure 2.5. Mathematical model with increased acetate production and cellular-debris exchange increases final densities of *S. enterica* during *E. coli*-specific T7 phage attack. A) Schematic of modified model of *E. coli*-specific T7 phage attack. Red text highlights the modifications of cellular-debris (cd) and a 50% increase in acetate production (p_{ac}) by T7-resistant *E. coli*. **B)** Relative *S. enterica* co-culture yields of modeling (left panel) and experimental (right panel) results. Results are relative to no phage (-T7) control communities. Base = base model described in figure 1; +50%Ac = T7-resistant *E. coli* produce 50% more acetate compared to T7-sensitive *E. coli*; CDE = cellular debris exchange model where *E. coli* cells lysed by T7 generate

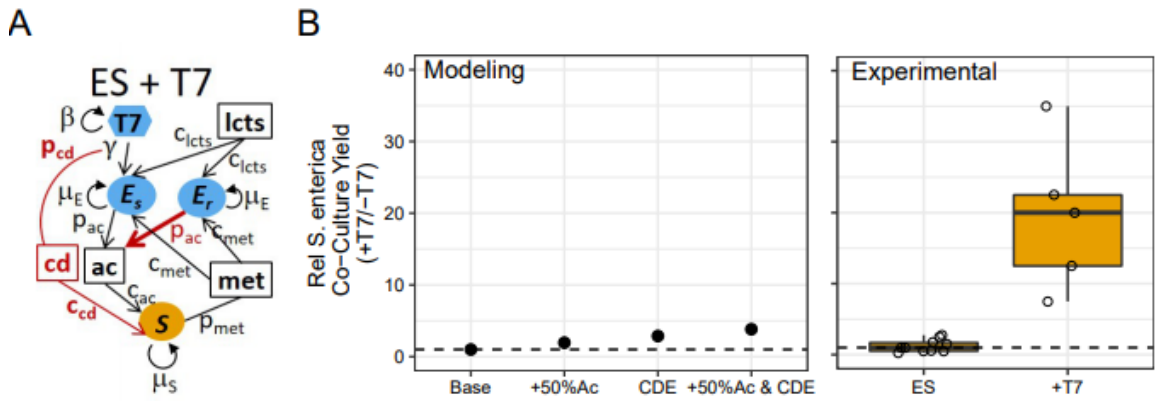

cellular debris that can be used by *S. enterica*; +50%Ac & CDE = model combining increase in acetate production when *E. coli* is resistant to T7 phage and consumption of cellular debris by *S. enterica*.

E. coli evolves partial resistance to phage, T7, increasing S. enterica yields.

E. coli isolates from replicate communities with T7 showed no inhibition of growth when cross streaked against T7 phage (Table S2.1). Additionally, evolved isolates grew in the presence of T7 while ancestral *E. coli* did not (Fig. 2.6b).

However, the mucoid phenotype of phage-resistant isolates suggested that partial resistance might contribute to the differential impact of T7 and P22*vir* phage on non-host bacteria. T7 phage-resistant *E. coli* formed mucoid colonies, while P22*vir*-resistant *S. enterica* did not (Fig. 2.6a, Table 2.1). Mucoidy is frequently associated with partial resistance, providing incomplete protection against phage by decreasing efficiency of adsorption.[92] Finally, T7 phage increased more than 10-fold on mucoid *E. coli* isolates, much less than the 100-fold increase observed on ancestral *E. coli* isolates (Fig. 2.6C). This is qualitatively different from the full resistance observed in *S. enterica*. From an inoculum of $1x10^6$ PFU/mL, P22*vir* phage on average reached $6.3x10^8 \pm 3x10^8$ PFU/mL on ancestral *S. enterica* and $1.3x10^6 \pm 7.5x10^5$ PFU/mL on P22*vir*-resistant after 48 hours of growth. Although growth of phage in evolved isolates may suggest T7 phage counter-adaptation, isolated ending phage populations and ancestral phage produced identical infection patterns when cross-streaked against evolved mucoid *E. coli* isolates (Table

S2.3). Furthermore, we note that similar phenotypes would be observed if a subset of the *E. coli* population reverted to the sensitive phenotype. However, it is unlikely that reversion instead of partial resistance would change the community-level interpretations we have suggested. These results suggest that evolved partially resistant *E. coli* isolates may continually be lysed throughout growth, increasing the total amount of cell debris available for *S. enterica* to consume.

Genome sequencing also supported partial resistance mechanisms in *E. coli* and a different mechanism in *S. enterica*. We whole-genome sequenced communities treated with either T7 or P22*vir* phage with Illumina sequencing and used *breseq* to identify mutations compared to reference genomes.[93] We focused on mutations unique to each phage treatment and >20% frequency in at least one replicate community. We identified two mutations in the intergenic region of the *clpx* and *lon* genes that reach high frequency in all T7-resistant *E. coli* populations (Table 2.2). Mutations in the *lon* gene encoding a protease of *E. coli* have been shown to cause mucoid phenotypes in *E. coli*.[94] We also identified a single mutation in four of five *S. enterica* genomes of P22*vir*-treated communities in a Gifsy-1 prophage terminase small subunit that rose to 80%-90% (Table 2.2).

Finally, we leveraged our model to assess the impact of *E. coli* partial resistance to T7 phage on yield of the non-host, *S. enterica*. We incorporated partial resistance by decreasing the T7 adsorption constant to reduce the frequency of successful phage infection of partially resistant *E. coli* which results in host cells lysing and releasing cellular debris throughout growth. Adding partial resistance, in addition to increasing acetate production of T7-resistant *E. coli* and allowing *S. enterica* to consume *E. coli* cellular debris, led to a maximum 55.2-fold increase in *S. enterica* yield, which is greater than the observed wet-lab increases of *S. enterica* (Fig. 2.6d). Furthermore, intermediate

adsorption values corresponding to partial resistance phenotypes led to the highest yields of *S. enterica* (Fig. 2.6d). These results suggest that multiple mechanisms including increased acetate production, consumption of phage-released cellular debris, and partial phage-resistance mechanisms all led to increase the final yield of *S. enterica* during T7 infection of *E. coli*.

Table 2.2. Mutations identified by whole-genome sequencing of communities.

Community Type	Genetic Element	Mutation Location	Mutation	Gene	# Reps
ES + P22*vir*	*S. enterica* genome	Coding Region (486/495bp)	Frameshift (+G)	STM2609 - DNA packaging-like protein, small terminase subunit, in *Gifsy-1* prophage	4/5
ES + T7	*E. coli* genome	Intergenic (+118/-67)	Δ5 bp :: repeat_region(+) +4 bp	*clpX* - *lon* intergenic region, upstream of *lon*	1/3
ES + T7	*E. coli* genome	Intergenic (+90/-93)	repeat_region (+) +6 bp :: Δ1 bp	*clpX* - *lon* intergenic region, upstream of *lon*	3/3

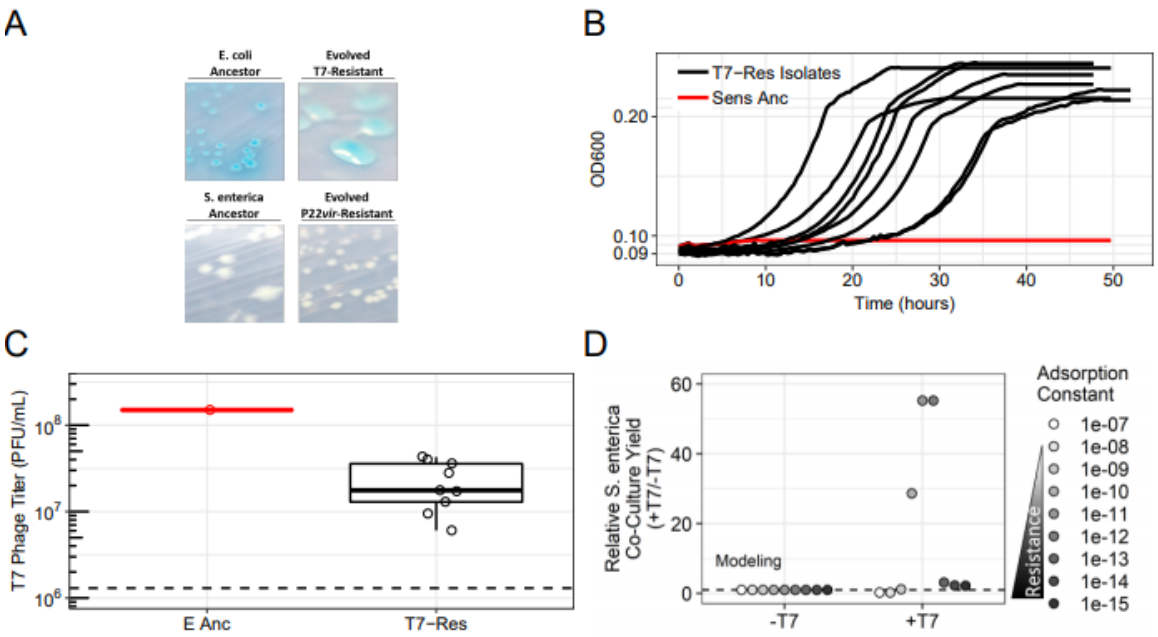

Figure 2.6. Experimental partial resistance quantification of *E. coli* mucoid T7-resistant and implications on non-host *S. enterica* yield during modeled T7 phage attack. A) Morphology comparison of representative *E. coli* T7-resistant isolate or representative P22*vir*-resistant *S. enterica* isolate and ancestor on lactose or acetate minimal media, respectively. **B)** Representative growth curves of ancestral *E. coli* (Anc E, red line) or T7-exposed *E. coli* isolates (black lines with T7 phage. Isolates were grown in lactose minimal medium supplemented with methionine with T7 phage (n = 9 isolates). **C)** Titers of T7 phage recovered from infection of *E. coli* isolates. Isolates were inoculated at 0.01 OD and ~10^6 T7 phage in lactose medium supplemented with methionine in triplicate. After culturing 72 hours in 30°C, phage lysates titered (n = 9 isolates, triplicate). Points are averages of three replicates. E Anc = Ancestral *E. coli*, T7-Res Isolates = mucoid evolved T7-resistant *E. coli* isolates. Dashed line = starting titer. **D)** *S. enterica* co-culture yields relative to no-phage treatment with adsorption constant = 1e-07. The mathematical model used had 50% increase in acetate production when *E. coli* is resistant to T7, the ability of *S. enterica* to consume cellular-debris, and partial resistance of *E. coli* against T7 phage as determined by the adsorption factor (adsorption factor = 1e-07, fully resistant). Dashed line = 1.

Discussion

In summary, our results suggest that lytic phage can dramatically impact communities of cooperating cross-feeding bacteria by changing yields of non-host species through multiple mechanisms. Previously published literature about responses to abiotic stressors lead us to initially predicted that attack of a host species with lytic phage would suppress the cross-feeding community. However, our resource-explicit models instead indicated that resistance could quickly evolve, leading to a temporary delay in community growth

before ultimately reaching similar yields and species ratios to those observed in communities not attacked by phage (Fig. 2.1). In agreement with the mathematical model, attack of *S. enterica* with P22*vir* phage delayed community growth in wet-lab experiments and had little effect on final species ratios (Fig. 2.2, Fig. S2.3). In contrast, *E. coli*-specific T7 attack dramatically altered the final species ratios in favor of *S. enterica*, the non-host, but caused a relatively small delay in community growth (Fig. 2.2, Fig. S2.3). Experimental and mathematical results suggest that a combination of several factors contributed to the increase of *S. enterica* in the presence of T7. These factors included changes in the extent of cross-feeding by resistant *E. coli* (Figs. 2.3,2.5), growth on cellular debris released from phage-lysed cells (Figs. 2.4,2.5), and the evolution of partial resistance in *E. coli* (Fig. 2.6). Our modeling suggests that divergent community responses to phage can be accurately predicted by incorporating metabolic mechanisms and the level of phage resistance.

We observed that the impact of phage extended beyond the targeted host to the other member of a cross-feeding pair. *P22vir* infection delayed growth of the non-host, while T7 infection facilitated growth of the non-host. In both cases the effect on growth of non-hosts was indirect and was mediated by changes in the metabolites available in the system. The *P22vir* results demonstrate that cross-feeding metabolic dependencies can make the entire community susceptible to perturbations of a single species, similar to previous findings with antibiotic and genetic perturbations,[74,75] and highlights the dangers of a cross-feeding lifestyle.[95] However, here we demonstrate that evolution of phage resistance can rapidly return cross-feeding co-cultures to the unperturbed state. In contrast, T7 had qualitatively distinct impacts on the community that were mediated by consumption of cellular debris. Release of nutrients through cell lysis is likely to generate indirect effects on species abundance independent of microbial interactions. Indeed, viral lysis of bacteria is thought to play a major role in shaping the composition of diverse

microbial communities.[2,78,79] Phage are frequently touted as tools for targeted treatment of pathogenic bacteria infections.[22,83] However, our results suggest that even strain-specific phage can have broader impacts on microbial communities, which could lead to diverse phage therapy outcomes.

We predict that an understanding of what metabolites mediate cross-feeding will make predicting indirect effects of phage more accurate. We have shown two contrasting effects of phage attack on a cross-feeding microbial community. One major reason for the divergent effects is likely the identity of the cross-fed nutrients. In our microbial community, *S. enterica* receives acetate from *E. coli,* while *E. coli* receives methionine from *S. enterica*. Bennett et. al. showed that intracellular pools of carbon-compounds are larger than intracellular pools of methionine.[96] Furthermore, it may be easier for cells to scavenge carbon from biomass components than methionine from proteins. Taken together, it is likely that *S. enterica* has easier access to required metabolites in cellular debris than *E. coli* because *S. enterica* reached higher densities on multiple cellular debris types than *E. coli* (Fig. 2.4, Table S2.4). Additionally, the nutritional quality of cellular debris appears to vary, as the difference between *S. enterica* and *E. coli* yields on cellular debris was larger on *E. coli* debris than on *S. enterica* debris (Fig. 2.4, Table S2.4). We acknowledge that the metabolites released by phage lysis are likely different from those released by sonication of uninfected cells due to phage-mediated host metabolism changes[97]; however, it is unlikely that these differences would qualitatively alter our results. These results suggest that metabolic mechanisms play a critical role in determining the impact of phage in cross-feeding systems and highlight the need for further methods to quantitatively incorporate these mechanisms in our models.[87]

In addition, the magnitude of the community response to T7 phage was influenced by the mechanism of phage resistance that evolved. Both mutations identified in *E. coli* genomes

exposed to T7 phage were upstream of the *lon* gene encoding the lon protease, a mutation consistent with a partial resistance phenotype.[94] Down-regulation of the lon protease has been found to cause a mucoid phenotype[94] and negatively regulates the activator of capsular genes, *rscA*.[98] Qimron et. al. showed that knocking out *rscA* also caused mucoidy and partial phage resistance against four phage, including T7.[99] Our model suggests that *E. coli*'s incomplete resistance significantly increased the indirect effects of *E. coli* – specific T7 phage on *S. enterica*. If complete resistance was modeled phage rapidly killed sensitive cells generating only a small pool of cellular debris. In contrast, partially resistant *E. coli* continued to lyse (though at a lower rate) and generate cell debris throughout growth. This continual lysis substantially increased yields of the non-host *S. enterica*. Partial resistance should also allow the phage population to be maintained and should therefore lead to lasting changes in species ratios barring further evolution by phage or host bacteria. In conclusion, evolution of partial resistance to phage infection has the potential to generate lasting changes in community composition due to the continual generation of consumable cellular debris.

Understanding the indirect impacts of phage in microbial communities is critical as we strive to manage microbial ecosystems. Four recent studies using phage therapy in mouse models also observed extensive indirect effects of phage in microbial communities.[59–62] All four studies reported that phage therapy changed abundances of non-host genera in mouse digestive tracts, however, no mechanisms were confirmed. Understanding how and why phage influence microbial communities is important for controlling bacteria populations, particularly in the food industry and medical field.[100,101] We conclude that understanding the ways in which bacteria interact, the ability of species to use nutrients from lysed bacteria, and the extent of phage resistance are paramount for predicting the effects of phage attack in diverse microbial communities.

Material and Methods

Mathematical Simulations.

We used resource-explicit ordinary differential equation models to simulate cooperative growth of *E. coli*, and *S. enterica* (Appendix 1). Growth of the bacterial species was governed by Monod kinetics with multiplicative limitation for resources. Production of cross-fed nutrients was growth-dependent. Our base model without phage infection used two equations to directly track *E. coli* (E) and *S. enterica* (S):

Where E or S is the bacterial population size, m_x is a species-specific growth rate (h^{-1}), k_x is a species- and metabolite-specific Monod constant, and *lcts*, *met*, and *ac* represent concentrations of lactose, methionine and acetate in g/200ml to compare to wet-lab results.

We added equations for *E. coli*-specific T7 or *S. enterica*-specific P22*vir* lytic phage infection (Fig. 2.1). For example, sensitive *E. coli* (Es) and T7 phage interacted through the following equations:

Models contain phage-sensitive (E_s or S_s) host strains, phage-resistant (E_r or S_r) host strains, or non-host (E or S) strains as needed. In a second model, we added an equation for cellular debris (cd) produced when sensitive host cells were killed by phage. The cellular debris was consumed by non-host species (Fig. 2.5). We altered metabolite production by changing the production parameters (p_x) and encoded partial resistance by changing the adsorption rate parameter (g). Our model assumes that resistant hosts were present at the beginning of the community growth and were seeded at 0.1% of the host population. All simulations were run in R with the DeSolve package, using the LSODA solver.[102] Supplementary Methods, Figures, Tables have details (Appendix 1).

Ancestral Bacterial Co-Culture System and Viral Strains.

Ancestral *E. coli* and *S. enterica* strains are previously described. Briefly, the ancestral *E. coli* K12 BW25113 *metB::kan* is a methionine auxotroph from the Keio collection with the lac operon restored. *S. enterica* LT2 was evolved to secrete methionine.[77] *E. coli* is tagged with a cyan fluorescent protein encoding gene integrated at the attB lambda integration site and driven by a constitutive lambda promoter. *S. enterica* is tagged with a yellow fluorescent protein encoding gene under the same promoter and at the same integration site. Co-cultures were grown in lactose hypho minimal medium (5.84 mM lactose, 7.26 mM K_2HPO_4, 0.88 mM NaH_2PO_4, 1.89 mM $[NH_4]_2SO_4$, 0.41 mM $MgSO_4$).[103] Monocultures of *E. coli* were supplemented with 80 mM of L-methionine and monocultures of *S. enterica* replaced lactose with acetate. T7 phage is an *E. coli*-specific lytic bacteriophage and P22*vir* phage is a *S. enterica*-specific lytic bacteriophage. Virus stocks were provided by I. J. Molineaux and were stored at -80°C. Working stocks of phage were grown on ancestral *E. coli* or *S. enterica* cultures in minimal medium and stored at 4°C.

Microbial Community Growth.

To measure bacteria community growth, mid-log cultures started from a single bacterial colony were used to inoculate 200ml of medium in a 96-well plate with 10^5 cells for each bacterial species per well, and 10^2 total phage (MOI = 0.01) where indicated (Table S2.2). The 96-well plates were incubated in a Tecan Pro200 plate reader for 96-120 hours at 30°C with shaking. OD600, *E. coli*-specific CFP (Ex: 430nm; Em: 490nm), and *S. enterica*-specific YFP (Ex: 500nm; Em: 530nm) fluorescence were read every 20 minutes. Fluorescent protein signals were converted to species-specific OD equivalents using an experimentally-determined conversion factor as described.[75] Five phage treatments and five controls were used in each experiment. Phage were tested in separate experiments

totaling five T7 treatments, five P22*vir* treatments, and 10 no-phage controls. Following growth, we plated for CFUs of both bacterial species - *E. coli* on lactose minimal medium plates with excess methionine and *S. enterica* on citrate minimal medium. X-gal (5-bromo-4-chloro-3-indolyl-β-D-galactopyranoside) in plates differentiated between *E. coli* and *S. enterica*. Phage population sizes were measured by plating for plaques on LB with 0.3% LB top agar with a lawn of the ancestral, sensitive host. Phage plates were incubated at 37°C and bacterial plates at 30°C.

Testing for Evolution of Phage Resistance: Cross-streaking Assays.

Three colonies per replicate community were isolated on minimal media plates. Resistance to ancestral phage was tested with cross-streaking assays on minimal media plates. Phage stock (~10^8 PFU) was spread in a line across an LB plate, bacterial isolates were streaked perpendicular to the phage culture, and plates were incubated at 30°C for 24-72 hours. Bacterial isolates with clearing around the phage streak were deemed sensitive and isolates with no clearing were resistant.

Phenotyping Phage Resistant Isolates.

Isolates were cultured alone or in cooperative co-culture as indicated in minimal medium in a 96-well plate. Bacteria were inoculated at 10^5 cells per well. OD600, and CFP or YFP fluorescence were recorded with the TecanPro200 shaking plate reader for 72 hours. Growth rates were calculated by fitting Baranyi growth curves[104] to fluorescent protein data transformed into OD-equivalents (see above) and compared to ancestral strains grown in either monoculture or cooperative co-culture.

Testing Phage-Mediated Cellular Debris Exchange.

E. coli was grown in lactose + methionine minimal medium and *S. enterica* was grown in acetate minimal medium. After stationary phase was reached (OD_{600} ~0.5), cells were pelleted, sonicated (10, 30s pulses), and filter sterilized with a 0.22μm filter. Filtered sonication supernatants were checked for sterility by plating. Ancestral bacteria were inoculated at $5x10^5$ cells/mL in lactose minimal medium supplemented with 25% filtered sonication supernatant and incubated at 30°C for 48 hours. Cultures were plated to enumerate CFUs.

Whole Genome Sequencing of Communities and Analysis.

Communities were inoculated from frozen stocks into lactose minimal media and grown at 30°C for 4 days. Total community DNA was isolated using the Zymo Quick-gDNA Miniprep Kit (11-317C). Illumina sequencing libraries were prepared according to the Nextera XT DNA Library Prep Kit protocol, submitted to the University of Minnesota Genomics Center for QC analysis, and sequenced on an Illumina Hi-Seq with 125bp paired-end reads. We used the *breseq* tool[93] version 0.28.1 to align Illumina reads to the following reference genomes: *Escherichia coli str. K-12 substr. MG1655* (Accession No: NC_000913.3), *Salmonella enterica subsp. enterica serovar Typhimurium str. LT2* (Accession No: NC_003197.2, NC_003277.2), Enterobacteria phage T7 (Accession No: NC_001604.1), and Enterobacteria phage P22 (Accession No: NC_002371.2) and predict polymorphisms (-p command). Mutations lists for resistant populations were filtered to remove mutations common between ancestral strains and reference genomes. We kept mutations that were unique to each phage treatment and arose in populations >20% (Table 2.2).

Acknowledgements

We would like to thank Ian J. Molineaux (UT-Austin) for the phage isolates; E. Adamowicz, S. Hammarlund, and the Institute of Molecular Virology at the University of Minnesota for constructive conversations; LF was funded by a Fellowship on the NIH T32 AI83196 training grant and a NIH RO1 GM121498-01A1 grant.

Chapter 3

Phage cocktail strategies for the suppression of a microbial cross-feeding coculture

This chapter is a reprint with minor alterations of *Environ Microbiol*. DOI: doi:10.1111/1751-7915.13650(2020). In Press. (accepted July 27th, 2020).

See Appendix 3 for supplemental figures and methods.

Lisa Fazzino[1,a,b], Jeremy Anisman[1,c,d], Jeremy M. Chacón[b,e], William R. Harcombe[b,e]

[1] These authors contributed equally to this manuscript.

[a] Department of Microbiology and Immunology, University of Minnesota, Minneapolis, MN, USA

[b] BioTechnology Institute, University of Minnesota, Saint Paul, MN, USA

[c] College of Continuing and Professional Studies, University of Minnesota, Minneapolis, MN, USA

[d] Department of Diagnostic and Biological Sciences, School of Dentistry, University of Minnesota, Minneapolis, MN, USA

[e] Department of Evolution, and Behavior, University of Minnesota, Saint Paul, MN, USA

Summary

Cocktail combinations of bacteria-infecting viruses (bacteriophage), can suppress pathogenic bacterial growth. However, predicting how phage cocktails influence microbial communities with complex ecological interactions, specifically cross-feeding interactions in which bacteria exchange nutrients, remains challenging. Here, we used experiments and mathematical simulations to determine how to best suppress a model pathogen, *E. coli*, when obligately cross-feeding with *S. enterica*. We tested whether the duration of pathogen suppression caused by a two-lytic phage cocktail was maximized when both phage targeted *E. coli*, or when one phage targeted *E. coli* and the other its cross-feeding partner, *S. enterica*. Experimentally, we observed that cocktails targeting both cross-feeders suppressed *E. coli* growth longer than cocktails targeting only *E. coli*. Two non-mutually-exclusive mechanisms could explain these results: 1) we found that treatment with two *E. coli* phage led to the evolution of a mucoid phenotype that provided cross-resistance against both phage, and 2) *S. enterica* set the growth rate of the co-culture, and therefore targeting *S. enterica* had a stronger effect on pathogen suppression. Simulations suggested that cross-resistance and the relative growth rates of cross-feeders modulated the duration of *E. coli* suppression. More broadly, we describe a novel bacteriophage cocktail strategy for pathogens that cross-feed.

Introduction

Phage have been used to treat pathogenic bacteria in human health, agriculture, and the food industry. Phage therapy and biocontrol often use multiple phage simultaneously in 'cocktails' to suppress pathogen growth.[4,7,83,105,106] Attacking a bacterial population with multiple phage can reduce the rate at which phage resistance evolves.[107–109] However, we understand less about how treatment outcomes are affected by complex interactions

among bacteria in a microbial community.[25] One bacterial interaction of particular interest is cross-feeding, in which metabolites secreted by one bacterium are used as a nutrient source by another. This is a common interaction in natural systems.[68–71,75] Understanding how complex ecological interactions involving pathogens affect phage treatment outcomes will be critical for designing effective therapies. Here, we explore how two important factors – the potential for cross-resistance evolution and relative bacterial growth rates – interact with targeting strategies to suppress growth of a focal pathogen cross-feeding in an engineered coculture.

Experiments using cocultures with well-defined interactions have helped elucidate a range of responses to phage infection which may be leveraged for phage therapy. For example, adding non-host bacteria that compete with phage hosts for nutrients limits phage resistance evolution, thereby magnifying the efficacy of the phage.[23,47,65,110,111] Microbes also can engage in cooperative mutualistic interactions, where bacteria depend on others to cross-feed nutrients.[68,69,71,75,112] Targeting one species in a cross-feeding mutualism can reduce the population of both mutualists, leading to the hypothesis that phage therapies could target a pathogen's mutualists.[25] However, it is unknown how cocktails should be assembled to maximize pathogen suppression in a community.

If pathogenic bacteria cross-feed with other community members, then we can consider novel strategies of phage cocktail design that also target the nonpathogenic cross-feeding partner. Phage cocktails classically contain multiple phage that target a focal species to better limit the growth of a pathogen while also decreasing the rate of resistance evolution.[110,113,114] However, cross-resistance can evolve during treatment with classic pathogen-targeting cocktails when a single mutation blocks infection to multiple phage.[3,115,116] We hypothesize that if a focal pathogen is engaged in an obligate mutualism, including a phage that targets the cross-feeding nonpathogen will increase

suppression of the pathogen. It has been shown that off-target inhibition of cross-feeding partners can inhibit focal bacterial strains.[72,75] Combining phage that target the pathogen and its cross-feeding partner in a 'multispecies-targeting' cocktail would require the coculture to evolve two resistance mutations – one in each cross-feeding partner – to continue growing. Here, we hypothesize that this novel cocktail strategy that targets pathogens and cross-feeding nonpathogens will eliminate cross-resistance evolution and lengthen pathogen suppression.

In this study, we test the efficacy of phage cocktail treatment strategies to suppress a model pathogen obligately cross-feeding in a synthetic coculture. We performed wet-lab experiments with an engineered obligate cross-feeding coculture of an *Escherichia coli* methionine auxotroph that provides carbon to a methionine-secreting *Salmonella enterica*.[77] Here, *E. coli* is the model pathogen to be suppressed. We introduced all pairwise combinations of *E. coli*-specific T7 and/or P1*vir* lytic phage, and the *S. enterica*-specific P22*vir* lytic phage (Fig. 3.1a). We then compared 'pathogen-targeting cocktails' with 'multispecies-targeting cocktails'. We hypothesized and observed that targeting both cross-feeding partners was more effective at suppressing *E. coli* than targeting only *E. coli* with cocktails in our wet-lab experiments. We combined wet-lab experiments and mathematical modeling to uncover two reasons for this. First, as anticipated, we found evidence that *E. coli* evolved cross-resistance in the pathogen-targeting cocktail treatment. Second, the multispecies-targeting cocktail inhibited the slowest-growing cross-feeding partner, *S. enterica*, which limited how fast the coculture recovered from phage treatments. In fact, treatment with a single phage infecting *S. enterica* was as effective as targeting both cross-feeding partners in wet-lab experiments and simulations. Ultimately, our study highlights a novel strategy for designing phage cocktails that suppress cross-feeding pathogens.

Results

We wondered whether the pathogen, *E. coli*, would be suppressed for longer by a phage cocktail combining two *E. coli*-targeting phage ('pathogen-targeting cocktail') or combining an *E. coli*-targeting phage with a *S. enterica*-targeting phage ('multispecies-targeting cocktail'). We grew control cocultures without phage ('phage-free'), and treatment cocultures with combinations of T7 and P1*vir* as *E. coli*-targeting phage and P22*vir* as a *S. enterica*-targeting phage. The growth of each strain was tracked with unique fluorescent proteins (see Experimental Procedures for details). We predicted that the multispecies-targeting cocktail would provide the longest *E. coli* suppression because cross-resistance would not be possible and two mutations in separate bacterial species would need to evolve for the coculture to grow.

We quantified the duration of *E. coli* suppression across phage treatments. To do this, we measured the amount of time required for a fluorescent protein in *E. coli* to reach 95% maximum intensity, which we refer to as time to maximum density. We calculated the relative suppression duration caused by each phage treatment as a fold-change relative to the phage-free cocultures, which required 34.4 hours to reach maximum density (Table S3.1). As anticipated, all phage treatments increased *E. coli* suppression duration (Fig 3.1b, Table S3.1 for absolute values). Notably, both of the multispecies-targeting cocktails delayed *E. coli* growth longer than the pathogen-targeting cocktail ($p<0.02$ for T7+P22*vir* and P1+P22*vir*), but were not significantly different from each other ($p=0.43$). Yet, the single phage treatment with the *S. enterica*-targeting phage P22*vir* suppressed *E. coli* equally as long as any of the cocktail treatments ($p>0.17$ for any cocktail) (Fig 3.1b, Table S3.1).

Two possible, but not mutually exclusive, reasons that targeting *S. enterica* suppressed *E. coli* growth longest are 1) that *E. coli* evolved cross-resistance to both phage in the

pathogen-targeting cocktail, reducing its efficacy and/or 2) that *S. enterica* sets coculture growth rate, and that targeting it maximizes suppression of both species including *E. coli*.

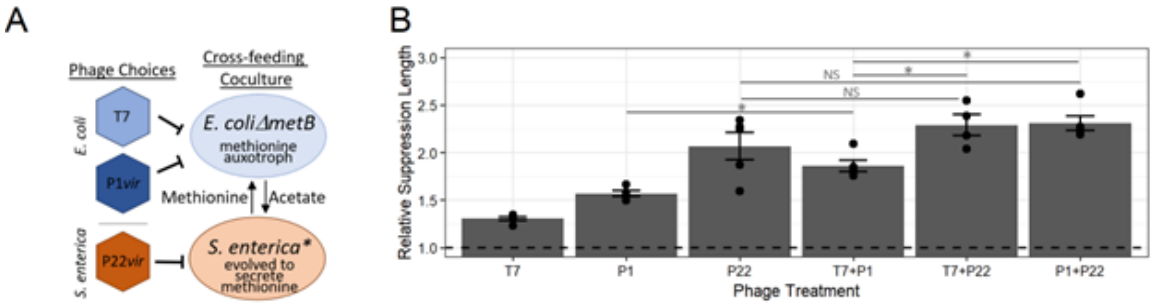

Figure 3.1. Phage cocktail and phage component suppression of cross-feeding microbial community. A) Schematic representation of the wet-lab engineered cross-feeding bacterial system with phage strains. *E. coli* = methionine auxotroph with cyan fluorescent protein, *S. enterica* = methionine secreter with yellow fluorescent protein. **B)** Relative *E. coli* suppression lengths of single and cocktail phage treatments standardized to the no phage control. Suppression length was calculated using 95% maximum cyan fluorescent protein measurement. Permutation statistical tests determined significance. $p>0.1$ (NS), $p<0.05$ (*). Exact p-values are in the text. Bars represent means ± SE (n = 4-5)

We hypothesized that cross-resistance may be one reason why the pathogen-targeting cocktail was less effective than the multispecies-targeting cocktails. Multiple studies have reported that phage cocktails suppress focal bacteria less than expected given single phage treatments, suggesting that evolution of cross-resistance may be common.[3,115,116] To determine if cross-resistance evolved, we measured phage resistance of *E. coli* isolates from each coculture with cross-streak assays. As expected, *E. coli* isolates from phage-free controls were sensitive to both *E. coli* phage (Table 3.1). Additionally, *E. coli* clones treated with a single phage were resistant to that phage, but remained sensitive to phage with which they had not been treated. Half of the *E. coli* clones from pathogen-targeting cocktail treatments evolved resistance to both *E. coli* phage, suggesting that cross-resistance may have evolved in some replicate cocultures. We also observed that all *E. coli* isolates from the pathogen-targeting cocktail treatments evolved mucoid phenotypes, which has previously been shown to cause cross-resistance by a single mutation in various genes involved in lipopolysaccharide production.[92,117–119]

Table 3.1. Resistance profiles and mucoid phenotypes of *E. coli* isolates to *E. coli*-specific phage.

Treatment	T7 Resistant[a] / Total Reps	P1vir Resistant[a] / Total Reps	Mucoid / Total Reps
No Phage	0/5	0/5	0/5
T7[b]	4/4	0/4	0/4
P1vir	0/5	5/5	0/5
T7 + P1vir[b]	2/4	4/4	4/4

[A] representative isolate per treatment replicate was cross-streaked against the indicated phage.

[b] One repeat each of a T7-only treated community and a T7+P1vir-treated community had no detectable *E. coli* at the end of growth and were omitted for phenotyping.

Additionally, we wondered whether the observed resistances to multiple phage were caused by two independent mutations or a single mutation conferring cross-resistance. We predicted how common resistance to both *E. coli* phage would be in populations unexposed to phage (i.e. standing variation of resistance). If resistance to the two *E. coli* phage required different mutations, then the frequency of resistance to both phage is the likelihood that each resistance mutation was acquired individually ($f_{cross\text{-}resistance} = f_{mut1} \times f_{mut2}$). To quantify standing variation of resistance, we compared the number of resistant colonies on a phage-covered plate with the number of colonies on a phage-free plate for each ancestral bacteria.[120] The frequency of resistance to both *E. coli* phage in the ancestral *E. coli* population was ~100-fold larger than predicted if resistance to both phage required two independent mutations (Fig 3.2 - T7+P1vir and red asterisk). These data suggest that the evolution of cross-resistance may be one reason the pathogen-targeting cocktail was less efficacious than the multispecies-targeting cocktail.

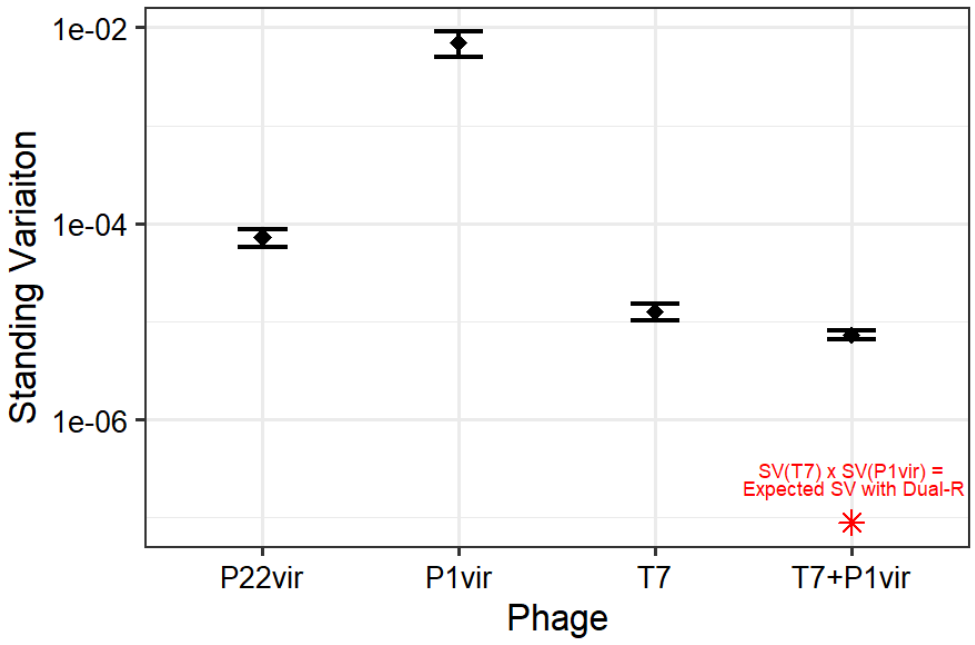

Figure 3.2. Resistance to phage standing genetic variation of ancestral bacterial species previously unexposed to phage. Standing variation frequencies are the number of bacterial colonies on plates with phage standardized to the number of colonies on plates without phage (black diamonds = means ± SE (n = 3)). Expected standing variation if dual-resistance occurred was calculated by multiplying the frequency of standing variation of T7 and P1*vir* (red asterisk).

Cross-resistance cannot explain another result: that a single phage targeting *S. enterica* is just as efficacious at increasing suppression of *E. coli* as any of the best cocktail treatments. A hypothesis which could explain this result is that *S. enterica*'s ability to recover from phage infection in the multispecies-targeting cocktail treatment set the coculture growth response. We tested two possible ways that *S. enterica* could act as a response-setting species: 1) that resistance to *S. enterica* phage was the least likely to evolve (i.e. smallest standing variation of phage resistance), or 2) that low *S. enterica* density caused by phage-mediated lysis delayed *E. coli* growth more than low *E. coli* density delayed *S. enterica* growth (i.e. *S. enterica* is the rate-limiting member of the co-culture).

To determine whether resistance to *S. enterica* phage was less likely to evolve than resistance to *E. coli* phage, we measured the standing variation in phage-free cultures of ancestral bacterial populations, or the frequency of resistance without exposure to phage. If the ability to evolve resistance was the determining factor of cocktail efficacy, then resistance to the *S. enterica* phage P22*vir* should have the lowest frequency of standing variation for resistance. Resistance to P22*vir* was more common than resistance to T7 ($p=0.050$, Fig 3.2) and less common than resistance to P1*vir* ($p = 0.047$, Fig 3.2), suggesting that resistance to T7, not P22*vir*, was hardest to evolve. If the ease of evolving resistance was the sole factor determining cocktail efficacy, then our results suggest that the longest suppression of *E. coli* should be caused by any treatment containing T7 phage. Yet, we observed that treatments including *S. enterica* phage P22*vir* suppressed *E. coli* growth the longest.

Alternatively, physiological differences between *S. enterica* and *E. coli* could cause a different co-culture response to phage. Other studies have illustrated asymmetrical responses of cross-feeding systems to perturbations caused by differences in growth rates or production rates of cross-fed nutrients.[72,121,122] Here, we examined the influence of physiology on co-culture rebound after a population size reduction by manipulating starting coculture frequencies without phage. This manipulation isolated the impact of phage-mediated population size reduction from the impact of phage replication and/or resistance evolution. We started cocultures with either *E. coli* or *S. enterica* at 0.01% instead of 50% of the coculture population and tracked *E. coli* growth as before. We found that reducing the density of *S. enterica* lengthened the time to *E. coli* maximum density more than reducing the starting density of *E. coli* ($p <0.01$, Fig 3.3).

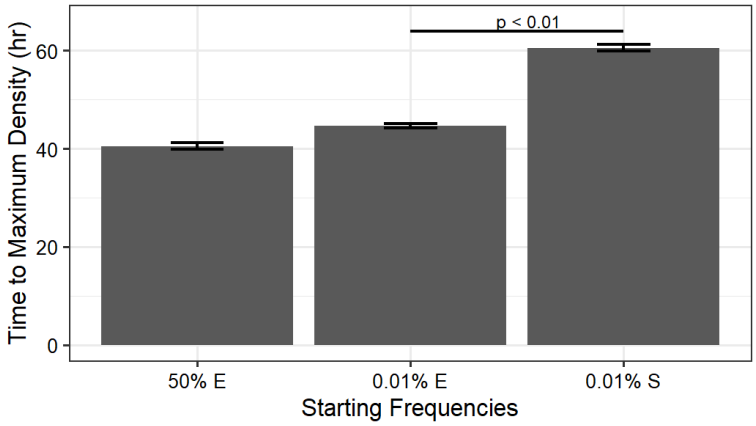

Figure 3.3. Time to maximum *E. coli* density when bacterial starting frequencies were altered in phage-free cocultures. Cocultures were grown as before with different initial starting densities of *E. coli* (E) or *S. enterica* (S). Statistics performed with permutation analysis. Means ± SE (n = 3).

Given that cross-resistance and phage-target identity both influenced the cocktail efficacies, we wondered whether one was more important to consider when predicting outcomes of cocktail treatment. We used a mathematical model to investigate this question. To start, we modified a resource-explicit model of the coculture that simulated the abundance of bacteria, phage, and resources through time (Fig 3.4a).[25] We used model parameters informed by literature values and used wet-lab experiments to measure maximum growth rates (Table S3.2, Fig 3.4b), and confirmed that the model accurately simulated the growth dynamics of the phage-free coculture (Fig 3.4c).[25] Phage-resistant bacteria were seeded in at low frequencies to approximate standing variation for phage resistance. We included two different phage resistance mechanisms and then manipulated phage target identity. Phage resistant mutants were either cross-resistant (resistant to two phage via one mutation) or dual-resistant (resistant to two phage via two independent mutations). The only difference between modeling resistance mechanisms was the doubly-resistant mutants' starting frequencies. For cross-resistance, we seeded in mutants resistant to both phage at a frequency equal to the sum of single resistant

mutant frequencies because resistance to either phage confers resistance to the other. For dual-resistance, doubly-resistant mutants were seeded in at a frequency equal to the product of single resistant mutant frequencies to approximate the likelihood that two independent mutations evolved by chance (Table S3). With this model, we simulated treatment with single phage and cocktail treatments. As expected, cross-resistance to two *E. coli* phage decreased the time to maximum *E. coli* density in pathogen-targeting cocktail treatments and the multispecies-targeting cocktails suppressed *E. coli* better than the pathogen-targeting cocktail when cross-resistance evolved (Fig 3.4d - dark bars). Furthermore, the relative efficacy of the cocktails depended on the resistance type. When we simulated cross-resistance, the multispecies-targeting cocktail was most effective (Fig 3.4d - dark bars); however, when we simulated dual-resistance the pathogen-targeting cocktail was most effective (Fig 3.4d - light bars). These simulations suggest that for our experimental coculture, the evolved resistance type determines which cocktail treatment is most effective. Note though, for both simulated resistance types, the single P22*vir* phage treatments targeting *S. enterica* suppressed communities equally as well as the multispecies-targeting cocktail, suggesting that phage-target identity also contributes to treatment efficacy.

We wanted to know if resistance type was always the determining factor of cocktail efficacy. Others have shown that differences in relative growth rates of cross-feeders change the recovery time from abiotic perturbations.[90,121,123] Therefore, we asked how changing relative growth rates of the cross-feeders altered phage treatment outcomes when simulating both dual- and cross-resistance mechanisms. In our experimental coculture, *E. coli* grows ~1.3x as fast as *S. enterica* (Fig 3.4b, Fig. 3.4e arrow). If we made *S. enterica* grow faster than *E. coli* (left side of fig 3.4e graphs), then the most effective cocktail was the pathogen-targeting cocktail (2E) or the multispecies-targeting cocktail

(1E+1S), depending on the resistance type (Fig 3.4e). Interestingly, the more similar the relative growth rates are, the smaller the differences in efficacy of cocktail treatment strategies. This suggests that targeting the slowest growing cross-feeding partner is important for effective suppression, but predicting which cocktail suppresses the pathogen the longest depends on the evolved resistance type and relative growth rates of cross-feeders.

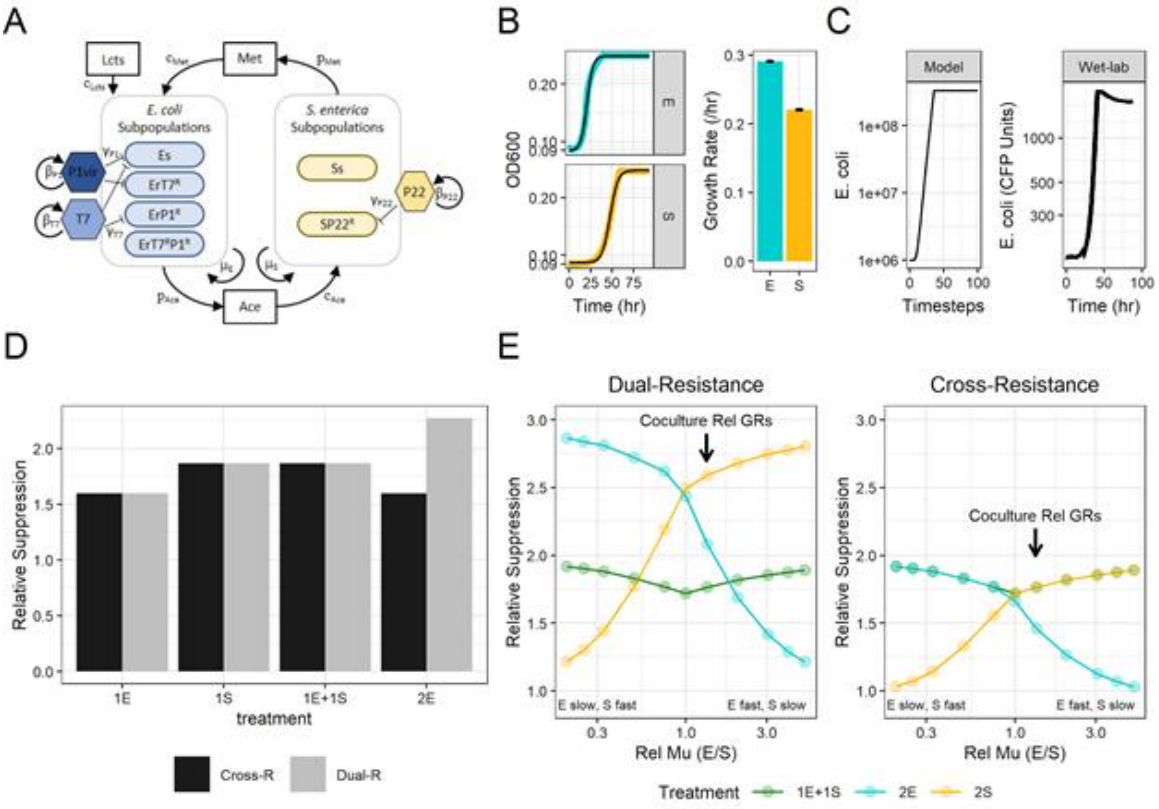

Figure 3.4. Simulations of coculture growth with phage treatments. A) Schematic showing cross-feeding interactions between *E. coli* (E) and *S. enterica* (S) subpopulations. Simulated bacterial subpopulations are listed in species boxes and allowed tracking sensitive (Xs) and phage-resistant (X^R) populations of *E. coli* (E) or *S. enterica* (S). Key tracked metabolites are in boxes. Arrows show direction of interactions. Key model parameters are next to associated arrows: μ_x = maximum growth rate of species X; p_m = production rate of metabolite; c_m = consumption rate of metabolite m; β_v= burst size of phage V; γ_v = adsorption rate of phage V. See Table S2 for details. **B)** Parametrizing bacterial growth rates from wet-lab data. The left panel are representative OD600 growth curves of *E. coli* (blue) and *S. enterica* (yellow) monocultures overlaid with Baranyi growth fits (black lines). The right panel shows calculated growth rates for each species. Bars are means ± SE (n = 5). **C)** Comparison of *E. coli*-specific phage-free coculture growth curves from the model and wet-lab experiments. Y-axis of the model growth curve is the total simulated *E. coli* biomass

and the y-axis of the wet-lab growth curve is measured with CFP fluorescence units. **D)** Relative suppression (time to maximum *E. coli* density relative to phage-free simulations) of either cross-resistance (Cross-R) or dual-resistance (Dual-R) simulations with experimentally determined growth rates. Simulating resistance mechanisms used different starting densities of phage-resistant subpopulations (see text and experimental procedures for details). **E)** Simulation of relative suppression while modulating relative bacterial growth rates under cross-resistance and dual-resistance mechanisms. Simulated phage treatments included multispecies-targeting cocktail (1E+1S - green), pathogen-targeting cocktail of two *E. coli* phage(2E - blue), or partner-targeting cocktail of two *S. enterica* phage (2S - yellow). Arrows indicate the relative growth rates of the experimental coculture measured in panel B. The multispecies-targeting and pathogen-targeting cocktails (green and blue lines) have experimental equivalents.

Discussion

We studied the optimal way to distribute two phage among two obligate cross-feeders to best suppress one focal bacterial species. In laboratory experiments, we found that a multispecies-targeting cocktail suppressed the model pathogen, *E. coli*, longer than pathogen-targeting cocktails. The simplest explanation for this result is that pathogen-targeting cocktails are overcome by a single *E. coli* mutation which confers cross-resistance to both phage. Consistent with this, we found an evolved mucoid phenotype in pathogen-targeting cocktails which did confer cross-resistance. However, we also found that even a single *S. enterica* phage suppressed *E. coli* as well as multispecies-targeting cocktails, which cannot be explained by cross-resistance. We first hypothesized that *E. coli* evolved resistance to T7 more easily than *S. enterica* evolved resistance to P22*vir*. However, resistance to P22*vir* was more common in *S. enterica* populations than resistance to T7 was in *E. coli* populations. An alternative hypothesis was rooted in population ecology: if *S. enterica* was the rate-limiting member of the obligate cross-feeding co-culture, then reducing its population would limit growth longer than a similar reduction to *E. coli*. Experiments without phage, but where initial densities were manipulated, support this hypothesis – a low starting density of *S. enterica* causes longer suppression than a similar low starting density of *E. coli*. Subsequent modeling showed that the cause of this effect was likely the differences in growth rate: *S. enterica* grows

more slowly than *E. coli*, and this slower growth interacted with the population decrease caused by phage to enhance *E. coli* suppression duration. Our results highlight a novel multispecies-targeting strategy for designing phage cocktails when pathogens obligately cross-feed with other bacteria that is affected by relative growth rates and evolved resistance type.

Our most effective cocktail strategy, the multispecies-targeting cocktail, included a phage that infected a nonpathogen, *S. enterica*, that cross-fed with our model pathogen, *E. coli*. This cocktail strategy used the ecological principle that inhibiting one cross-feeding partner effectively inhibits growth of other cross-feeding partners. By leveraging the same ecological principle, our lab previously showed that growth of a cystic fibrosis pathogen, *Pseudomonas aeruginosa*, can be inhibited by targeting its cross-feeding anaerobic partners with antibiotics.[75] While we are not the first to consider using multispecies-targeting cocktails, others have used them with a different goal - to target co-occurring pathogens.[124–128] Additionally, others have explored phage treatment of pathogens in competitive ecological contexts, but limited their analysis to single phage treatments that targeted the focal bacterial species only.[23,47,65,110,111] Our research extended these foundational studies by including both pathogen-targeting and multispecies-targeting cocktails, and by addressing the role of cooperative cross-feeding between a pathogen and another coculture member. We highlight an additional way to leverage microbial ecological interactions to control pathogens.

We identified two independent factors that contributed to increased efficacy of the multispecies-targeting cocktail compared to the pathogen-targeting cocktail. First, the evolution of cross-resistance limited efficacy of the pathogen-targeting cocktail. We avoided this complication by using a multispecies-targeting cocktail strategy in which the individual phage could not infect both *E. coli* and *S. enterica*. Others have suggested

alternative methods to prevent the evolution of cross-resistance. For example, Yu and colleagues designed cocktails with 'guard' phage that inhibit the evolution of phage resistance because they were previously experimentally evolved to infect likely-to-evolve resistant cells.[129] However, many researchers have described multiple rounds of phage-host coevolution suggesting that protection by guard phage may be temporary on an evolutionary time scale, although this has not been tested.[33,130] Others have used molecular techniques to identify phage binding sites and subsequently design cocktails that use multiple binding sites to increase both the number of mutations required for resistance and the cost of resistance.[107] While this would protect against receptor-mediated evolution of resistance, it would not prevent general resistance mechanisms that inhibit phage access to the cell surface, such as the evolution of mucoidy, which we observed when treating the cocultures with the pathogen-targeting cocktail. Yet, others have described phage that degrade this mucoid barrier and facilitate infection by other phage.[131] We identified an additional method for preventing cross-resistance from reducing the efficacy of phage cocktails.

Second, we found that including a phage that targeted the slower-growing cross-feeding partner was key to effectively suppressing pathogen growth. We used mathematical simulations to determine that relative growth rates of the cross-feeding partners altered how effective including a phage targeting the slower-grower was (Fig 3.4e). In fact, inhibiting the slower-grower, *S. enterica*, with a single phage was as effective as inhibiting with the multispecies-targeting cocktails in experiments (Fig 3.1b) and in simulations (Fig 3.4d). Our findings agree with other studies that suggest that changes in relative growth rates of community members,[132,133] particularly cross-feeders[90,134] can alter responses to perturbations. To expand on these foundational studies, we used mathematical simulations to explore how relative growth rates impact the magnitude of response to

perturbations. We found that the more similar the relative growth rates of the cross-feeders were, the smaller the difference in efficacy of cocktail strategies. Conversely, the more different the relative growth rates were, the more benefit we observed in targeting the slower-growing cross-feeding partner. While our simulations suggest that a *S. enterica*-targeting cocktail would be most effective at suppressing *E. coli* if cross-resistance did not evolve (Fig 3.4e), we were unable to test this because our efforts to find a second *S. enterica* phage that replicated in our coculture were unsuccessful (Fig S3.1). Our results suggest that including at least one phage targeting the slower-grower in a cross-feeding coculture is an effective method to extend pathogen suppression. Furthermore, our results indicate that if the relative growth rates of a pathogen and its cross-feeding partner are unknown, adding a nonpathogen-targeting phage could be one way to maximize the odds of inhibiting the pathogen.

A complication in a clinical setting or agricultural application could be that absolute pathogen population size, or pathogen load, may be more critical to treatment outcomes than how long the growth of a pathogen can be suppressed. Here, in two of fifteen communities treated with the T7 *E. coli*-targeting phage either alone or in a cocktail we observed complete eradication of *E. coli* populations and lower final *E. coli* densities in cocultures in which *E. coli* was not eradicated (Fig S3.3). This would indicate that directly targeting the pathogen would be the fastest way to immediately decrease pathogen load. But the rate of resistance evolution would determine how long population sizes are kept low. Our results indicate that including phage targeting cross-feeding partners is one way to limit the recovery of knocked-down pathogen populations. These approaches are not mutually exclusive - phage cocktails could include multiple phage targeting the pathogen, and one or more phage targeting its cross-feeding partner.

An alternative method for targeting multiple species in a community is with polyvalent phage treatment, or phage with host ranges that encompass multiple species. Descriptions of polyvalent phage have increased over the past five years likely due to directed changes in phage isolation protocols.[135–137] In fact, Zhao and colleagues used a soil-carrot microcosm system to compare the efficacy of a cocktail that included phage targeting two different plant pathogens with a treatment of a single polyvalent phage that infected both pathogens.[128] They found that both treatments effectively limited the growth of both pathogens, but the polyvalent phage treatment disturbed the soil microbiome less than the multipathogen-targeting cocktail. Some challenges with using polyvalent phage might include differences in host preference based on receptor-phage binding strength. If binding strength were different enough, the polyvalent phage should function like a phage that targeted a single species. However, one benefit is that phage populations could grow faster because more hosts would be available, although no studies have directly tested this yet. We suggest that future research could test including polyvalent phage with different cocktail strategies.

In conclusion, we have illustrated a novel phage cocktail strategy for targeting cross-feeding pathogens. Our strategy limits cross-resistance evolution and maximizes pathogen suppression by targeting both the slower-growing partner and the pathogen. These and other results indicate that leveraging microbial community ecological interactions is a promising approach to help control pathogen growth in a variety of applications in human health, agriculture, and food safety.

Experimental Procedures

Bacterial and Phage Strains in the Cooperative Co-Culture System

The bacterial strains used in this experiment have been previously described (Fig 3.1A).[77] Briefly, the *E. coli* K12-derivative has a *metB* deletion and cyan fluorescent protein (CFP) in the attB lambda integration site. *S. enterica* is an LT2 strain with mutations in *metA* and *metJ* causing methionine secretion and yellow fluorescent protein (YFP) in the *attB* lambda integration site.[138,139] *E. coli* metabolizes lactose and excretes acetate which *S. enterica* consumes. *S. enterica* excretes methionine which is used by *E. coli*. Bacterial stocks were stored at -80°C in 20% glycerol. *E. coli*-specific phage T7 and P22*vir* were provided by Ian Molineaux (UT Austin) and *S. enterica*-specific P1*vir* by Ross Carlson (Montana State University). Phage stocks were grown on monocultures of ancestral *E. coli* or *S. enterica* in lactose or acetate minimal medium at 30°C. Cells were lysed with chloroform, centrifuged to pellet cell debris, and stored at 4°C.

Monoculture and co-culture experiments used a defined minimal medium (14.5 mM K_2HPO_4, 16.3 mM NaH_2PO_4, 0.814 mM $MgSO_4$, 3.78 mM Na_2SO_4, 3.78 mM $(NH_4)_2SO_4$) supplemented with trace metals (1.2 μM $ZnSO_4$, 1 μM $MnCl_2$, 18 μM $FeSO_4$, 2 μM $(NH_4)_6Mo_7O_{24}$, 1 μM $CuSO_4$, 2 mM $CoCl_2$, 0.33 μM Na_2WO_4, 20 μM $CaCl_2$) as described.[103] Carbon sources were 2.78 mM D-lactose or acetate, as indicated. Monocultures of *E. coli* were supplemented with 20μM L-methionine.

Measuring E. coli Suppression in the Cross-Feeding Co-Culture

Bacterial growth at 30°C was tracked every 20 min with OD600 and fluorescence measurements using a shaking plate reader (Tecan Infinite ProM200). *E. coli* was measured with CFP (Ex: 430 nm; Em: 490 nm), and *S. enterica* with YFP (Ex: 500 nm; Em: 530 nm). We used four - five replicates of each treatment, as indicated. To wells in a 96-well plate, 10^5 cells each of mid-log phase *E. coli* and *S. enterica* were inoculated into 200μL of lactose minimal media with $5x10^2$ virions as indicated (MOI = 0.05 per phage).

Cultures incubated for 5 days until stationary phase was reached. *E. coli* suppression length in hours was estimated by calculating the time to 95% maximum CFP measurement.

Profiling Resistance to Phage via Cross-Streak Assays

To assay for acquired phage resistance, we used cross-streak assays with representative isolates from treatments. 30µL of ancestral phage stock (10^8 to 10^9 PFU/mL) was dripped down a minimal medium agar plate and left to dry. Overnight cultures of isolates grown in minimal medium were streaked perpendicular to the phage. Plates were incubated at 30°C until growth was visible. Isolates were determined to be resistant if streaks were uniform across the phage line and sensitive if bacterial growth was interrupted.

Resistance to Phage due to Standing Variation in Ancestral Bacterial Stocks

To determine frequency of phage resistance of ancestral bacteria, we quantified the number of cells that grew on phage-saturated agar plates. Ancestral *E. coli* and *S. enterica* monocultures were grown in lactose + methionine or acetate minimal media, respectively, for 3 days at 30°C. LB plates were saturated with 1ml of ancestral phage stock (~$1x10^9$ PFU/mL), dried, and spotted with 5µl of bacterial monocultures in 10-fold dilutions. Plates were incubated at 30°C until phage-resistant colonies were counted. We compared the number of colonies of plates with and without phage for each phage-host combination.

Assessing the Effect of Starting Frequency of Microbial Partners on Coculture Growth

We tested the time to maximum density of *E. coli* in the coculture when starting frequencies were altered in the absence of phage We started the rare partner of cocultures at 0.03% while holding the common species at 10^5 cells/well in lactose minimal medium

(n=5). Community growth was as described above (see Methods: *Measuring Experimental Cross-Feeding…).*

In silico Modeling of Communities

To represent our cross-feeding microbial community, we modified a series of resource-explicit ordinary differential equations to simulate an *E. coli* and *S. enterica* cross-feeding system in which one species grows on nutrients secreted by the other.[25] We used Monod equations with multiplicative limitation of lactose and methionine essential nutrients for *E. coli*. The model mimics the metabolic network of the synthetic experimental coculture.

The major metabolites – lactose, acetate, and methionine – are tracked throughout simulations. Lactose is seeded in and is depleted as *E. coli* grows. Acetate is produced by *E. coli* growth, and is depleted by *S. enterica* growth. Methionine is produced during *S. enterica* growth, and is depleted during *E. coli* growth. Simulated cocultures grow until all lactose is consumed.

Each species has multiple genotypes to simulate resistance to different phage, with the amount seeded in representing mutation rarity. Resistant genotypes had founder population sizes at a maximum of 0.1% of the sensitive genotype to simulate rare resistance. *E. coli* had four genotypes: Es for sensitive to both phage, ErT7 for resistant to only T7, ErP1 for resistant to only P1*vir*, and ErT7P1 for resistant to both phage. *S. enterica* had two genotypes: Ss for sensitive to P22*vir*, and Sr for resistant to P22*vir*. Resistance was modeled as complete and without cost. The replication of each phage strain– T7, P1*vir*, and P22*vir* – was determined by adsorption rates and burst sizes. Each phage species can only kill sensitive genotypes of a single bacterial species. Model parameters are informed by literature values and were parameterized to approximate coculture growth dynamics without phage (Fig 3.4, Table S3.2).[25] Bacterial growth rates

were measured from wet-lab monoculture experiments (*E. coli* grown in lactose + methionine and *S. enterica* grown in acetate) where OD600 was measured every 20min. Growth curves were fit with a non-linear least-squares Baranyi function of the growth rate parameter, as described.[104]

Figure 3.4 shows a schematic representation of the following equations and parameters.

E. coli (E) growth:

$$\frac{dEs}{dt} = \mathrm{Es} * \mu_{\mathrm{E}} * \frac{\mathrm{Lcts}}{\mathrm{Lcts} + \mathrm{k}_{\mathrm{ELcts}}} * \frac{\mathrm{Met}}{\mathrm{Met} + \mathrm{k}_{\mathrm{EMet}}}$$

S. enterica (S) growth:

$$\frac{dSs}{dt} = \mathrm{Ss} * \mu_{\mathrm{S}} * \frac{\mathrm{Ace}}{\mathrm{Ace} + \mathrm{k}_{\mathrm{SAce}}}$$

Population sizes (E or S) are multiplied by their species-specific growth rates per hour (μ_x) and a Monod saturation function with a species and resource explicit constant (k) for each necessary resource. During phage infection, cell lysis is simulated. For example, when P1vir infects an *E. coli* that is only T7-resistant:

$$\frac{dErT7}{dt} = \left(ErT7 * \mu_{\mathrm{E}} * \frac{\mathrm{Lcts}}{\mathrm{Lcts} + \mathrm{k}_{\mathrm{Elcts}}} * \frac{\mathrm{Met}}{\mathrm{Met} + \mathrm{k}_{\mathrm{EMet}}}\right) - (Es * P1 * Adsorption\ Constant)$$

New phage are added with host death:

$$\frac{dP1}{dt} = P1 * Burst\ size * ErT7 * Adsorption\ Constant$$

E. coli, *S. enterica*, and phage equations are repeated for each individual genotype and phage.

Simulations were run in R with the DeSolver package, using the LSODA solver.[102]

Acknowledgements

We would like to thank Sarah P. Hammarlund, Harcombe Lab members, and the UMN Institute for Molecular Virology community for useful discussions. L. Fazzino was supported by a Fellowship from the Institute for Molecular Virology Training Program (NIH T32 AI083196). Research was also supported through the NIH (GM121498-01A1, to William Harcombe). The authors declare no conflict of interest.

Chapter 4

Impacts of phage infection and cross-feeding interactions on rates of adaptation in an experimentally-evolved synthetic coculture

See Appendix 4 for supporting figures and tables.

Lisa Fazzino[a,b] and William R. Harcombe[b,c]

[a] Department of Microbiology and Immunology, University of Minnesota, Minneapolis, MN, USA

[b] BioTechnology Institute, University of Minnesota, Saint Paul, MN, USA

[c] Department of Evolution, and Behavior, University of Minnesota, Saint Paul, MN, USA

Summary

Microbial communities experience multiple evolutionary pressures at the same time. Two such pressures are predation pressure from bacterial viruses (phage) and maintenance of ecological interactions, like mutualistic cross-feeding. Two ecological theories, the 'Red Queen' and the 'Red King' hypotheses predict that phage infection will increase rates of adaptation while cross-feeding will decrease rates of adaptation. We completed an experimental evolution with a cross-feeding synthetic system of *Escherichia coli* and *Salmonella enterica* that was exposed to an *E. coli*-specific phage and quantified changes in rates of adaptation with phenotypic- and genomic-based measurements. After 20 batch culture transfers, we found marginally increased rates of adaptation caused by phage infection and marginally decreased rates of adaptation caused by cross-feeding, but no interaction between the two evolutionary pressures. Furthermore, we found almost no mutational signature of either evolutionary pressure, indicating a lack of convergent evolution. We suggest that evolutionary pressures that supposedly are opposing might in fact function independently in a cross-feeding community context.

Introduction

In microbial communities bacteria interact in diverse ways with other bacteria and with viruses known as bacteriophage (phage). Biotic interactions can generate strong selection pressures;[42,76] however, it remains unclear how multiple types of biotic interactions (e.g. antagonistic and mutualistic) combine to influence evolutionary processes.[140] Here, we use a synthetic microbial coculture to explore how multiple biotic evolutionary pressures influence evolution in microbial communities. Specifically, we investigate how a mutualistic interaction—cross-feeding of exchanged essential nutrients—and a predator-prey interaction—phage infection—impact rates of adaptation in a synthetic bacterial coculture.

Phage infection and cross-feeding are individually predicted to have opposing effects on the rate of microbial adaptation. By comparing the Red Queen and Red King theories that can address how antagonistic or mutualistic interactions alter rates of adaptation respectively, we can hypothesize evolutionary outcomes that could result from communities simultaneously experiencing phage infection and cross-feeding evolutionary pressures. Van Valen's 'Red Queen Effect', when applied to a phage-host system, hypothesizes that antagonistic arms races govern the evolution of phage-bacterial interactions and result in never-ending and fast evolutionary cycles.[42–44] Accelerated rates of adaptation in the presence of phage increases the likelihood that hosts evolve resistance to current parasites and persist over evolutionary time with counter adapting, or coevolving, phage. In contrast, Bergstrom and Lachmann's 'Red King Effect', theorized that mutualists, such as cross-feeding bacteria, have slower rates of adaptation which results in advantageous maintenance of mutualism and enhanced exchange benefits.[76] When selection pressures from both phage and bacterial cross-feeding partners are simultaneously present, their effects may simply be additive and cancel out, or the interaction between these selective pressures could change the impact of one in the presence of the other.

Rates of adaptation have been measured through both phenotypic and genomic approaches. Phenotypic-based methods of measuring rates of adaptation are varied and depend on which selection pressure is being applied to a system. For example, Adamowicz and colleagues quantified changes in antibiotic resistance over time (rate of adaptation) of a coculture and found that cocultures with obligate cross-feeding interactions adapt more slowly than monocultures.[141] In comparison, genomic-based

measurements of rates of adaptation frequently use whole-genome sequencing of evolved isolates or populations to calculate the number of DNA base-pair changes over time when exposed to a selection pressure. For example, Betts and colleagues used whole genome sequencing of evolved phage-resistant isolates to suggest that rates of adaptation increase with antagonistic phage-host interactions compared to phage-free cultures.[114] Here, we use a combination of phenotypic- and genomic-based measurements to quantify rates of adaptation.

In this study, we determined the impacts of phage infection and cross-feeding on rates of adaptation by introducing phage into a synthetic cross-feeding system.[25,77,138,139] The bacterial system involves an *Escherichia coli* auxotrophic for methionine that produces carbon (acetate and galactose) consumed by a methionine-secreting *Salmonella enterica* strain (Fig. 4.1). We performed experimental evolution of *E. coli* monocultures and cross-feeding cocultures with and without *E. coli*-specific T7 lytic phage. After 20 batch culture transfers, we tested for differences in rates of adaptation with a combination of phenotypic assays and genomic-based measurements using whole genome sequencing of entire communities. We found that phage and bacteria co-existed throughout the experiment and that *E. coli* evolved mucoid phenotypes in the presence of T7 phage in monoculture and coculture. Furthermore, rates of adaptation trended toward an increase in the presence of phage (as predicted by the Red Queen hypothesis) and toward a decrease when hosts were cross-feeding (as predicted by the Red King hypothesis). We hypothesize that supposedly opposing evolutionary forces might, in fact, act independently in certain environmental conditions.

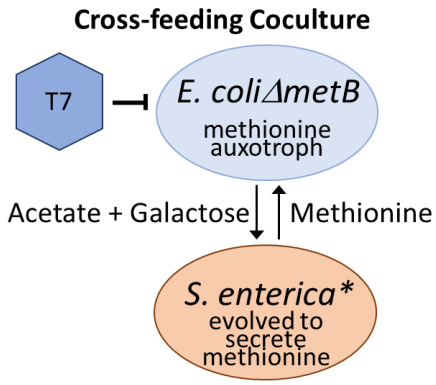

Figure 4.1. Synthetic cross-feeding coculture system. *E. coli* auxotrophic for methionine (blue) exchanges acetate and galactose for methionine with methionine-secreting *S. enterica* (orange). T7 phage (blue hexagon) can infect *E. coli*.

Results

Phage and host are stably maintained in experimental evolution of a cross-feeding coculture.

As a first measure of adaptability, we determined whether all three organisms were maintained throughout experimental evolution. We might expect to observe extinctions. Slow adaptation of *E. coli* or T7 could result in loss of one of these populations, if either the bacteria did not evolve resistance or the phage did not evolve around resistance rapidly enough.[31] Similarly, rapid evolution of 'cheater' bacteria that do not provide nutrients but still use exchanged nutrients, has been shown to cause extinction of cross-feeding populations.[77] We observed that all populations were maintained throughout the evolution experiment in each replicate (Fig. 4.2). Plating for plaques showed that T7 phage were maintained at a minimum of ($2x10^4$) PFU/ml in both monoculture and cross-feeding scenarios (Fig. 4.2b). Furthermore, selective plating showed that *E. coli* hosts (Fig. 4.2a) and *S. enterica* cross-feeding partners (Fig. 4.2c) were also maintained. Plating results were consistent with OD600 measurements of the whole community (Fig. S4.1), indicating that no communities experienced long-term population crashes or extinctions.

Although all three organisms were maintained, their population dynamics were not the same across all treatments. It appears that T7 phage-containing *E. coli* monocultures only reached maximum carrying capacity in the last two transfers of the experiment. However, the phage-containing cross-feeding coculture reached maximum carrying capacity much earlier. In addition, phage treatments appeared to increase variability of *E. coli* and T7 population sizes, but not of *S. enterica* (Fig. 4.2 – pale lines).

E. coli *mucoid phenotype sweeps phage-containing monocultures and cocultures.*

As a phenotypic measure of rate of adaptation, we tracked the emergence of mucoid phenotypes over time by plating. We and others have shown that mucoid phenotypes evolve in response to phage infection and confer varying levels of resistance to phage infection.[25,34,92] Here, we classified individual colonies as mucoid or non-mucoid (Fig. 4.3a). Mucoid *E. coli* phenotypes evolved only in response to phage infection and swept to fixation (i.e. 100% frequency) within three transfers in phage-containing monocultures and in cocultures (Fig. 4.3bc). However, the frequency of mucoidy appeared higher after the first passage in phage-containing monocultures than phage-containing cocultures, but was not statistically-significant (Fig 4.3b, p=0.089).

Rates of bacterial adaptation trend toward faster during phage infection and slower during cross-feeding.

Given the phenotypic signature of adaptation to phage, we explored whether genomic-based measures of adaptation rates differed between treatments. To determine if phage infection or cross-feeding changed the number of mutations—a genomic-based proxy for rate of adaptation—that were acquired during evolution, we sequenced entire communities at the end of the experiment for the *E. coli* (E), *E. coli* + T7 phage (E+T7), *E.*

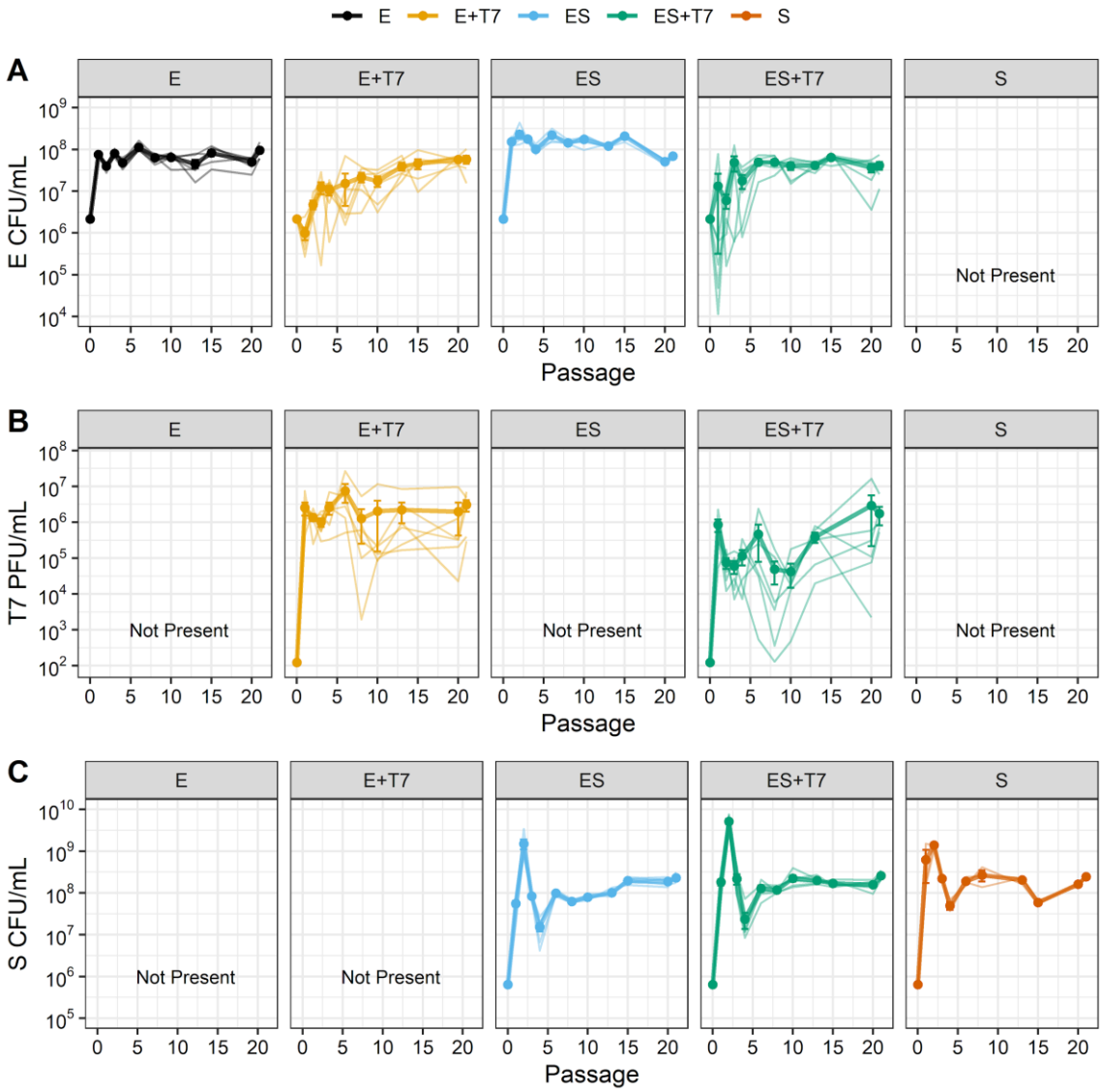

Figure 4.2. Ecological dynamics of community members over time. A) *E. coli* CFU/ml, **B**) T7 PFU/ml, and **C**) *S. enterica* CFU/ml population sizes over time measured with selective plating. Dark points and thick lines represent the mean population density ± SE (n=6, except for S treatment where n=3). Treatment abbreviations: E = *E. coli* only, E+T7 = *E. coli* + T7 phage, ES = *E. coli* + *S. enterica*, ES+T7 = *E. coli* + *S. enterica* + T7 phage, S = *S. enterica* only. Light thin lines show individual replicates. "Not Present" indicates that plating resulted in zero colonies or plaques.

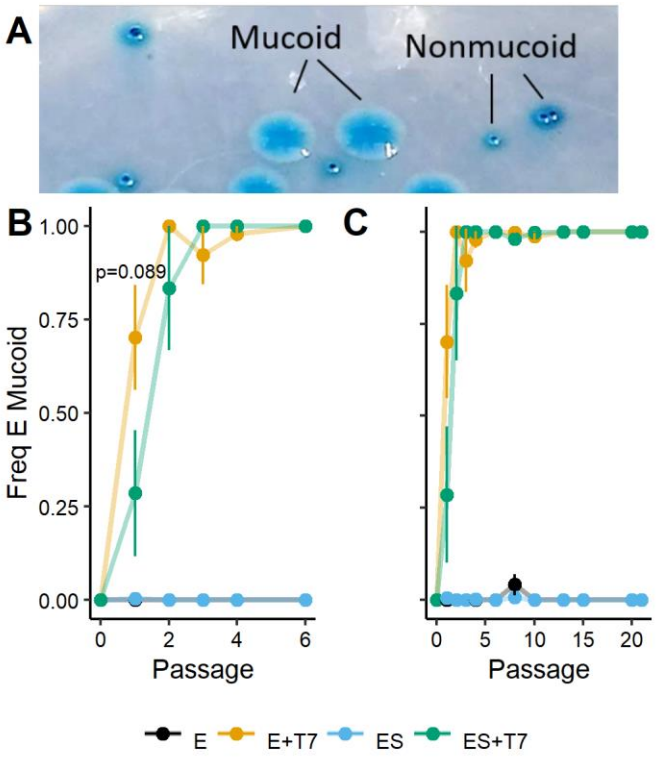

Figure 4.3. Rise of mucoid *E. coli* phenotypes over time. A) An example of mucoid and non-mucoid colonies from a single mixed community on an *E. coli* selective plate (lactose + methionine + Xgal). **B)** Frequency of mucoidy in the first 6 passages, and **C)** all 20 passages. Mucoid *E. coli* sub-populations swept to fixation only in the E + T7 and ES + T7 treatments. Mean frequency of mucoid *E. coli* isolates ± SE was determined by plating periodically during the experimental evolution (n=6). Statistical significance at passages 1 was determined by a t-test.

coli + *S. enterica* (ES), *E. coli* + *S. enterica* + T7 phage (ES+T7) (n = 6 per treatment), and *S. enterica* (S, n = 3). Using *breseq*, a whole genome mutational analysis tool, we identified all mutations that accumulated throughout experimental evolution in the three organisms. We identified ancestral mutations for each organism and mutations that likely resulted from selective pressure of culturing methods (e.g. medium choice, oxygen levels in shaking tubes, etc.) with two different methods (Table 4.1). We also filtered for mutations that reached >25% frequency in at least one replicate community. After mutation curation, the two different filtering methods resulted in largely the same number of mutations identified (Table 4.2, Fig. S4.2). We analyzed the remaining mutations, which should represent responses to either T7 phage infection or maintenance of cross-feeding,

although genetic drift could also influence mutations that arose. For simplicity, we present the "N-2" filtering method results in the main text, but using an alternative filtering method ("75% reps & 90% freq") did not qualitatively affect results (Fig. S4.3).

Table 4.1. Ancestral filtering method descriptions.

Ancestral Filtering (Short Name)	Ancestral Mutation Criteria
N-2 communities (N-2)	A mutation was identified in a minimum of two fewer communities than the total number of communities in which an organism was included (e.g. 24 sequenced communities had *E. coli*, a mutation identified in 22 or more communities was identified as ancestral).
75% replicate communities and 90% frequency (75% reps & 90% freq)	A mutation was identified in 75% of expected communities and rose to at least 90% frequency in all communities in which it was identified.

Table 4.2. Number of mutations identified at each stage of ancestral filtering.

Genome	# Raw Muts	# Ancestral Mutations			# Mutations		# Functional Mutations [A]		# Considered Mutations [B]		
		N-2	75% reps + 90% freq	N-2 + manual curation	N-2	75% reps + 90% freq	N-2	75% reps + 90% freq	N-2	75% reps + 90% freq	N-2 + manual curation
E	2513	213	41	355	2300	2200	322	222	274	174	142
S	3415	1253	1197	1279	2162	2308	87	140	71	100	49
T7	236	32	136	32	204	204	123	123	121	121	121

[A] Functional mutations = mutations (SNPs , indels, and intergenic regions) that are not synonymous and arose to 25% frequency in at least one community in which the mutation was found

[B] Considered mutations = functional mutations in which sequencing quality has been manually confirmed

To determine how phage infection and cross-feeding affected rates of adaptation, we compared the number of mutations that accumulated in each genome over 20 passages, a proxy for adaptation rate, among treatments. We found that more *E. coli* mutations occurred in cultures that contain phage regardless of monoculture or coculture status ($F(1,21)=3.20$, $p=0.088$), and that fewer *E. coli* mutations evolved in cocultures regardless

of phage status (F(1,21)=3.20, p=0.088), although these trends were not statistically significant (Fig. 4.4a, S4.3a). We also found that the number of *S. enterica* mutations was significantly larger when cocultured with phage than in phage-free cocultures for N-2 ancestral filtering method (F(1,12)=5.023, p=0.044)(Fig. 4.4b, S4.3b). In contrast, there was no statistically significant difference in the number of mutations that accumulated in the *S. enterica* genome as a response to cross-feeding (F(1,12)=0.11, p=0.74) or in the number of accumulated T7 mutations of monocultures or cocultures containing phage (T=1.09, p=0.31)(Fig. 4.4bc, S4.3bc).

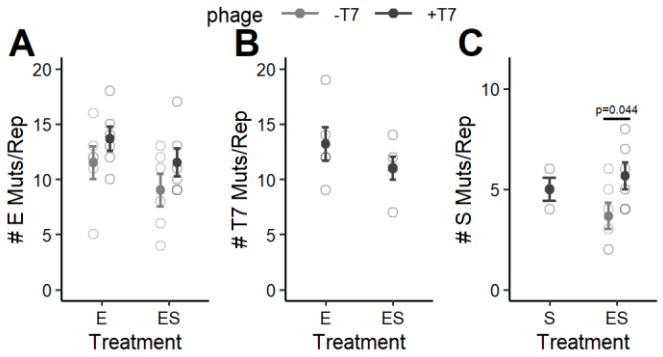

Figure 4.4. Number of mutations per replicate community after 20 passages. Mutations were filtered with N-2 method and the total number of mutations per replicate community (# Muts/Rep) in the A) *E. coli* (E) genome, B) T7 phage (T7) genome, and C) *S. enterica* (S) genome were calculated. Light grey points = number of mutations in individual replicate communities, black points = mean number of mutations ± SE (n=6, expect S treatment where n=3). See Methods for statistics details.

Weak clustering of mutational profiles detected from phage and cross-feeding treatments indicating non-convergent evolution.

We tested for mutational signatures, and therefore parallel (convergent) evolution, from either cross-feeding or phage treatment with hierarchical clustering of mutations for each genome. Hierarchical clustering is an unsupervised algorithm that determines if samples can be grouped together based on similarity of, for example, mutations (refs). If evolved

mutations were driven by phage infection, then phage-containing monocultures should be more similar to phage-containing cross-feeding cocultures than phage-free monocultures. Clustering tendency was tested for with the Hopkins statistic (*H)* where 0.5 represent no clustering and 0 or 1 represent strong clustering. All three genomes showed weak clustering tendencies ($0.59 \leq H \geq 0.71$) (Fig. 4.5). This was also evident from a visual assessment of clustering tendencies (VAT) that showed limited block structure, which should have been present if there was strong similarity among samples within a treatment (Fig. S4.4). To illustrate the lack of clustering, we calculated Bray-Curtis dissimilarity of genome for each sample to capture differences in both the presence/absence and frequency of mutations among samples.

If there was strong convergent evolution within treatments, then we would have expected treatments to cluster together in a dendrogram, which would have indicated sample similarity. However, we did not observe strong treatment clustering as samples of the same treatment (indicated by color) are not necessarily found in the same cluster, in agreement with the *H*-statistic and VAT analysis (Fig. 4.5, Fig. S4.4).

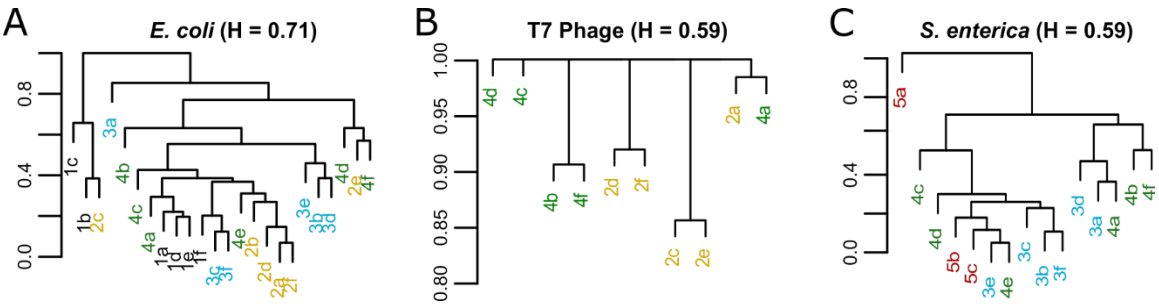

Figure 4.5. Dendrogram of hierarchical clustering analysis of each organism. A) Mutations in *E. coli* genomes only were analyzed. **B)** Mutations in T7 phage genome were analyzed. **C)** Mutations in *S. enterica* genomes only were analyzed. Dissimilarity matrix was calculated with Bray-Curtis distances and hierarchical clustering performed with the "complete" method. *H* = Hopkins statistic to measure clustering tendency. Labels represent communities. letters =

replicates and numbers = treatments. 1 (black) = *E. coli* monoculture, 2 (yellow) = *E. coli* + T7, 3 (blue) = *E. coli* + *S. enterica*, 4 (green) = *E. coli* + *S. enterica* + T7, 5 (red) = *S. enterica* monoculture.

Discussion

We studied how phage infection and cross-feeding interactions influence long-term dynamics of coexistence and rates of adaptation in a synthetic coculture. We found that during a batch culture evolution experiment, phage and bacterial hosts coexisted for all 20 transfers in monoculture and cocultures (Fig. 4.2), and that *E. coli* evolved mucoid phenotypes in response to T7 phage infection (Fig. 4.3). Despite these phenotypic differences in phage-containing and phage-free treatments, we found weak trends of differences in rates of adaptation caused by phage or cross-feeding treatments (Fig. 4.4), but no distinct mutational profiles (Fig. 4.5, Fig. S4.4). In general, phage infections tended to increase rates of adaptation while cross-feeding tended to decrease rates of adaptation, which is consistent with the Red King theory and Red Queen theory predictions. Our results suggest that supposedly opposing evolutionary forces (phage = faster, cross-feeding = slower) can have independent effects on rates of adaptation and that a diverse set of mutations may drive these differences, resulting in weak signatures at the mutation level.

We observed tendencies toward faster rates of adaptation caused by phage treatment and slower rates of adaptations caused by cross-feeding interactions. Continued evolution would likely amply these trends as more mutations accumulated in genomes. These trends support both the Red Queen hypothesis of antagonistic parasite-host interactions and the Red King hypothesis for constraining effects of mutualism. Although it could have been hypothesized that Red Queen and Red King effects would cancel out each other and leave rates of adaptation unchanged, we saw weak effects of both phage and cross-

feeding. Analyzing the total number of mutations that accumulated over the entire evolution experiment does not take into account the fact that *E. coli* populations sizes were smaller in phage-containing treatments than phage-free treatments, meaning that fewer cellular divisions occurred in which to acquire mutations. Standardizing to the number of cellular divisions would likely amplify the impact of phage on the number of *E. coli* mutations. This suggests that predation and cross-feeding had opposing effects but independent effects on evolutionary rates, although an alternative interpretation may be that since effects on rates of adaptation were weak, that the phage and cross-feeding evolutionary pressures did partially diminish the effects of each other.

We observed a weak decrease in rates of adaptation due to cross-feeding interaction – as hypothesized by the Red King Effect. A similar effect of slower evolution when cross-feeding has been shown in cross-feeding cocultures adapting to antibiotic pressures.[141] However, others suggest that mutualisms - especially symbionts with vertical transmission - adapt faster than monocultures.[72,140,142–146] The effect of vertically transmitted symbiosis-based mutualisms may be different from cross-feeding based mutualism as the partner feedback is stronger with physically-connected species. In addition, rapid evolution of cross-feeding between previously non-interacting bacterial species[140] and of the ability to recover from strong bottleneck pressures[72] has been reported. One interpretation could be that there is a distribution of effects on rates of adaptation caused by cross-feeding that may be, on average, slow, but need not always be so.

Although we did not detect significant changes in rates of adaptation caused by phage, we did observe a striking phenotypic response to phage treatments - the evolution of mucoidy. We hypothesized a larger mutational signature from the combination of cross-

feeding and phage treatments because those evolutionary pressures have significantly different predicted selection targets. For example, mutations in phage tails or host cell surface receptor structures that mediate phage entry are often targets of adaptation during phage infection,[9,147] while mutations to genes that enhance partner fidelity,[77,86,148] or minimize costs of mutualisms through compensatory mutations[149] are likely to evolve in response to cross-feeding. Yet, despite the large phenotypic difference in phage-containing and phage-free cocultures, there was a weak mutational signature of convergence within phage treatments when measured with Hopkin's statistic and hierarchical clustering. There may be a diverse set of mutations that result in a mucoid phenotype, thereby eliminating the signal of convergent evolution at the level of mutations. This hypothesis is supported by the sparseness of our mutation data set - we identified 207 mutations with N-2 ancestral filtering, but only 43 occurred in two or more community replicates, indicating that most mutations only evolved in a single community (Table S4.2). Perhaps higher-order clustering analysis, such as at a pathway-level, would reveal stronger convergent evolution.

Mucoidy, an excess of exopolysaccharide, is a frequently observed evolutionary response that confers resistance to phage infection in multiple systems (refs), including our cross-feeding system.[25] Our results suggest that mucoidy may facilitate coexistence of phage and bacterial hosts, as suggested by others.[34] Previously, we observed that mucoid *E. coli* isolates that evolved in a single growth curve in response to T7 phage infection were partially-resistant to phage infection. We hypothesize that partial resistance results in enough phage replication for phage to survive the dilution in a batch culture evolution experiment, allowing long-term coexistence. While this could be interpreted to imply that Red Queen dynamics were not at play because phage were 'good enough' at infecting

mucoid cells to survive and might not be under strong selection, we identified numerous mutations identified in phage tail proteins – genes associated with host recognition (e.g. gene 19 - tail fibers). We suggest these mutations, which are not conserved across communities, are a signature of coevolution between phage and *E. coli* hosts in response to partial resistance. Others have described coevolutionary Red Queen dynamics for partial, not full, resistance and infectivity coevolution in plant-pathogen systems.[150]

We also observed differences in the variation of population sizes in phage-containing cocultures. *E. coli* and T7 population sizes were more varied across replicate communities than *S. enterica* population sizes. Our previous work suggested that the cellular contents released during phage lysis of partially-resistant mucoid *E. coli* could support *S. enterica* growth.[25] Others have described similar effects[2,52,89,151]. We hypothesize that the consumption of cellular debris released by phage lysis of cross-feeding partners impact community composition on an evolutionary timescale. In fact, *S. enterica* appears to benefit from T7 infection of *E. coli* throughout the evolution experiment, perhaps with diminishing effects, which may have complicated feedback mechanisms on *E. coli* growth (Fig. S4.5).

In conclusion, we showed long-term coexistence of phage and hosts in cross-feeding communities. Using phenotype-based and genomic-based measurements, we showed that rates of adaptation were marginally increased during phage infection and marginally decreased when engaged in cross-feeding. We suggest that evolutionary forces that at first glance appear in opposition might in fact work independently when different mutational targets are likely.

Methods

Bacterial and phage strains. Ancestral strains of bacteria and phage are previously described.[25,77,138,139] Briefly, ancestral *E. coli* (Eo) is a K12 BW25113 *metB::kan* methionine auxotroph derivative from the Keio collection[152] in which the lactose operon has been reinserted by transduction. The ancestral *S. enterica* strain (So) was evolved from *S. enterica* LT2 to secrete methionine in a two-step process on agar plates.[77] Ancestral T7 phage stock was provided by I. J. Molineaux. All bacteria and phage strains were stored at -80°C.

Experimental coevolution - tracking population dynamics and mucoid phenotypes. Bacterial and viral combinations were grown in 3ml of minimal hypho medium[103] supplemented with carbon and methionine as indicated in a 15ml 16mm glass tube at 30°C, shaking. For E, E + T7, ES, and ES + T7 treatments, six replicate communities were used. For S and S + T7 treatments, three replicate communities were used. The S + T7 treatment was stopped following 2 consecutive transfers because there was no detectable T7 phage. Every three days, cultures were transferred with a 1:101 dilution scheme (30μl culture into 3ml fresh media) for a total of 20 transfers. At each transfer, OD600 was read with a TecanPro shaking plate reader. Also, at each transfer, cultures were frozen in a 1:4 dilution with 80% glycerol and stored at -80°C for later analysis. For some transfers, cultures were plated on selective media to count CFUs of *E. coli* (lactose + methionine + Xgal) and *S. enterica* (acetate + Xgal). In addition, T7 phage PFUs were plated by making a phage lysate with the addition of chloroform and centrifugation, and plated on 0.3% LB top agar with ancestral *E. coli*. Phage lysates were also frozen as described above for subsequent analysis. CFU plates were incubated at 30°C until countable colonies were

visible (2-4 days), and PFU plates were incubated at 37°C until plaques were visible (12-24 hours). *E. coli* colonies were also tracked for mucoid phenotypes by plating.

Whole genome sequencing. We sequenced whole-community samples of each replicate at the end of growth of the 20 transfers. DNA from each replicate community was isolated with Zymo Quick-gDNA Miniprep Kit (11-317C) from 0.3ml of frozen glycerol stock. Illumina sequencing libraries were prepared according to the Nextera XT DNA Library Prep Kit protocol. All samples were sequenced using NEXTSeq platform 2x150 paired-end reads by the University of Minnesota Genomics Center. Following sequencing, we trimmed samples with TrimGalore with --paired and --nextera options (version 0.6.0, Babraham Bioinformatics). Mutations were called by comparing all evolved populations to reference genomes (Table S1) using *breseq*, a mutation calling program for haploid organisms (version 0.28).[93] We used the standard settings to identify polymorphic mutations, i.e. mutations reached a frequency of at least 0.05 in the population and occurred on at least two reads from each strand.

Curating the evolved mutation list. Two methods were used to filter out ancestral mutations (Table 4.1). First, ancestral mutations were considered any mutation that was identified in N-2 expected replicate communities, called N-2 method. For example, it was expected that a total of 24 samples contained *E. coli*. If a mutation was found in at least 22 samples, it was considered an ancestral mutation and removed from the analysis. The second filtering method was to consider any mutation that evolved in at least 75% of replicate communities in which an organism was present and rose to at least 90% frequency in all communities in which it was identified, called 75% reps & 90% freq method. Either filtering method could remove massively parallel evolved mutations, which are likely rare. To

further focus the sequencing analysis on mutations with strong selection, we analyzed mutations that reached a minimum of 25% in at least one sequenced population. All remaining mutations across the three organisms were then manually curated to remove mutations called because of misalignment or poor coverage, and to consolidate sequential insertions or deletions identified by *breseq*.

Mutation analysis. Mutations including SNPs, indels and intergenic mutations, were assigned to a genome according to genomic elements (Table S4.1). The total number of mutations per genome (*E. coli*, *S. enterica*, or T7 phage) were calculated. Statistical analysis was completed in R (version 4.0.1). *E. coli* mutations were compared with a two-way ANOVA, *S. enterica* mutations with a one-way ANOVA, and T7 mutations with a t-test. Clustering tendency was assessed with the Hopkins statistic and VAT (visual assessment of clustering tendency) with the factoextra R package (version 1.0.7). Differences between treatments were tested with hierarchical clustering in R using the vegan package[153] (version 2.5-6) with Bray-Curtis dissimilarity metric and the “complete” clustering method.

Acknowledgements

We would like to thank Leno Smith, Sarah Hammarlund, and Mitchell Chiesl for technical help, Jeremy Chacón for statistics advice, and other Harcombe Lab Members and the UMN Institute for Molecular Virology community for useful discussions. We acknowledge the University of Minnesota Genomics Core and Minnesota Supercomputing Institute (MSI) for providing resources and expertise for sequencing and sequencing analysis (http://www.msi.umn.edu). LF was supported by a Fellowship from the Institute for

Molecular Virology Training Program (NIH T32 AI083196) and research funds from the NIH (GM121498-01A1, to Dr. William Harcombe).

Chapter 5

Conclusions and future directions

Summary

Overall, my thesis focused on describing ecological and evolutionary processes that dictate community-level responses to phage infection. By focusing on communities that include cross-feeding interactions between bacterial community members, I highlighted an understudied, but commonly occurring, ecological interaction that could differentiate responses from communities with predominantly antagonistic or competitive interactions. I drew on concepts from marine biology (the viral shunt in Chapter 2), treatment of pathogenic infections (phage therapy in Chapter 3), and evolutionary responses (Red Queen and Red King Effects in Chapter 4) to better understand phage- community dynamics. This thesis helps to set a baseline expectation of how phage infection influences cross-feeding microbial communities. Ultimately, this knowledge may help design applications of phage for human services, such as phage therapy treatments or strategies combatting agricultural pathogens. I will first summarize the three research chapters and provide immediate next steps. Then I will propose future research directions related to effects of phage in cross-feeding coculture and roadblocks to applying phage to microbial communities that provide a variety of human services.

Chapter 2 laid the foundation of my thesis by exploring how a two-species cross-feeding coculture was altered by infection with a single phage at a time. As anticipated, phage resistance evolved for applications of either *E. coli*-specific T7 phage or *S. enterica*-specific P22 phage. Unexpectedly, I observed more *S. enterica* when *E. coli* was infected by an *E. coli* - specific phage than in phage-free co-cultures. This observation contradicted expectations of how cross-feeding microbial communities respond to disturbances. Typically, cross-feeding bacteria are limited by each other and follow similar growth patterns.[72] However, these patterns had typically been studied by limiting nutrients, which leaves bacterial cells intact. In comparison, phage burst open infected bacterial cells to

release new phage. In doing so, the burst bacterial cells also release any nutrients that were previously contained, which serve as a new resource for the coculture. In addition, mathematical modeling showed that phage resistance needed to be incomplete to increase *S. enterica* growth, meaning that phage replicated poorly compared to phage infecting sensitive *E. coli*. Using a combination of mathematical modeling and wet-lab experiments, I showed that nutrients released by burst *E. coli* cells were consumed by *S. enterica* and facilitated independent *S. enterica* growth, all within a single 4-day growth curve.

While I was able to identify a likely mutation upstream of the *lon* gene that caused mucoidy (it occurred in almost all phage-containing cocultures and reached frequencies of >70%), an obvious next step would be to perform genetic experiments to confirm the causality and sufficiency of this mutation- engineering the *lon* mutation into a clean ancestral genetic background to determine if it is necessary and sufficient to cause the mucoidy phenotype. It would also be interesting to examine the repeatability of this phenotype - perhaps upstream of the *lon* gene serves as a mutational hotspot. In addition, genetic analyses investigating multiple mutations in pathways whose disruption is known to produce mucoid phenotypes would shed light on whether this specific mutation was necessary to facilitate *S. enterica* consumption of cellular debris or whether any mutation that resulted in a mucoid phenotype was sufficient. Partial resistance could be considered a continuous trait whose magnitude could affect how well the cross-feeding partner grows during phage infection.

Furthermore, food-web analyses, like those used to discover the viral shunt, could indicate how cellular debris released by phage infections are used in a more complex microbial community where effects of cellular debris release are likely to be distributed among additional bacterial species. In addition, genome-scale metabolic modeling of

multi-species cross-feeding communities, which has been used to study the gut microbiome,[154] could help track the fates of different cellular debris components (nucleotides, amino acids, metabolites) depending on the scavenging ability of different community members (e.g. saccharolytic vs proteolytic bacteria) (see appendix 5 for a detailed description of possible genome-scale study of the dental microbiome).

In Chapter 3, I extended the experimental set-up to model phage therapy's use of multiple phage in formulations called 'cocktails' to treat recalcitrant bacterial infections. To increase the complexity and applicability of my experimental system, I used cocktails of two phage and measured changes in the length of time that these cocktails suppressed bacterial growth. In addition, I asked whether the bacterial targets of phage altered the length of growth suppression (i.e. whether both phage attacked the same single bacteria or both cross-feeding bacteria). The goal was to determine what factors influence bacterial suppression when treating a focal (pathogenic) bacteria engaged in cross-feeding was treated with phage cocktails. With *E. coli* as the target in the cross-feeding system, I discovered that to suppress a target pathogen was more important to include a phage that infected the cross-feeding bacteria with the slowest growth rate than to specifically target the focal pathogenic bacterial species. In our system, the slow grower was *S. enterica*. I used a generalized mathematical model to illustrate that this observation is not an experimental artifact of our system, but is a general principle of how cross-feeding systems respond to phage cocktails. In effect, I described a novel cocktail formulation that included not only phage targeting that focal pathogenic bacterial species, but also its cross-feeding partners.

An extension of this project would be to test the prediction that targeting the slower-grower in a cross-feeding community best impedes growth of a focal pathogen in a complex microbial community. Several human-associated microbial communities involve

cross-feeding between multiple species. For example, *Pseudomonas aeruginosa* and multiple anaerobic bacteria in the lungs of cystic-fibrosis patients[155,156] or the *Bifidobacterium* and butyrate-producing anaerobes in the gut microbiome.[157] To take this research one step further, the effects of phage with broad host ranges that include multiple bacterial species (polyvalent phage) should be investigated. One study that used a polyvalent phage in a soil-carrot microcosm system found that polyvalent phage decreased pathogen numbers equally as well as a phage cocktail but caused less perturbation of the microbial community, a desirable response.[128] Additional similar studies with cross-feeding communities could begin to illuminate how complex phage communities influence complex microbial communities.

Lastly, in Chapter 4, I increased the experiment's complexity by investigating how *E. coli* evolved with phage when cross-feeding with *S. enterica* over long time periods. I hypothesized that engaging in cross-feeding relationships changed the rate of adaptation of any of the community members. There are two theories that set clear expectations for impacts of phage infections and cross-feeding on rates of adaptation. The Red Queen hypothesis[42–44] posits that phage infection will increase the rate of adaptation while the Red King hypothesis[76] predicts that cross-feeding interactions will decrease the rate of adaptation. Faster adaptation to a pathogen would increase the likelihood of 'winning' the evolution race while slower adaptation to a mutualistic partner would ensure that no mutation is detrimental to the partnership. In this coculture system, phage infection and cross-feeding evolutionary pressures occur simultaneously and could either cancel out each other or one could become the dominant pressure. I used a batch culture experimental evolution set-up to grow *E. coli*, *S. enterica*, and an *E. coli* - specific phage (T7) together for ~150 generations, or 20 transfers. I used a combination of phenotypic- and genomic-based measurements to quantify rates of adaptation. Specifically, I used the

evolution of mucoidy, a common evolutionary response to phage infection, as a phenotypic trait of *E. coli* and the total number of acquired mutations, determined by whole-community whole-genome sequencing, as a genomic-based proxy for rate of adaptation. I found that phage infection marginally increased the rate of adaptation and that cross-feeding tended to decrease the rate of adaptation, which supports the Red Queen and Red King hypotheses, respectively. However, I did not find that phage infection and cross-feeding evolutionary pressures interacted. The supposedly opposing evolutionary pressures of cross-feeding and phage infection, one that should decrease rates of adaptation while the other should increase rates of adaptation, can in fact interact independently within a community context.

While there was only a weak signature at the mutation level of either phage infection or cross-feeding treatments, it is possible that higher-level analysis could uncover broader patterns of mutational identity - for example at the gene, operon, or pathway level. In fact, many mutations in phage-containing communities showed mutations that affected genes involved in lipopolysaccharide biosynthesis, a pathway known to contribute to mucoidy phenotypes. Furthermore, while I focused on end-point analysis of genomic-based measurements of rates of adaptation, there are likely complex dynamics occurring throughout the evolution[37] of mutational sweeps or clonal interference, that occurred throughout the evolution experiment, like those described in plasmid-host systems,[158] in phage-host systems.[13,51] Sequencing analysis of additional timepoints could uncover such transitory interactions between phage and hosts.

Reflections on phage in microbial communities

Additionally, it remains unclear whether phage infection in natural systems elicits arms-race dynamics or fluctuating selection dynamics. Arms-race dynamics, also called 'tit-for-tat', are classic pathogen-host responses predicted by the Red Queen hypothesis, and have been described extensively, particularly in experiments using cultures of a single host and phage.[31] Others have described fluctuating selection, also called frequency-dependent dynamics, where lineages of phage-resistance bacteria rise and fall in accordance with the most common phage genotype.[2] In fact, at least one paper found that long-term experimental evolution between *Pseudomonas fluorescens* and a parasitic phage (lytic) initially showed arms-race dynamics that gave way to fluctuating selection dynamics as the cost of resistance became too costly.[13] It remains unknown whether a cross-feeding community context could exacerbate small fitness costs that are tolerable in monoculture but are selected against when in a cross-feeding context. However, two studies would suggest that this is true. First, phage resistance costs have been described as context-dependent in plant-associated microbiomes.[12] Second, trade-offs between phage and other selection pressures, specifically antibiotic resistance, have been documented.[159,160] If phage resistance interacted with cross-feeding, such as decreasing the amount of cross-fed nutrient produced, then it is likely that such costs could be tolerated in monoculture but not in a cross-feeding coculture.

Furthermore, small fitness costs should be more pronounced in natural systems when competing for nutrients with other bacteria, or even other microbes like fungi and archaea, and being eaten by other predators like protozoa, single-celled eukaryotes that consume bacteria. Surprisingly, some of the same molecular mechanisms used to evade phage are also used to evade predation by protists - masking by changing cell surface receptors that identify bacteria to protists.[161] Such potential overlap of resistance

mechanisms lays the groundwork for some interesting interplay between phage resistance and protist resistance evolution dynamics. For example, resistance to one pressure may confer cross-resistance to the other.

This thesis has focused on exploring and describing evolutionary responses to phage infection of a simple and isolated cross-feeding community. Others have increased complexity to study phage infection of microbial communities within host-associated microbiomes.[33,62] However, tracking mechanisms beyond host-phage interactions thus far has been difficult in such systems, particularly if the host bacterial species is not yet culturable. Technological improvements in sequencing, *in situ* analysis, and genetics may help tease apart such mechanisms underlying evolutionary processes in complex microbial communities. For example, Hi-C sequencing of naturally communities[162] spiked with phage-host combinations (such as[51]) could help elucidate the role of spatial segregation in microbial communities by linking physically close pieces of DNA together. Other methods of tracking metabolite movement through a complex community (e.g. C-13 labeling, heavy water) could shed light on the fate of cellular debris released by phage. A first step could be using mesocosms such as the soil microcosms of Gomez and Buckling.[51] Another axis of complexity to explore is the combination of phage and antibiotics, a growing field that is particularly relevant for human-health based applications of phage.[160,163]

While improvements in scientific technology will be needed to greatly increase experiment complexity, that is not the only improvement required for large-scale use of phage in applied settings. Broad use of phage, particularly in human health applications, will remain stunted until regulatory entities like the United States Federal Drug Administration, work to redefine guidelines for approval of phage-based technologies.[164]

Currently, there is not a path for broad phage-therapy approval. As such, phage therapy is only used as experimental last resort treatment with many success stories.[3]

Ultimately, accurate and efficient use of phage in applied settings without unanticipated side effects will likely require two things: strong predictive power of how phage effects could ripple out into the entire microbial community to affect other bacteria, fungi, protists, and archaea that might have mutualistic or competitive relationships with a focal bacterial strain; and identification of a way to limit the effects of phage in community settings. This is a complex set of interaction variables with many possible outcomes. However, it is possible generalizable ecological and evolutionary principles hold true in most situations. Defining those processes well would greatly increase our ability to predict microbial community reactions to perturbations in general, not only to phage infections.

Concluding remarks

Phage infection can have strong effects on microbial community structure, but since 1915 when discovered, phage have largely been studied in isolation with a host species. Putting phage into a community context has been gaining traction; there is a rich body of scientific literature about phage in complex marine ecosystems, and a growing body of literature of phage in plant or animal host-associated contexts. Such complex environments make drawing mechanistic conclusions difficult. Here, I have described some of the numerous ways that phage can influence microbial community structure and function, largely focusing on direct changes in host population sizes and the fate of released cellular debris. As researchers increase the complexity of microbial communities used to study phage influences — including studying more types of bacterial interactions like cross-feeding— and as techniques used in natural communities are improved, it is likely that even more

complex interactions among phage, their hosts, and ecological partners of their hosts will be revealed.

Bibliography

1. Meaden, S. & Koskella, B. Exploring the risks of phage application in the environment. *Front. Microbiol.* **4**, (2013).
2. Breitbart, M., Bonnain, C., Malki, K. & Sawaya, N. A. Phage puppet masters of the marine microbial realm. *Nat. Microbiol.* **3**, 754–766 (2018).
3. Kortright, K. E., Chan, B. K., Koff, J. L. & Turner, P. E. Phage therapy: A renewed approach to combat antibiotic-resistant bacteria. *Cell Host Microbe* **25**, 219–232 (2019).
4. Mahony, J., Casey, E. & van Sinderen, D. The impact and applications of phages in the food industry and agriculture. *Viruses* **12**, (2020).
5. Jorge, P. *et al.* Antimicrobial resistance three ways: Healthcare crisis, major concepts and the relevance of biofilms. *FEMS Microbiol. Ecol.* **95**, 1–17 (2019).
6. D'herelle, F. Bacteriophage as a treatment in acute medical and surgical infections. *Bull. Newyord Acad. Med.* **7**, 329–348 (1931).
7. Gordillo Altamirano, F. L. & Barr, J. J. Phage therapy in the postantibiotic era. *Clin. Microbiol. Rev.* **32**, 1–25 (2019).
8. Serwer, P., Wright, E. T., Hakala, K. W. & Weintraub, S. T. Evidence for bacteriophage T7 tail extension during DNA injection. *BMC Res. Notes* **1**, 1–6 (2008).
9. Labrie, S. J., Samson, J. E. & Moineau, S. Bacteriophage resistance mechanisms. *Nat. Rev. Microbiol.* **8**, 317–327 (2010).
10. Hyman, P. & Abedon, S. T. *Bacteriophage host range and bacterial resistance. Advances in applied microbiology* **70**, (Elsevier Inc., 2010).
11. Samson, J. E., Magadán, A. H., Sabri, M. & Moineau, S. Revenge of the phages: defeating bacterial defences. *Nat. Rev. Microbiol.* **11**, 675–87 (2013).
12. Meaden, S., Paszkiewicz, K. & Koskella, B. The cost of phage resistance in a plant pathogenic bacterium is context-dependent. *Evolution.* **69**, 1321–1328 (2015).
13. Hall, A. R., Scanlan, P. D., Morgan, A. D. & Buckling, A. Host-parasite coevolutionary arms races give way to fluctuating selection. *Ecol. Lett.* **14**, 635–642 (2011).
14. Forde, S. E., Thompson, J. N., Holt, R. D. & Bohannan, B. J. M. Coevolution drives temporal changes in fitness and diversity across environments in a bacteria-bacteriophage interaction. *Evolution.* **62**, 1830–1839 (2008).
15. Lenski, R. E. & Levin, B. R. Constraints on the coevolution of bacteria and virulent phage : A model, some experiments, and predictions for natural communities. *Am. Nat.* **125**, 585–602 (1985).
16. Schrag, S. J. & Mittler, J. E. Host-parasite coexistence: The role of spatial refuges in stabilizing bacteria-phage interactions. *Am. Nat.* **148**, 348–377 (1996).
17. Wang, I.-N., Smith, D. L. & Young, R. Holins: The protein clocks of bacteriophage Infections. *Annu. Rev. Microbiol.* **54**, 799–825 (2000).
18. Parikka, K. J., Le Romancer, M., Wauters, N. & Jacquet, S. Deciphering the virus-to-prokaryote ratio (VPR): Insights into virus–host relationships in a variety of ecosystems. *Biol. Rev.* **92**, 1081–1100 (2017).
19. Parada, V., Herndl, G. J. & Weinbauer, M. G. Viral burst size of heterotrophic prokaryotes in aquatic systems. *J. Mar. Biol. Assoc. United Kingdom* **86**, 613–621 (2006).
20. Wright, R. C. T., Brockhurst, M. A. & Harrison, E. Ecological conditions determine extinction risk in co-evolving bacteria-phage populations. *BMC Evol. Biol.* **16**, 1–6 (2016).

21. Smith, J. M. A comment on the Red Queen. *Am. Nat.* **110**, 325–330 (1976).

22. Levin, B. R. & Bull, J. J. Population and evolutionary dynamics of phage therapy. *Nat. Rev. Microbiol.* **2**, 166–173 (2004).

23. Brockhurst, M. A., Fenton, A., Roulston, B. & Rainey, P. B. The impact of phages on interspecific competition in experimental populations of bacteria. *BMC Ecol.* **6**, 19 (2006).

24. Prasad, Y., Arpana, Kumar, D. & Sharma, A. K. Lytic bacteriophages specific to *Flavobacterium columnare* rescue catfish, *Clarias batrachus* (Linn.) from columnaris disease. *J. Environ. Biol.* **32**, 161–168 (2011).

25. Fazzino, L., Anisman, J., Chacón, J. M., Heineman, R. H. & Harcombe, W. R. Lytic bacteriophage have diverse indirect effects in a synthetic cross-feeding community. *ISME J.* **14**, 123–134 (2020).

26. Abedon, S. T. Impact of phage properties on bacterial survival. in *Contemporary Trends in Bacteriophage Research* (ed. Adams, H. T.) 217–235 (Nova Science Publishers, Inc, 2009).

27. Chao, L., Levin, B. R. & Stewart, F. M. A complex community in a simple habitat: An experimental study with bacteria and phage. *Ecology* **58**, 369–378 (1977).

28. Górski, A. *et al. Phage as a modulator of immune responses: Practical implications for phage therapy*. *Advances in Virus Research* **83**, (2012).

29. Leung, C. Y. & Weitz, J. S. Modeling the synergistic elimination of bacteria by phage and the innate immune system. *J. Theor. Biol.* **429**, 241–252 (2017).

30. Roach, D. R. *et al.* Synergy between the host immune system and bacteriophage is essential for successful phage therapy against an acute respiratory pathogen. *Cell Host Microbe* **22**, 38–47 (2017).

31. Bohannan, B. J. M. & Lenski, R. E. Linking genetic change to community evolution: Insights from studies of bacteria and bacteriophage. *Ecol. Lett.* **3**, 362–377 (2000).

32. De Paepe, M. & Taddei, F. Viruses' life history: Towards a mechanistic basis of a trade-off between survival and reproduction among phages. *PLoS Biol.* **4**, e193 (2006).

33. Koskella, B. & Brockhurst, M. A. Bacteria-phage coevolution as a driver of ecological and evolutionary processes in microbial communities. *FEMS Microbiol. Rev.* **38**, 916–931 (2014).

34. Chaudhry, W. *et al.* Mucoidy, a general mechanism for maintaining lytic phage in populations of bacteria. *bioRxiv* doi:10.1101/775056 (2019).

35. Heilmann, S., Sneppen, K. & Krishna, S. Sustainability of virulence in a phage-bacterial ecosystem. *J. Virol.* **84**, 3016–22 (2010).

36. Koskella, B. Resistance gained, resistance lost: An explanation for host-parasite coexistence. *PLoS Biol.* **16**, e3000013 (2018).

37. Lenski, R. E. Experimental evolution and the dynamics of adaptation and genome evolution in microbial populations. *ISME Journal* **11**, 2181–2194 (2017).

38. Wandro, S. *et al.* Predictable molecular adaptation of coevolving *Enterococcus faeciumand* lytic phage EfV12-phi1. *Front. Microbiol.* **10**, 1–11 (2019).

39. Wang, J., Gao, Y. & Zhao, F. Phage-bacteria interaction network in human oral microbiome. *Environ. Microbiol.* **18**, 2143–2158 (2015).

40. Marston, M. F. *et al.* Rapid diversification of coevolving marine *Synechococcus* and a virus. *Proc. Natl. Acad. Sci.* **109**, 4544–4549 (2012).

41. Frickel, J., Sieber, M. & Becks, L. Eco-evolutionary dynamics in a coevolving host-virus

system. *Ecol. Lett.* **19**, 450–459 (2016).

42. Van Valen, L. A new evolutionary law. *Evol. Theory* **1**, 1–30 (1973).

43. CM, L. & V, A. No Title. in *Ecology of Infectious Diseases in Natural Populations* (eds. BT, G. & AP, D.) 421–449 (Cambridge Univ Press, 1995).

44. Woolhouse, M. E. J., Webster, J. P., Domingo, E., Charlesworth, B. & Levin, B. R. Biological and biomedical implications of the co-evolution of pathogens and their hosts. *Nature Genetics* **32**, 569–577 (2002).

45. Azam, A. H. & Tanji, Y. Bacteriophage-host arm race: an update on the mechanism of phage resistance in bacteria and revenge of the phage with the perspective for phage therapy. *Appl. Microbiol. Biotechnol.* **103**, 2121–2131 (2019).

46. Quance, M. A. & Travisano, M. Effects of temperature on the fitness cost of resistance to bacteriophage T4 in *Escherichia coli*. *Evolution.* **63**, 1406–1416 (2009).

47. Harcombe, W. R. & Bull, J. J. Impact of phages on two-species bacterial communities. *Appl. Environ. Microbiol.* **71**, 5254–5259 (2005).

48. Held, N. L. & Whitaker, R. J. Viral biogeography revealed by signatures in *Sulfolobus islandicus* genomes. *Environ. Microbiol.* **11**, 457–466 (2009).

49. Vos, M., Birkett, P. J., Birch, E., Griffiths, R. I. & Buckling, A. Local adaptation of bacteriophages to their bacterial hosts in soil. *Science.* **325**, 833 (2009).

50. Koskella, B. Bacteria-phage interactions across time and space: Merging local adaptation and time-shift experiments to understand phage evolution. *Am. Nat.* **184**, S9–S21 (2014).

51. Gómez, P. & Buckling, A. Bacteria-phage antagonistic coevolution in soil. *Science (80-.).* **332**, 106–109 (2011).

52. Wilhelm, S. W. & Suttle, C. A. Viruses and nutrient cycles in the sea: Viruses play critical roles in the structure and function of aquatic food webs. *Bioscience* **49**, 781–788 (1999).

53. Poorvin, L., Rinta-Kanto, J. M., Hutchins, D. A. & Wilhelm, S. W. Viral release of iron and its bioavailability to marine plankton. *Limnol. Oceanogr.* **49**, 1734–1741 (2004).

54. Shelford, E. J., Middelboe, M., Møller, E. F. & Suttle, C. A. Virus-driven nitrogen cycling enhances phytoplankton growth. *Aquat. Microb. Ecol.* **66**, 41–46 (2012).

55. Weitz, J. S. & Wilhelm, S. W. Ocean viruses and their effects on microbial communities and biogeochemical cycles. *F1000 Biol. Rep.* **4**, 2–9 (2012).

56. Jover, L. F., Effler, T. C., Buchan, A., Wilhelm, S. W. & Weitz, J. S. The elemental composition of virus particles: Implications for marine biogeochemical cycles. *Nat. Rev. Microbiol.* **12**, 519–528 (2014).

57. Mirzaei, M. K. & Maurice, C. F. Ménage à trois in the human gut: Interactions between host, bacteria and phages. *Nat. Rev. Microbiol.* **15**, 397–408 (2017).

58. Morella, N. M., Gomez, A. L., Wang, G., Leung, M. S. & Koskella, B. The impact of bacteriophages on phyllosphere bacterial abundance and composition. *Mol. Ecol.* **27**, 2025–2038 (2018).

59. Hsu, B. B. *et al.* Dynamic modulation of the gut microbiota and metabolome by bacteriophages in a mouse model. *Cell Host Microbe* **25**, 803–814 (2019).

60. Galtier, M. *et al.* Bacteriophages to reduce gut carriage of antibiotic resistant uropathogens with low impact on microbiota composition. *Environ. Microbiol.* **18**, 2237–2245 (2016).

61. Mai, V. *et al.* Bacteriophage administration significantly reduces *Shigella* colonization and shedding by *Shigella*-challenged mice without deleterious side effects and distortions in

the gut microbiota. *Bacteriophage* **5**, e1088124 (2015).

62. Reyes, A., Wu, M., McNulty, N. P., Rohwer, F. L. & Gordon, J. I. Gnotobiotic mouse model of phage-bacterial host dynamics in the human gut. *Proc. Natl. Acad. Sci.* **110**, 20236–41 (2013).

63. Geredew Kifelew, L., Mitchell, J. G. & Speck, P. Mini-review: efficacy of lytic bacteriophages on multispecies biofilms. *Biofouling* **35**, 472–481 (2019).

64. Chhibber, S., Bansal, S. & Kaur, S. Disrupting the mixed-species biofilm of *Klebsiella pneumoniae* B5055 and *Pseudomonas aeruginosa* PAO using bacteriophages alone or in combination with xylitol. *Microbiol. (United Kingdom)* **161**, 1369–1377 (2015).

65. Yu, P., Mathieu, J., Yang, Y. & Alvarez, P. J. J. Suppression of enteric bacteria by bacteriophages: Importance of phage polyvalence in the presence of soil bacteria. *Environ. Sci. Technol.* **51**, 5270–5278 (2017).

66. Maslov, S. & Sneppen, K. Population cycles and species diversity in dynamic Kill-the-Winner model of microbial ecosystems. *Sci. Rep.* **7**, 39642 (2017).

67. Chacón, J. M. & Harcombe, W. R. The power of metabolism for predicting microbial community dynamics. *mSystems* **4**, e00146-19 (2019).

68. Zelezniak, A. *et al.* Metabolic dependencies drive species co-occurrence in diverse microbial communities. *Proc. Natl. Acad. Sci.* **112**, 201522642 (2015).

69. Mee, M. T., Collins, J. J., Church, G. M. & Wang, H. H. Syntrophic exchange in synthetic microbial communities. *Proc. Natl. Acad. Sci.* **111**, E2149–E2156 (2014).

70. D'Souza, G. *et al.* Less is more: Selective advantages can explain the prevalent loss of biosynthetic genes in bacteria. *Evolution.* **68**, 2559–2570 (2014).

71. Schink, H. Synergistic interaction in the microbial world. *Antoinie van Leeuwenhoek* **81**, 257–261 (2002).

72. Shou, W., Ram, S. & Vilar, J. M. G. G. Synthetic cooperation in engineered yeast populations. *Proc. Natl. Acad. Sci.* **104**, 1877–1882 (2007).

73. Harcombe, W. R. *et al.* Metabolic resource allocation in individual microbes determines ecosystem interactions and spatial dynamics. *Cell Rep.* **7**, 1104–1115 (2014).

74. Chubiz, L. M., Harcombe, W. R., Granger, B. R. & Segrè, D. Species interactions differ in their genetic robustness. *Front. Microbiol.* **6**, 271 (2015).

75. Adamowicz, E. M., Flynn, J., Hunter, R. C. & Harcombe, W. R. Cross-feeding modulates antibiotic tolerance in bacterial communities. *ISME J.* **12**, 2723–2735 (2018).

76. Bergstrom, C. T. & Lachmann, M. The Red King effect: When the slowest runner wins the coevolutionary race. *Proc. Natl. Acad. Sci.* **100**, 593–598 (2003).

77. Harcombe, W. R. Novel cooperation experimentally evolved between species. *Evolution.* **64**, 2166–2172 (2010).

78. Sullivan, M. B., Weitz, J. S. & Wilhelm, S. Viral ecology comes of age. *Environ. Microbiol. Rep.* **9**, 33–35 (2017).

79. Suttle, C. A. Marine viruses-major players in the global ecosystem. *Nat. Rev. Microbiol.* **5**, 801–812 (2007).

80. Rosenwasser, S., Ziv, C., Creveld, S. G. van & Vardi, A. Virocell metabolism: Metabolic innovations during host–virus interactions in the ocean. *Trends Microbiol.* **24**, 821–832 (2016).

81. Santos, S. B., Costa, A. R., Carvalho, C., Nóbrega, F. L. & Azeredo, J. Exploiting bacteriophage proteomes: The Hidden biotechnological potential. *Trends Biotechnol.* **36**,

966–984 (2018).

82. de Melo, A. G., Levesque, S. & Moineau, S. Phages as friends and enemies in food processing. *Curr. Opin. Biotechnol.* **49**, 185–190 (2018).

83. Kakasis, A. & Panitsa, G. Bacteriophage therapy as an alternative treatment for human infections: A comprehensive review. *Int. J. Antimicrob. Agents* **53**, 16–21 (2019).

84. Scanlan, P. D. Bacteria–bacteriophage coevolution in the human gut: Implications for microbial diversity and functionality. *Trends Microbiol.* **25**, 614–623 (2017).

85. Fahimipour, A. K., Anderson, K. E. & Williams, R. J. Compensation masks trophic cascades in complex food webs. *Theor. Ecol.* **10**, 245–253 (2017).

86. D'Souza, G. *et al.* Ecology and evolution of metabolic cross-feeding interactions in bacteria. *Nat. Prod. Rep.* **35**, 455–488 (2018).

87. Carlson, R. P. *et al.* Competitive resource allocation to metabolic pathways contributes to overflow metabolisms and emergent properties in cross-feeding microbial consortia. *Biochem. Soc. Trans.* **46**, 269–284 (2018).

88. Haraldsson, M. *et al.* Microbial parasites make cyanobacteria blooms less of a trophic dead end than commonly assumed. *ISME J.* **12**, 1008–1020 (2018).

89. Weitz, J. S. *et al.* A multitrophic model to quantify the effects of marine viruses on microbial food webs and ecosystem processes. *ISME J.* **9**, 1352–1364 (2015).

90. Hammarlund, S. P., Chacón, J. M. & Harcombe, W. R. A shared limiting resource leads to competitive exclusion in a cross-feeding system. *Environ. Microbiol.* (2018). doi:10.1111/1462-2920.14493

91. Hoek, T. A. *et al.* Resource availability modulates the cooperative and competitive nature of a microbial cross-feeding mutualism. *PLOS Biol.* **14**, e1002540 (2016).

92. Scanlan, P. D. & Buckling, A. Co-evolution with lytic phage selects for the mucoid phenotype of *Pseudomonas fluorescens* SBW25. *ISME J.* **6**, 1148–58 (2012).

93. Deatherage, D. E. & Barrick, J. E. Identification of mutations in laboratory evolved microbes from next-generation sequencing data using breseq. *Methods Mol. Biol.* **1151**, 165–188 (2014).

94. Torres-Cabassa, A. S. & Gottesman, S. Capsule synthesis in *Escherichia coli* K-12 is regulated by proteolysis. *J. Bacteriol.* **169**, 981–989 (1987).

95. Oliveira, N. M., Niehus, R. & Foster, K. R. Evolutionary limits to cooperation in microbial communities. *PNAS* **111**, 17941–17946 (2014).

96. Bennett, B. D. *et al.* Absolute metabolite concentrations and implied enzyme active site occupancy in *Escherichia coli*. *Nat. Chem. Biol.* **5**, 593–9 (2009).

97. Birch, E. W., Ruggero, N. A. & Covert, M. W. Determining host metabolic limitations on viral replication via integrated modeling and experimental perturbation. *Plos Comput. Biol.* **8**, e1002746 (2012).

98. Gottesman, S., Trisler, P. & Torres-Cabassa, A. S. Regulation of capsular polysaccharide synthesis in *Escherichia coli* K-12: Characterization of three regulatory genes. *J. Bacteriol.* **162**, 1111–1119 (1985).

99. Qimron, U., Marintcheva, B., Tabor, S. & Richardson, C. C. Genomewide screens for *Escherichia coli* genes affecting growth of T7 bacteriophage. *PNAS* **103**, 19039–44 (2006).

100. Baker, J. L. & Edlund, A. Exploiting the oral microbiome to prevent tooth decay: Has evolution already provided the best tools? *Front. Microbiol.* **9**, 3323 (2018).

101. Szafrański, S. P., Winkel, A. & Stiesch, M. The use of bacteriophages to biocontrol oral biofilms. *J. Biotechnol.* **250**, 29–44 (2017).

102. Soetaert, K., Petzoldt, T. & Setzer, R. W. Solving differential equations in R: Package deSolve. *J. Stat. Softw.* **33**, (2010).

103. Delaney, N. F. *et al.* Development of an optimized medium, strain and high-throughput culturing methods for *Methylobacterium extorquens*. *PLoS One* **8**, e62957 (2013).

104. Baranyi, J. & Roberts, T. A. A dynamic approach to predicting bacterial growth in food. *Int. J. Food Microbiol.* **23**, 277–294 (1994).

105. Pires, D. P., Melo, L. D. R., Vilas Boas, D., Sillankorva, S. & Azeredo, J. Phage therapy as an alternative or complementary strategy to prevent and control biofilm-related infections. *Curr. Opin. Microbiol.* **39**, 48–56 (2017).

106. Culot, A., Grosset, N. & Gautier, M. Overcoming the challenges of phage therapy for industrial aquaculture: A review. *Aquaculture* **513**, 734423 (2019).

107. Filippov, A. A. *et al.* Bacteriophage-resistant mutants in *Yersinia pestis*: Identification of phage receptors and attenuation for mice. *PLoS One* **6**, (2011).

108. Ramírez, M., Neuman, B. & Ramírez, C. A. Bacteriophages as promising agents for the biological control of moko disease (*Ralstonia solanacearum*) of banana. *Biol. Control* **149**, 104238 (2020).

109. Gu, Y. *et al.* Identification of novel bacteriophage vB_EcoP-EG1 with lytic activity against planktonic and biofilm forms of uropathogenic *Escherichia coli*. *Appl. Microbiol. Biotechnol.* **103**, 315–326 (2019).

110. Wang, X. *et al.* Parasites and competitors suppress bacterial pathogen synergistically due to evolutionary trade-offs. *Evolution.* **71**, 733–746 (2017).

111. Testa, S. *et al.* Phage efficacy in infecting dual-strain biofilms of *Pseudomonas aeruginosa*. *Commun. Biol.* 551754 (2019). doi:10.1101/551754

112. D'Souza, G. & Kost, C. Experimental evolution of metabolic dependency in bacteria. *PLOS Genet.* **12**, 1–27 (2016).

113. Chan, B. K. & Abedon, S. T. Bacteriophage adaptation, with particular attention to issues of phage host range. in *Bacteriophages in Dairy Processing* (eds. Quiberoni, A. & Reinheimer, J.) 25–52 (Nova Science Publishers, 2012).

114. Betts, A., Gray, C., Zelek, M., MacLean, R. C. & King, K. C. High parasite diversity accelerates host adaptation and diversification. *Science.* **360**, 907–911 (2018).

115. Cairns, B. J. & Payne, R. J. H. Bacteriophage therapy and the mutant selection window. *Antimicrob. Agents Chemother.* **52**, 4344–4350 (2008).

116. Wei, Y., Kirby, A. & Levin, B. R. The population and evolutionary dynamics of *Vibrio cholerae* and its bacteriophage: Conditions for maintaining phage-limited communities. *Am. Nat.* **178**, 715–725 (2011).

117. Radke, K. L. & Siegel, E. C. Mutation preventing capsular polysaccharide synthesis in *Escherichia coli* K-12 and its effect on bacteriophage resistance. *J. Bacteriol.* **106**, 432–437 (1971).

118. Skurray, R. A., Hancock, R. E. W. & Reeves, P. Con- mutants: class of mutants in *Escherichia coli* K 12 lacking a major cell wall protein and defective in conjugation and adsorption of a bacteriophage. *J. Bacteriol.* **119**, 726–735 (1974).

119. Mizoguchi, K. *et al.* Coevolution of bacteriophage PP01 and *Escherichia coli* O157:H7 in continuous culture. *Appl. Environ. Microbiol.* **69**, 170–176 (2003).

120. Luria, S. E. & Delbrück, M. Mutations of bacteria from virus sensitivity to virus resistance.

Genetics **28**, 491–511 (1943).

121. La Sarre, B., McCully, A. L., Lennon, J. T. & McKinlay, J. B. Microbial mutualism dynamics governed by dose-dependent toxicity of cross-fed nutrients. *ISME J.* **11**, 337–348 (2017).

122. McCully, A. L., LaSarre, B. & McKinlay, J. B. Growth-independent cross-feeding modifies boundaries for coexistence in a bacterial mutualism. *Environ. Microbiol.* **19**, 3538–3550 (2017).

123. Hom, E. F. Y. & Murray, A. W. Niche engineering demonstrates a latent capacity for fungal-algal mutualism. *Science.* **345**, 94–98 (2014).

124. Carson, L., Gorman, S. P. & Gilmore, B. F. The use of lytic bacteriophages in the prevention and eradication of biofilms of *Proteus mirabilis* and *Escherichia coli*. *FEMS Immunol. Med. Microbiol.* **59**, 447–455 (2010).

125. Lehman, S. M. & Donlan, R. M. Bacteriophage-mediated control of a two-species biofilm formed by microorganisms causing catheter-associated urinary tract infections in an in vitro urinary catheter model. *Antimicrob. Agents Chemother.* **59**, 1127–1137 (2015).

126. Oliveira, A., Sousa, J. C., Silva, A. C., Melo, L. D. R. & Sillankorva, S. Chestnut honey and bacteriophage application to control *Pseudomonas aeruginosa* and *Escherichia coli* biofilms: Evaluation in an ex vivo wound model. *Front. Microbiol.* **9**, 1–13 (2018).

127. Milho, C. *et al. Escherichia coli* and *Salmonella enteritidis* dual-species biofilms: interspecies interactions and antibiofilm efficacy of phages. *Sci. Rep.* **9**, 1–15 (2019).

128. Zhao, Y. *et al.* Comparing polyvalent bacteriophage and bacteriophage cocktails for controlling antibiotic-resistant bacteria in soil-plant system. *Sci. Total Environ.* **657**, 918–925 (2019).

129. Yu, L. *et al.* A guard-killer phage cocktail effectively lyses the host and inhibits the development of phage-resistant strains of *Escherichia coli*. *Appl. Microbiol. Biotechnol.* **102**, 971–983 (2018).

130. Jariah, R. O. A. & Hakim, M. S. Interaction of phages, bacteria, and the human immune system: Evolutionary changes in phage therapy. *Rev. Med. Virol.* **29**, 1–14 (2019).

131. Kim, M. S. *et al.* Phage-encoded colanic acid-degrading enzyme permits lytic phage: Infection of a capsule-forming resistant mutant *Escherichia coli* strain. *Appl. Environ. Microbiol.* **81**, 900–909 (2015).

132. Banks, M. K. & Bryers, J. D. Bacterial species dominance within a binary culture biofilm. *Appl. Environ. Microbiol.* **57**, 1974–1979 (1991).

133. Raskin, L., Rittmann, B. E. & Stahl, D. A. Competition and coexistence of sulfate-reducing and methanogenic populations in anaerobic biofilms. *Appl. Environ. Microbiol.* **62**, 3847–3857 (1996).

134. Turner, P. E., Souza, V. & Lenski, R. E. Tests of ecological mechanisms promoting the stable coexistence of two bacterial genotypes. *Ecology* **77**, 2119–2129 (1996).

135. Hamdi, S. *et al.* Characterization of two polyvalent phages infecting *Enterobacteriaceae. Sci. Rep.* ***7****, 1–12 (2017).*

136. Duc, H. M. *et al.* Isolation, characterization and application of a polyvalent phage capable of controlling *Salmonella* and *Escherichia coli* O157:H7 in different food matrices. *Food Res. Int.* **131**, 108977 (2020).

137. Li, Z. *et al.* Exploring the effects of phage cocktails in preventing *Vibrio* infections in juvenile sea cucumber (*Apostichopus japonicus*) farming. *Aquaculture* **515**, 734599 (2020).

138. Douglas, S. M., Chubiz, L. M., Harcombe, W. R., Ytreberg, F. M. & Marx, C. J. Parallel

mutations result in a wide range of cooperation and community consequences in a two-species bacterial consortium. *PLoS One* **11**, (2016).

139. Douglas, S. M., Chubiz, L. M., Harcombe, W. R. & Marx, C. J. Identification of the potentiating mutations and synergistic epistasis that enabled the evolution of inter-species cooperation. *PLoS One* **12**, (2017).

140. Lawrence, D. *et al.* Species interactions alter evolutionary responses to a novel environment. *PLoS Biol.* **10**, e1001330 (2012).

141. Adamowicz, E. M., Muza, M. A., Chacón, J. M. & Harcombe, W. R. Cross-feeding modulates the rate and mechanism of antibiotic resistance evolution in a model microbial community of *Escherichia coli* and *Salmonella enterica*. *PLoS Pathog.* **16**, e1008700 (2020).

142. Lilja, E. E. & Johnson, D. R. Substrate cross-feeding affects the speed and trajectory of molecular evolution within a synthetic microbial assemblage. *BMC Evol. Biol.* **19**, 129 (2019).

143. Sachs, J. L., Essenberg, C. J. & Turcotte, M. M. New paradigms for the evolution of beneficial infections. *Trends in Ecology and Evolution* **26**, 202–209 (2011).

144. Guimarães, P. R., Jordano, P. & Thompson, J. N. Evolution and coevolution in mutualistic networks. *Ecol. Lett.* **14**, 877–885 (2011).

145. Peek, A. S., Vrijenhoek, R. C. & Gaut, B. S. Accelerated evolutionary rate in sulfur-oxidizing endosymbiotic bacteria associated with the mode of symbiont transmission. *Mol. Biol. Evol* **15**, 1514–1523 (1998).

146. Gast, R. J. & Caron, D. A. Molecular phylogeny of symbiotic dinoflagellates from planktonic foraminifera and radiolaria. *Mol. Biol. Evol.* **13**, 1192–1197 (1996).

147. Paterson, S. *et al.* Antagonistic coevolution accelerates molecular evolution. *Nature* **464**, 275–278 (2010).

148. Rosenthal, A. Z., Matson, E. G., Eldar, A. & Leadbetter, J. R. RNA-seq reveals cooperative metabolic interactions between two termite-gut spirochete species in co-culture. *ISME J.* **5**, 1133–1142 (2011).

149. Thommes, M., Wang, T., Zhao, Q., Paschalidis, I. C. & Segrè, D. Designing metabolic division of labor in microbial communities. *mSystems* **4**, 263–281 (2019).

150. Antonovics, J., Thrall, P. H., Burdon, J. J. & Laine, A. L. Partial resistance in the linum-melampsora host-pathogen system: Does partial resistance make the red queen run slower? *Evolution.* **65**, 512–522 (2011).

151. Daly, R. A. *et al.* Viruses control dominant bacteria colonizing the terrestrial deep biosphere after hydraulic fracturing. *Nat. Microbiol.* **4**, 352–361 (2019).

152. Baba, T. *et al.* Construction of *Escherichia coli* K-12 in-frame, single-gene knockout mutants: the Keio collection. *Mol. Syst. Biol.* (2006). doi:10.1038/msb4100050

153. Condit, R, Pitman, N, Leigh, E.G., Chave, J., Terborgh, J., Foster, R.B., Nuñez, P., Aguilar, S. & Valencia, R., Villa, G., Muller-Landau, H.C., Losos, E. & Hubbell, S. P. Beta-diversity in tropical forest trees. *Science.* **295**, 666–669 (2002).

154. Sen, P. & Orešič, M. Metabolic modeling of human gut microbiota on a genome scale: An overview. *Metabolites* **9**, 22 (2019).

155. Flynn, J. M., Niccum, D., Dunitz, J. M. & Hunter, R. C. Evidence and role for bacterial mucin degradation in cystic fibrosis airway disease. *PLoS Pathog.* **12**, 1–21 (2016).

156. Flynn, J. M. *et al.* Disruption of cross-feeding inhibits pathogen growth in the sputa of patients with cystic fibrosis. (2020). doi:10.1128/mSphere.00343-20

157. Belenguer, A. *et al.* Two routes of metabolic cross-feeding between *Bifidobacterium adolescentis* and butyrate-producing anaerobes from the human gut. *Appl. Environ. Microbiol.* **72**, 3593–3599 (2006).

158. Hughes, J. M. *et al.* The role of clonal interference in the evolutionary dynamics of plasmid-host adaptation. (2012). doi:10.1128/mBio.00077-12

159. Chan, B. K. *et al.* Phage selection restores antibiotic sensitivity in MDR *Pseudomonas aeruginosa*. *Sci. Rep.* **6**, 1–8 (2016).

160. Burmeister, A. R. *et al.* Pleiotropy complicates a trade-off between phage resistance and antibiotic resistance. *Proc. Natl. Acad. Sci.* **117**, 201919888 (2020).

161. Wildschutte, H., Wolfe, D. M., Tamewitz, A. & Lawrence, J. G. Protozoan predation, diversifying selection, and the evolution of antigenic diversity in Salmonella. *Proc. Natl. Acad. Sci.* **101**, 10644–10649 (2004).

162. Marbouty, M., Thierry, A. & Koszul, R. Phages - bacteria interactions network of the healthy human gut. *bioRxiv* doi:10.1101/2020.05.13.093716 (2020). doi:10.1101/2020.05.13.093716

163. Segall, A. M., Roach, D. R. & Strathdee, S. A. Stronger together? Perspectives on phage-antibiotic synergy in clinical applications of phage therapy. *Current Opinion in Microbiology* **51**, 46–50 (2019).

164. Mathew, S. K. & Kanungo, R. Bacteriophages: A new (yet old) weapon against infections. in *Regenerative Medicine and Plastic Surgery* 69–79 (2019). doi:10.1007/978-3-030-19958-6

Appendices

Appendix 1: Supplemental figures and methods from Ch. 2

An Ordinary Differential Equation Model Exploring Phage Effects on a

Cross-Feeding Microbial Co-culture Community in R

1. Resource-Explicit ODE Model of Phage Infection of a Bipartite Cross-Feeding Microbial Community

We used the following systems of ordinary differential equations to model changes in biotic populations of an engineered mutualistic co-culture community comprised of *Escherichia coli* (E) and *Salmonella enterica* (S).[1] We added equations to model the effects of E-specific phage (T7) and S-specific phage (P22*vir* or P22). Replication of phage populations depended on whether host bacterial populations were actively replicating. Bacterial populations were comprised of phage-sensitive (s) and phage-resistant (r) individuals, indicated by a lowercase letter. The model used the units of cells/200mL and g/200mL for nutrient resources. Definitions of model parameters are in Supplemental Table 1. Parameters include interactions between biotic populations, phage population parameters, nutrient uptake, and conversion parameters. Although we used parameter values and variable names that mimic the *E. coli* / *S. enterica* wet-lab community, these models are generalizable to any species and phage system.

1.1 Base Monod Growth Model Without Phage Infection

We started with the following set of equations as a base model of *E. coli* and *S. enterica* cross-feeding interactions in lactose minimal medium without phage infection:

Biotic Equations:

$$\frac{dEs}{dt} = (Es)(\mu_{Es})\left(\frac{lcts}{lcts + k_{Elcts}}\right)\left(\frac{met}{met + k_{Emet}}\right)$$

Example Abiotic Equation:

$$\frac{dlcts}{dt} = (Es)(\mu_{Es})\left(\frac{lcts}{lcts + k_{Elcts}}\right)\left(\frac{met}{met + k_{Emet}}\right) * c_{Elcts}$$

where represent isolate-specific growth rates. In this model formulation, *E. coli* growth is limited by lactose (lcts) and methionine (met) concentrations in a multiplicative manner, and saturates with Monod half-saturation parameter (k_x). Accumulation of produced metabolites is growth-dependent. Relative maximum growth is equal to the multiplicative Monod constant.

1.2 Modelling Phage Infection of Cross-Feeding Bacterial Community

We added phage infection of either host species to the model equations by including a phage equation, a resistant host equation with a different maximum growth rate parameter (μ_{Er}), and a term in the sensitive host to represent phage-mediated death. Phage-mediated death is modeled using a classic, linear, host-parasite interaction. However, since T7 phage reproduction significantly decreases on stationary phase cells [2], in our model, T7 phage only produced new progeny from actively growing hosts. To accomplish this, we allowed phage replication only if multiplicative Monod constants were >0.0001 using ifelse statements. Abiotic equations were also changed to accurately represent metabolite consumption and production by additional bacterial genotypes.

The following example set of equations model T7 phage infection of *E. coli:*

Biotic Equations:

$$\frac{dEs}{dt} = (Es)(\mu_{Es})\left(\frac{lcts}{lcts + k_{Elcts}}\right)\left(\frac{met}{met + k_{Emet}}\right) - Es\,(T7)(\gamma)$$

$$\frac{dT7}{dt} = (T7)(\beta)(Es)(\mu_{Es})\left(\frac{lcts}{lcts + k_{Elcts}}\right)\left(\frac{met}{met + k_{Emet}}\right)(\gamma)$$

$$\frac{dEr}{dt} = (Er)(\mu_{Er})\left(\frac{lcts}{lcts + k_{Elcts}}\right)\left(\frac{met}{met + k_{Emet}}\right)$$

$$\frac{dS}{dt} = (S)(\mu_{S})\left(\frac{ac}{ac + k_{Sac}}\right)$$

Example Abiotic Equation:

$$\frac{dlcts}{dt} = (Es)(\mu_{Es})\left(\frac{lcts}{lcts + k_{Elcts}}\right)\left(\frac{met}{met + k_{Emet}}\right) * c_{Elcts} + (Er)(\mu_{Er})\left(\frac{lcts}{lcts + k_{Elcts}}\right)\left(\frac{met}{met + k_{Emet}}\right) * c_{Elcts}$$

where represents the number of sensitive *E. coli* host cells killed by T7 phage infection with the adsorption constant ( ), β is the phage burst size, and Er represents the phage-resistance genotype that is seeded in at 0.1% of the sensitive population level.

To model P22*vir* infection of *S. enterica*, similar equations as above were used with Ss, Sr, and P22 equations to replace Es, Er, and T7 equations.

2. Resource-Explicit ODE Model Including Phage-Lysis Mediated Exchange of Cellular Debris

To our base model, we added the ability of non-host cells to consume cellular debris released during phage lysis of host cells. To accomplish this, we added a metabolite equation to represent cellular debris (cd). Production of cellular debris occurred when phage hosts died by phage lysis, with production rate parameter p_e_cd. Non-hosts (S) could grow using cellular debris with Monod kinetics. The consumption parameter c_s_cd describes the amount of cellular debris required to produce an *S. enterica* cell from cellular debris. *S. enterica* cells growing on acetate and cellular debris could grow faster than *S. enterica* cells growing on either resource alone because acetate and cellular debris could be used as substitutes for each other. Furthermore, growth on both substrates was additive.

Specifically, to model attacking *E. coli* with T7 phage allowing *S. enterica* to consume lysed *E. coli* cellular debris, we modified the previous set of equations describing phage infection of the host to include a cellular debris metabolite equation, and added a growth term to the non-host species to describe growth of cellular debris. Other metabolite equations were modified to include consumption of metabolites by cells that had been lysed during that time step.

3. Model Parameters

Table of model parameters with references can be found in Supplemental Table S2.1.

4. Simulation Framework

ODE models were numerically integrated using the lsoda solver from the deSolve package in R. Time was in units of hours. We set hmax = 0.001, rtol =$1x10^{-10}$ (default), and atol = $1x10^{-13}$, which improved the solutions. Code to run a sample model with a subset of parameters is included in the supplementary R script below.

References

[1] Harcombe WR. Novel cooperation experimentally evolved between species. Evolution. 2010;64:2166–72.

[2] Yin, J. A quantifiable phenotype of viral propagation. Biochem. Biophys. Res. Comms. 1991;174,2:1009-1014.

[3] Harcombe WR, Riehl WJ, Dukovski I, Granger BR, Betts A, Lang AH, et al. Metabolic resource allocation in individual microbes determines ecosystem interactions and spatial dynamics. Cell Rep. 2014;7:1104–15.

[4] De Paepe M and Taddei F (2006) Viruses' Life History: Towards a Mechanistic Basis of a Trade-Off between Survival and Reproduction among Phages. PLoS Biology 4(7): e193

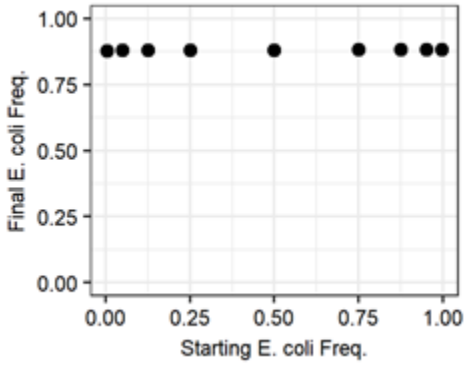

Supplemental Figure 2.1. Species frequencies converge in simulated growth regardless of starting frequencies. We began the simulation with various *E. coli* and *S. enterica* frequencies. Total beginning biomass was 2 x 10^6 cells regardless of starting ratio. We simulated cooperative growth until all lactose was consumed. Final *E. coli* frequencies of the total bacterial population (E + S) were calculated. Frequencies converged to ~0.88 (88% *E. coli*).

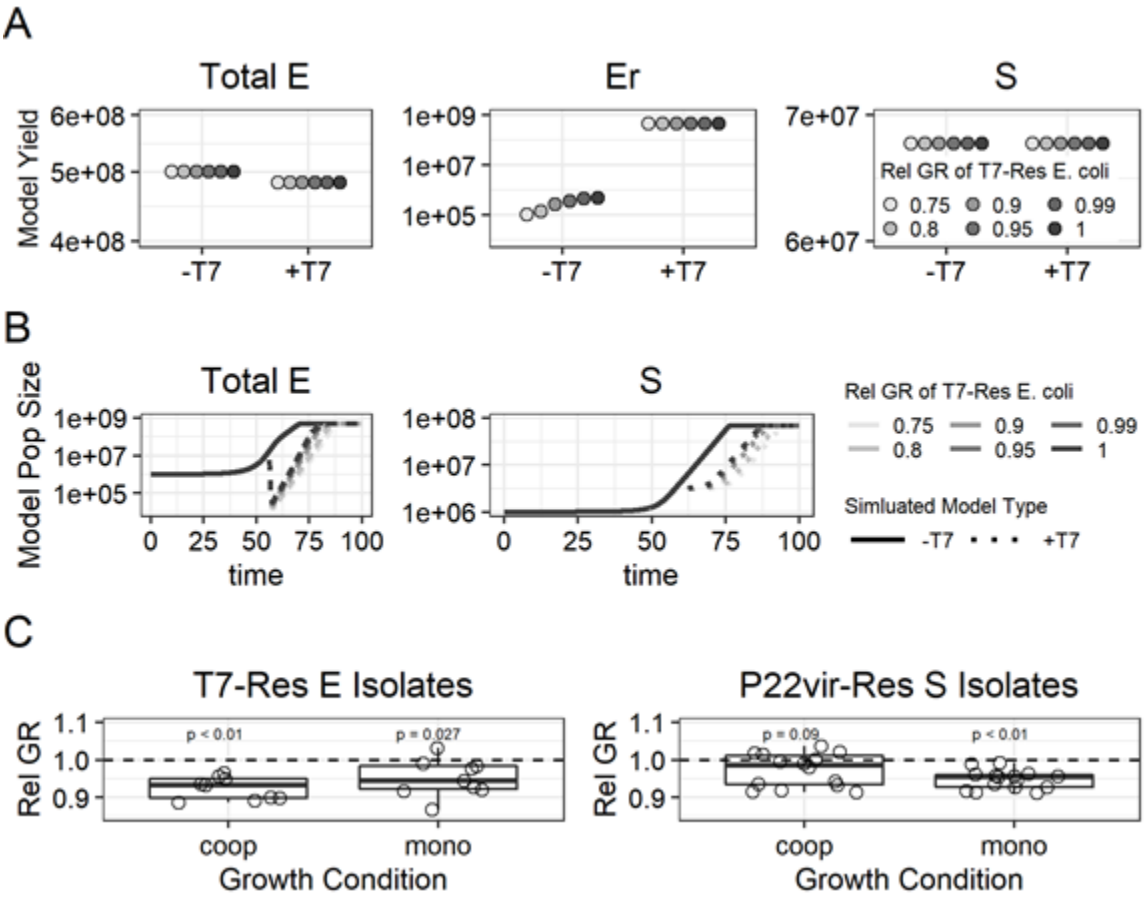

Supplemental Figure 2.2. Simulated and measured costs of resistance do not qualitatively change growth dynamics. In mathematical models, costs of resistance were simulated by decreasing the maximum growth rate of T7-resistant *E. coli* genotypes. Costs varied from 100% maximum relative growth rate (0% cost) to 75% maximum relative growth rate (25% cost). Simulations were run with and without phage. Costs did not change **A)** simulated yields of *E. coli* or *S. enterica*, but slightly alter final yields of resistant *E. coli* in cooperative co-cultures without phage. **B)** Costs also caused small growth delays. **C)** In wet-lab experiments, costs of resistance were measured for isolates by comparing growth rates in monoculture or co-culture with the ancestral isolate or co-cultured pair. Measured growth rates were standardized to ancestral growth rates. Average costs ranged from 0%-8% depending on the host species and growth conditions. Statistical significance determined with a one-sided T-test with mu = 1.

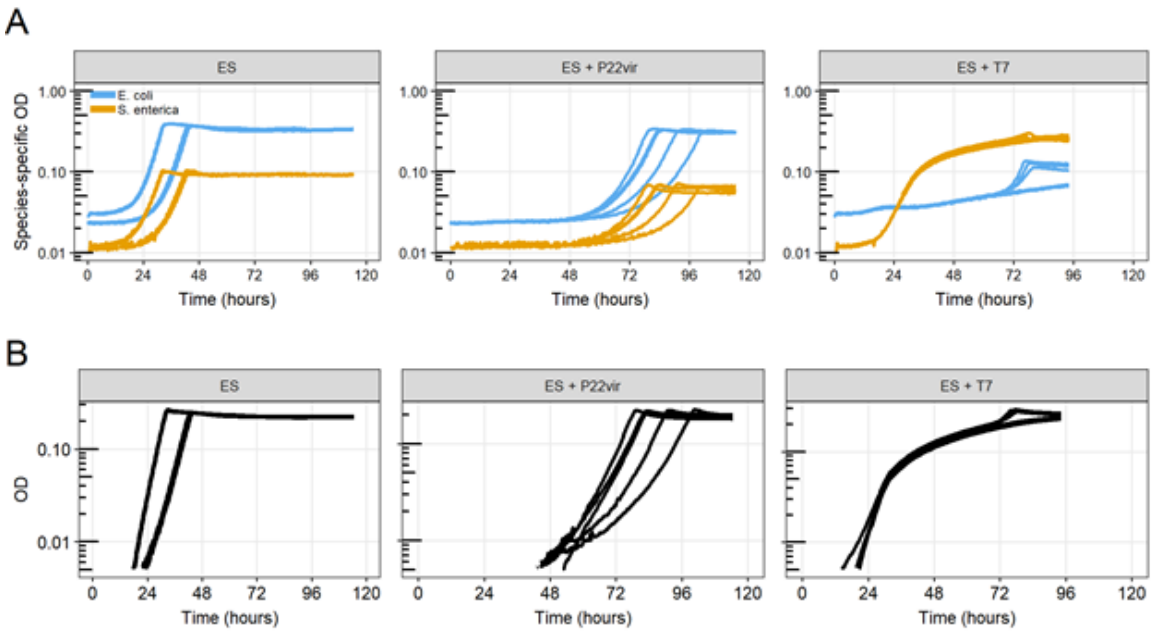

Supplemental Figure 2.3. Community OD shows more delayed growth during P22*vir* attack than T7 attack. A) Species-specific growth curves calculated by transforming fluorescence into species-specific OD for three treatments: no phage (ES), *S. enterica*-specific P22*vir* phage (ES + P22), or *E. coli*-specific T7 phage (ES + T7). *E. coli* (CFP) = blue, *S. enterica* (YFP) = yellow. Note: In ES + T7 panel (right), lower blue lines are two communities in which *E. coli* went extinct. CFP is not zero in these communities due to bleed-through from YFP channel. **B)** OD growth curves of cooperating communities treated with the indicated phage were measured every 20min in a shaking plate reader. OD is a proxy for growth of the whole bacterial community.

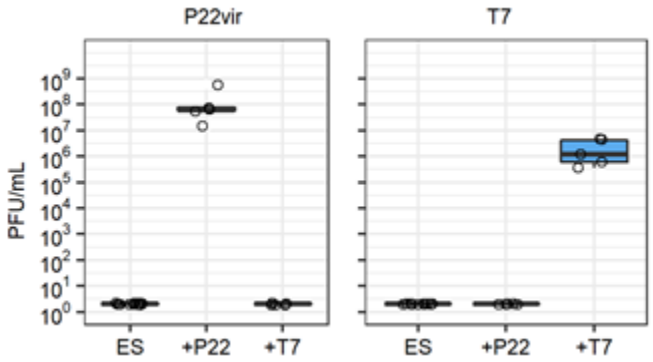

Supplemental Figure 2.4. Phage PFU measurements from wet-lab co-culture experiments. Phage titers of **A)** P22*vir* and **B)** T7 were measured for no phage controls (ES, n=10), co-culture with P22*vir* (+P22, n = 5), and co-cultures with T7 (+T7, n = 5).

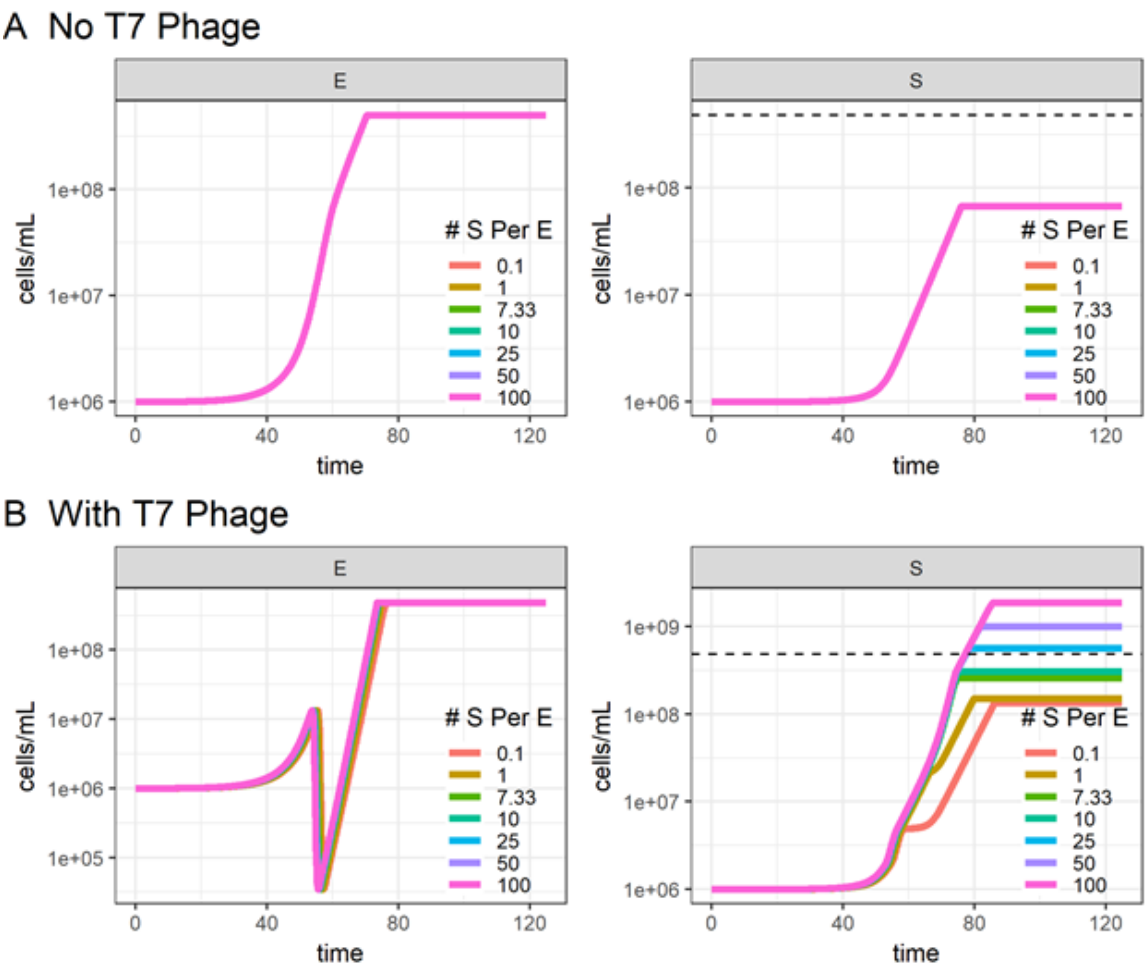

Supplemental Figure 2.5. Mathematic modeling a range of cellular debris conversion rates shows quantitative differences in non-host final yields. In mathematical models, conversion rates were simulated by including a scaling variable for the consumption of cellular debris parameter by *S. enterica*. Conversion rates ranging from 0.1 to 100 *S. enterica* cells produced per *E. coli* cell lysed by T7 phage did not affect A) simulated cooperative co-culture growth without T7 phage infection, and B) quantitatively, not qualitatively, changed only *S. enterica* yields in simulated growth with T7 phage attack of *E. coli*. Dashed line = observed median final *S. enterica* yields from wet-lab experiments.

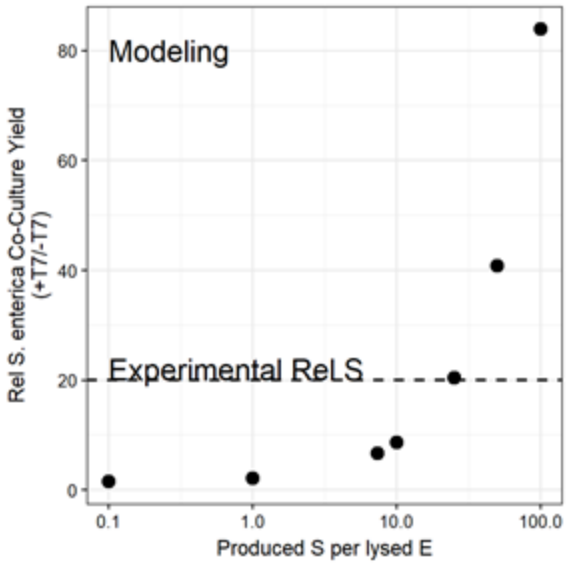

Supplemental Figure 2.6. Mathematically modeling a range of cellular debris conversion rates shows quantitative differences in non-host final yields. In mathematical models, conversion rates were simulated by including a scaling variable for the production of cellular debris parameter by *E. coli*. Simulating experimental relative S yields required production of ~ 25 *S. enterica* per lysed *E. coli*.

Supplemental Table S2.1. Resource-explicit mathematical model parameters.

Parameter	Description	Value	Units	Reference
μE	E, Es, Er growth rate (hr^{-1})	0.550 (lcts)	h^{-1}	This study
μS	S, Ss, Sr growth rate (hr^{-1})	0.156 (ac)	h^{-1}	This study
p_{ac}	Es & Er acetate production (base)	4×10^{-13} 6×10^{-13}	g/cell	[3] (Adjusted)
p_{met}	S methionine production	1×10^{-12}	g/cell	[3] (Adjusted)
p_{cd}	E production of cellular debris	2×10^{-12}	g/cell	This study
c_{ac}	S acetate consumption	3×10^{-12}	g/cell	[3] (Adjusted)
c_{cd}	S cellular debris consumption	2×10^{-12}	g/cell	This study
c_{lcts}	Es & Er lactose consumption	2×10^{-12}	g/cell	[3] (Adjusted)
c_{met}	Es & Er methionine consumption	5×10^{-14}	g/cell	[3] (Adjusted)
b	Burst size	100	phage progeny/infected cell	[4] (Adjusted)[a]
g	Adsorption rate (successful infection	10^{-9}	min^{-1}	[4] (Adjusted)[a]
k_{ac}	Michaelis-Menton acetate saturation	3×10^{-7}	g/200ml	[3] (Adjusted)
k_{cd}	Michaelis-Menton cellular debris	3×10^{-7}	g/200ml	This study
k_{lcts}	Michaelis-Menton lactose saturation	7×10^{-7}	g/200ml	[3] (Adjusted)
k_{met}	Michaelis-Menton methionine saturation	3×10^{-7}	g/200ml	[3] (Adjusted)

[a] De Paepe & Taddei (2006) [4] used *E. coli* strain MG1655 at 37°C in LB to measure parameters. We decreased our model burst rate (b) and adsorption rate (g) parameters to accommodate slower growth in 30°C growth in lactose minimal media.

Supplemental Table S2.2. Measured starting densities and MOIs.

Experiment #	Community Type	E (cells/well)	S (cells/well)	Phage (Type) (PFU/well)	MOI
1	ES	$2.25x10^5$	$1.77x10^5$	NA	NA
1	ES + T7	$2.25x10^5$	$1.77x10^5$	$1.6x10^3$ (T7)	0.007
2	ES	$1.1x10^5$	$1.16x10^4$	NA	NA
2	ES + P22*vir*	$1.1x10^5$	$1.16x10^4$	$2.1x10^2$ (P22*vir*)	0.018

Supplemental Table S2.3. Phage communities cross-streaked against evolved isolates.

Bacterial Isolates	Host Species	Comm. Rep #[a]	Community Treatment	Phage Lysate Community Replicate #[b]				
				1	2	3	4	5
Anc E	*E. coli*	NA	NA	S	Growth	S	Growth	S
1a	*E. coli*	1	ES + T7	PR (m)	R (m)	R (m)	R (m)	R (m)
1b	*E. coli*	1	ES + T7	PR (m)	R (m)	R (m)	R (m)	R (m)
1c	*E. coli*	1	ES + T7	PR (m)	R (m)	R (m)	R (m)	R (m)
3a	*E. coli*	3	ES + T7	PR (m)	R (m)	R (m)	R (m)	R (m)
3b	*E. coli*	3	ES + T7	PR (m)	R (m)	R (m)	R (m)	R (m)
3c	*E. coli*	3	ES + T7	PR (m)	R (m)	R (m)	R (m)	R (m)
5a	*E. coli*	5	ES + T7	PR (m)	R (m)	R (m)	R (m)	R (m)
5b	*E. coli*	5	ES + T7	PR (m)	R (m)	R (m)	R (m)	R (m)
5c	*E. coli*	5	ES + T7	PR (m)	R (m)	R (m)	R (m)	R (m)
Anc S	*S. enterica*	NA	NA	S	S	S	S	S
1a	*S. enterica*	1	ES + P22*vir*	R (nm)	R (nm)	R (nm)	R (nm)	R (nm)
1b	*S. enterica*	1	ES + P22*vir*	No Growth	No Growth	No Growth	No Growth	No Growth
1c	*S. enterica*	1	ES + P22*vir*	R (nm)	R (nm)	R (nm)	R (nm)	R (nm)
2a	*S. enterica*	2	ES + P22*vir*	R (nm)	R (nm)	R (nm)	R (nm)	R (nm)
2c	*S. enterica*	2	ES + P22*vir*	R (nm)	R (nm)	R (nm)	R (nm)	R (nm)
2b	*S. enterica*	2	ES + P22*vir*	R (nm)	R (nm)	R (nm)	R (nm)	R (nm)
3a	*S. enterica*	3	ES + P22*vir*	R (nm)	R (nm)	R (nm)	R (nm)	R (nm)

3b	*S. enterica*	3	ES + P22*vir*	R (nm)	R (nm)	R (nm)	R (nm)	R (nm)
3c	*S. enterica*	3	ES + P22*vir*	R (nm)	R (nm)	R (nm)	R (nm)	R (nm)
4a	*S. enterica*	4	ES + P22*vir*	R (nm)	R (nm)	R (nm)	R (nm)	R (nm)
4b	*S. enterica*	4	ES + P22*vir*	R (nm)	R (nm)	R (nm)	R (nm)	R (nm)
4c	*S. enterica*	4	ES + P22*vir*	R (nm)	R (nm)	R (nm)	R (nm)	R (nm)
5a	*S. enterica*	5	ES + P22*vir*	R (nm)	R (nm)	R (nm)	R (nm)	R (nm)
5b	*S. enterica*	5	ES + P22*vir*	R (nm)	R (nm)	R (nm)	R (nm)	R (nm)
5c	*S. enterica*	5	ES + P22*vir*	R (nm)	R (nm)	R (nm)	R (nm)	R (nm)

[a] *E. coli* in ES + T7 communities #2 and #4 went extinct.

[b] S = Sensitive, PR = Partial Resistant, R = Resistant, (nm) = non-mucoid, (m) = mucoid

Supplemental Table S2.4. Cellular debris conversions – cells produced per lysed cell equivalents.

Bacterial Cellular Debris Provided	# Cell-equivalents of cellular debris provided	Bacterial Species Produced	# Cells Produced	# Cells Produced Per Cell Lysed
E. coli	$1.8x10^7$	*S. enterica*	$1.32x10^8$	7.33
E. coli	$1.8x10^7$	*E. coli*	$6.03x10^5$	0.03
S. enterica	$4.1x10^7$	*S. enterica*	$2.56x10^6$	0.06
S. enterica	$4.1x10^7$	*E. coli*	$1.92x10^6$	0.05

Appendix 2: Nature Research Microbiology Community Blog Post associated with Ch. 2

This chapter is a reprint, with minor alterations, of a published Nature Research Microbiology Community blog post.

https://naturemicrobiologycommunity.nature.com/users/312265-will-harcombe/posts/54510-bacteriophage-serving-up-bacterial-buffets

Behind the Paper: Bacteriophage: Serving up bacterial buffets

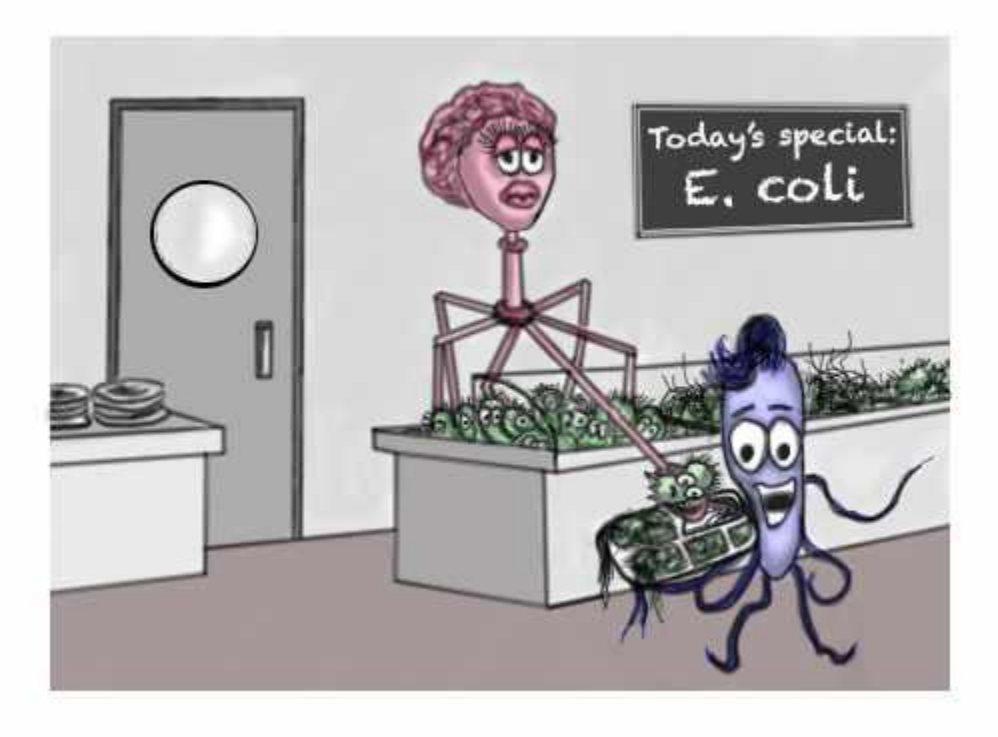

artwork by Brady King

Bacteriophage, or viruses that infect bacteria, are everywhere! They are thought to kill 10-25% of the bacteria in Earth's oceans every day1, meaning these viruses can significantly affect bacterial communities. Bacteriophage (phage) typically have a narrow host range; however in addition to directly killing cells, previous work has shown that phage can indirectly impact the abundance of non-hosts by altering the strength of competition between bacteria.2-4 I study how phage affect cooperative cross-feeding systems in which metabolites are exchanged between species. Our lab has developed a model cross-feeding co-culture of *Escherichia coli* and *Salmonella enterica*.5 These two bacterial strains form an obligate mutualism in which acetate and methionine are exchanged. We

found that phage infection can impact the non-host partner in diverse and under-appreciated ways. In some cases, the non-host is prevented from growing until phage resistance evolves in the host. In other instances, the non-host reaches higher final yields when its partner is decimated by phage infection, meaning phage infection breaks the cross-feeding dependency.

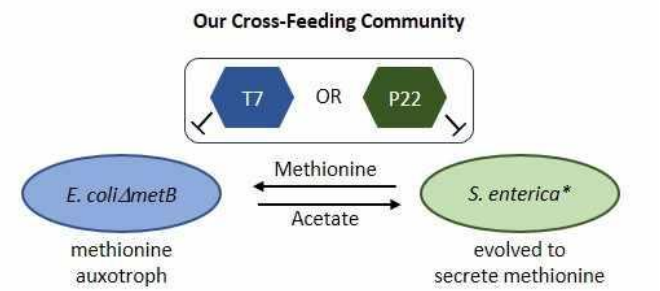

Mathematical modeling and previous work from our lab led us to predict that phage attack of either member of our cross-feeding coculture would slow community growth, but have little effect on final yields.6 Bench experiments showed that both *E. coli*-specific T7 phage and *S. enterica*-specific P22*vir* phage did indeed slow community growth, but there were some unexpected impacts on final yields. When *E. coli* was infected with T7, *S. enterica* reached HIGHER yields than in co-cultures without phage. The mathematical model completely missed the surprising benefit to *S. enterica* during T7 phage infection.

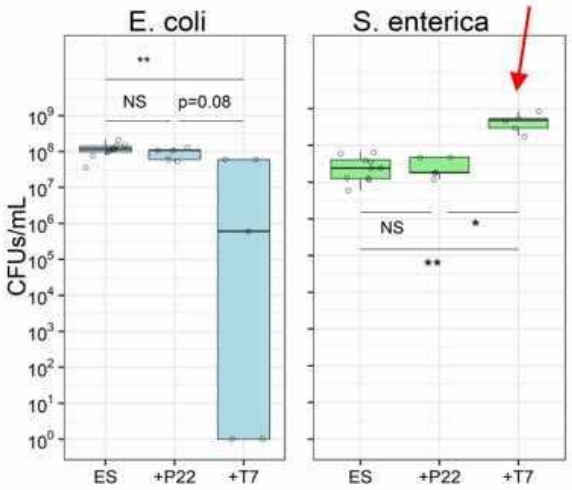

We used a combination of experiments and mathematical modeling to figure out two reasons why *S. enterica* benefited from phage infection when it should have suffered with its cross-feeding partner *E. coli*. First, the *S. enterica* consumed the cellular debris released by phage by lysed *E. coli*. We showed that dead *E. coli* were readily consumed by *S. enterica*, but dead *S. enterica* were hardly used by *E. coli*. Basically, *S. enterica* is happy to go to an *E. coli* carbon buffet, but *E. coli* is a picky eater - because it requires methionine from *S. enterica*, not carbon.

Second, PARTIAL phage resistance increased the benefit to *S. enterica*. *E. coli* isolates from the end of our T7 experiments were all mucoid! Mucoidy is extra exopolysaccharide that acts as a goopy physical barrier limiting phage infection. Mucoid *E. coli* were able to grow in the presence of phage, but the phage were still able to infect at some rate. Our models showed that partial resistance led to continual release of cellular debris over the course of growth, in contrast to the small burst of cellular debris released from sensitive

cells right after phage addition. To continue the metaphor, partial resistance allowed the carbon buffet to be continually restocked by phage.

It was surprising to find that phage could either constrain OR enhance growth of a cross-feeding partner. We are excited about the new questions this work has raised. Do these ecological dynamics continue through evolutionary time? Would multiple phage strains better prevent community-level bacterial growth? Overall, considering how the ecology and metabolism of phage hosts change consequences of infection could reveal new ways that phage control bacterial communities - including bacterial communities important to human health or food production.

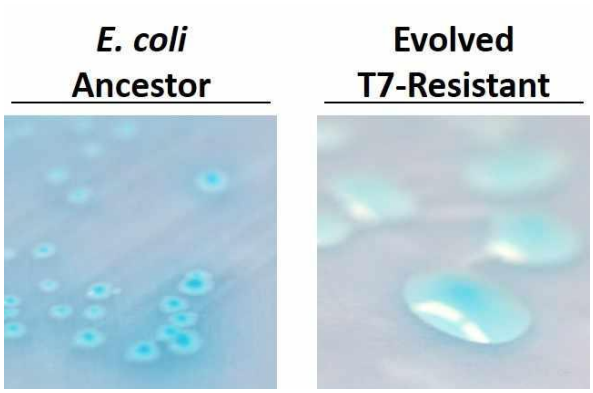

References:

(1) Suttle. Nat Rev Microbiol. (2007) 5, 801–437

(2) Harcombe & Bull. AEM (2005) 7:9, 5254-5259

(3) Brookhurst *et. al.* BMC Ecology (2006) 6:19

(4) Yu *et. al.* Environmental Science & Technology (2017) 51, 5270−5278

(5) Harcombe. Evolution (2010) 64-7, 2166–2172

(6) Adamowicz *et. al.*. The ISME J (2018) 12:11, 2723-2735

Appendix 3: Supporting figures & tables from Ch. 3

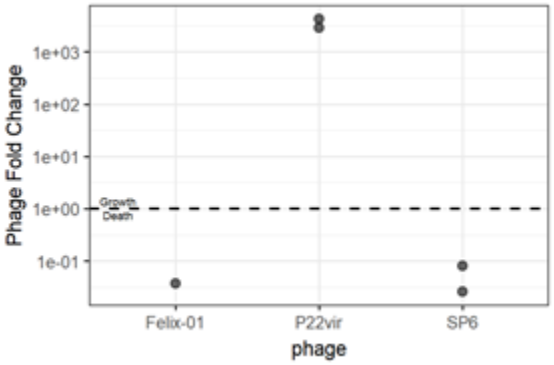

Supplemental Figure 3.1. Screening of *S. enterica*-specific phage activity in cooperative coculture. P22*vir*, SP6, and Felix-01 *S. enterica*-specific phages were inoculated into *E. coli-S. enterica* cocultures and grown at 30°C while shaking until stationary phase was reached (4-5 days, n = 1-2). Initial and final PFU/ml were measured by plating with ancestral *S. enterica.* Only P22*vir* increased in concentration over the growth period.

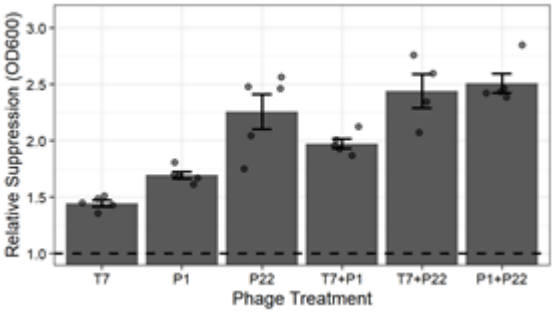

Supplemental Figure 3.2. Coculture-level suppression lengths caused by phage treatments. Relative coculture suppression lengths of single and cocktail phage treatments standardized to the no phage control. Suppression length was calculated using 95% maximum OD600. Bars represent means ± SE (n = 4-5).

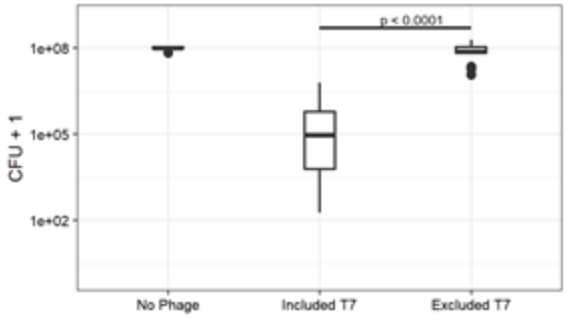

Supplemental Figure 3.3. Boxplots of final *E. coli* densities after phage treatments. Including T7 phage in treatments lowered final *E. coli* population size. Cocultures were grown with single phage treatments and cocktails and bacterial populations sizes were counted by plating with selective plates. Statistical significance was tested with a Two-sample Mann–Whitney U. (n = 15)

Supplemental Table S3.1. Absolute and relative suppression lengths of phage treatments.

Phage Treatment	Treatment Type	Absolute Suppression Length (hrs ± SE)	Relative Suppression Length (standardized to phage-free)
Phage-free	None	34.44 ± 0.0	1.00 ± 0.0
T7	Single phage	49.74 ± 2.05	1.44 ± 0.06
P1vir	Single phage	58.37 ± 2.35	1.69 ± 0.07
P22vir	Single phage	77.7 ± 12.0	2.26 ± 0.35
T7+P1vir	Pathogen-targeting	67.98 ± 3.28	1.97 ± 0.10
T7+P22vir	Multispecies-targeting	84.03 ± 10.42	2.44 ± 0.30
P1vir + P22vir	Multispecies-targeting	86.3 ± 6.56	2.5 ± 0.19

Supplemental Table S3.2. Parameters for resource-explicit ODE mathematical model.

Parameter (name in model)	Parameter value
E. coli growth rate (mu_e)	0.291/hr
S. enterica growth rate (mu_s)	0.221/hr
E. coli production of ace (p_e_ace)	4e-12 grams produced/*E. coli* cell
S. enterica consumption of ace (c_s_ace)	3e-12 grams consumed/*S. enterica* cell
S. enterica production of met (p_s_met)	4e-12 grams produced/*S. enterica* cell
E. coli consumption of met (c_s_met)	3e-12 grams consumed/*E. coli* cell
E. coli-specific T7 burst size (burst_T7)	100 phage/burst *E. coli* cell
E. coli-specific T7 adsorption rate	1e-9 /phage**E. coli* cell
E. coli-specific P1*vir* burst size (burst_P1)	100 phage/burst *E. coli* cell
E. coli-specific P1*vir* adsorption rate	1e-9 /phage**E. coli* cell
S. enterica-specific P22*vir* burst size (burst_P22)	100 phage/burst *S. enterica* cell
S. enterica-specific P22*vir* adsorption rate	1e-9 /phage**E. coli* cell

Supplemental Table S3.3. Starting densities of cross- and dual-resistance modeling.

Simulated Organism	Organism Description	Cross-Resistance	Dual-Resistance
Es	Sensitive *E. coli*	9.98999e5	9.97999e5
ErT7	T7-resistance *E.coli*	0	1e3
ErP1vir	P1vir-resistant *E. coli*	0	1e3
Er	T7- and P1vir-resistant *E. coli*	1.001e3	1
Ss	Sensitive *S. enterica*	9.98999e5	9.97999e5
SrP22vir	P22vir-resistant *S. enterica*	0	1e3
Sr2	Phage2-resistant *S. enterica* [a]	0	1e3
Sr	P22vir and Phage2-resistant *S. enterica*	1.001e3	1
Total Biomass	Sum of all bacterial biomass	1e6	1e6

[a] Phage 2 is for simulation purposes only and does not correspond to a second experimental *S. enterica* phage.

Appendix 4: Supporting figures & tables from Ch. 4

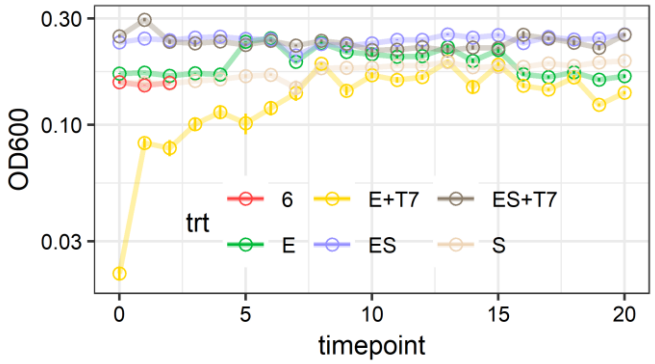

Figure S4.1. Community-level OD600-based growth curves. All plotted points show mean population OD600 measurements ± SE (n=6).

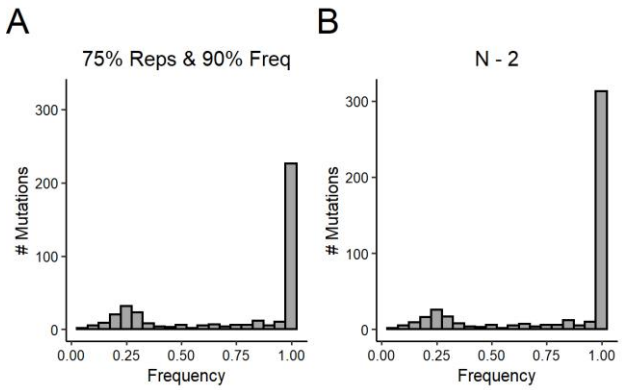

Figure S4.2. Ancestral mutation filtering robustness analysis. Distributions of mutations not identified as ancestral were plotted for A) ancestral mutations that were found in 75% of expected communities and arose to 90% in all communities in which a mutation was identified, B) ancestral mutations that were in N-2 expected communities

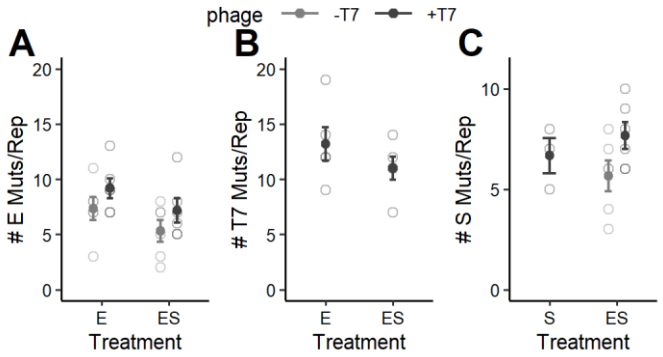

Figure S4.3. Number of mutations per replicate community with ancestral filtering = 75% replicates and at least 90% frequency in all replicates. Mutations were filtered with 75% reps and 90% frequency method and the total number of mutations per replicate community (# Muts/Rep) in **A)** the *E. coli* (E), **B)** T7 phage (T7), and **C)** *S. enterica* (S) genomes were calculated. Results were not qualitatively different from N-2 ancestral filtering method (see main text). *E. coli* acquired more mutations when exposed to phage ($F(1,21)=3.46$, $p=0.077$) and fewer in coculture ($F(1,21)=4.12$, $p=0.055$). The number of *S. enterica* mutations were larger when cocultured with phage ($F(1,12)=4.08$, $p = 0.067$), but no difference when cross-feeding ($F(1,12)=0.0$, $p=1.0$). The number of T7 mutations was not affected by coculturing either ($T:1.09$, $p=0.31$). Light grey points = number of mutations in individual replicate communities, black points = mean number of mutations ± SE (n=6, expect S treatment where n=3). Statistical significance was determined with two-way ANOVA for E mutations, t-test for T7 mutations, and one-way ANOVA for S mutations.

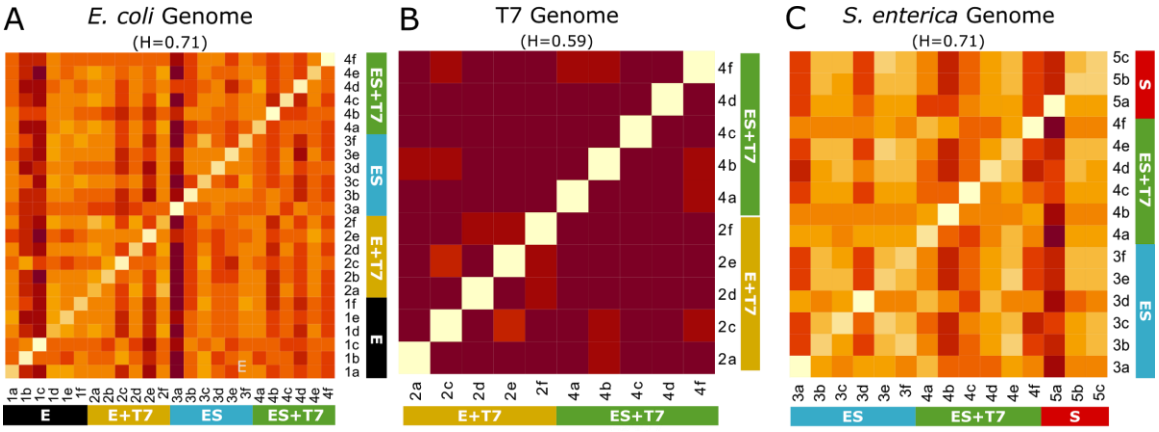

Figure S4.4. Visual assessment of clustering tendency of mutations from the A) *E. coli* genome, B) T7 phage genome, or C) *S. enterica* genome. H = Hopkin's statistic where 0.5 is random patterns and 1 is strong clustering. There is weak clustering in *E. coli* and *S. enterica* genomes, and almost no clustering in T7 genomes. Heatmaps were made from a Bray-Curtis dissimilarity matrix calculated with the vegan package and are a visual representation of Hopkin's statistic. If samples are similar based on mutational signatures, then there would be blocks of light yellow around samples of the same treatment. Red = dissimilar, Light yellow = similar.

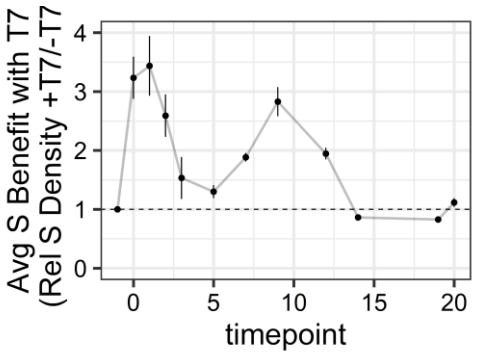

Figure S4.5. Benefit to *S. enterica* when cocultured with *E. coli* and T7 phage. Population sizes of *S. enterica* in phage-containing cocultures were standardized to the average *S. enterica* population size in phage-free coculture as a relative benefit metric. Here the dotted line (y = 1) represents when the population sizes in phage-containing and phage-free cocultures are equal.

Supplemental Table S4.1. Reference genomes and accession numbers.

Genetic Element	Genome	Accession Number
Escherichia coli str. K-12 substr. MG1655	*E. coli*	NZ_CP009273.1
Escherichia coli F-plasmid	*E. coli*	NC_002483.1
Salmonella enterica subsp. *enterica* serovar *Typhimurium* str. LT2	*S. enterica*	NC_003197.2
Salmonella enterica plasmid pSLT	*S. enterica*	NC_003277.1
Salmonella enterica plasmid pR27 transposon Tn10	*S. enterica*	NG_035265.1
T7 phage genome	T7	V01146.1

Supplemental Table S4.2 Evolved Mutations Filtered with N-2 Method

	Frequency of Mutation									
sample	1a	1b	1c	1d	1e	1f	2a	2b	2c	2d
treatment	E	E	E	E	E	E	E+T7	E+T7	E+T7	E+T7
Mutation (Genome, Basepair Number, New Base)										
NC_002483 52320 A	0.8551	0.0000	0.0000	0.7129	0.7702	0.8381	0.8485	0.7703	0.0000	0.8310
NC_002483 61959 CT	1.0000	1.0000	1.0000	1.0000	1.0000	1.0000	1.0000	1.0000	1.0000	1.0000
NC_002483 61960 T	0.0000	0.0000	0.0000	0.0000	0.0000	0.0000	0.0000	0.0000	0.0000	0.0000
NC_002483 63485 NA	0.0000	1.0000	0.0000	1.0000	0.0000	1.0000	1.0000	1.0000	1.0000	1.0000
NC_002483 63526 C	1.0000	0.0000	0.0000	1.0000	1.0000	1.0000	1.0000	1.0000	0.0000	1.0000
NC_002483 63577 C	0.3016	0.0000	0.0000	0.0000	0.0000	0.0000	0.0000	0.0000	0.0000	0.0000
NC_002483 63655 T	1.0000	0.0000	0.0000	1.0000	1.0000	1.0000	1.0000	1.0000	1.0000	1.0000
NC_002483 63842 A	0.0000	1.0000	0.0000	0.0000	0.0000	1.0000	0.0000	0.0000	1.0000	0.0000
NC_002483 63843 G	0.8000	1.0000	0.0000	0.0000	0.0000	0.0000	0.0000	0.8667	1.0000	0.0000
NC_002483 65446 NA	1.0000	1.0000	1.0000	1.0000	1.0000	1.0000	1.0000	1.0000	1.0000	1.0000
NC_002483 65618 T	1.0000	1.0000	0.0000	1.0000	1.0000	1.0000	1.0000	1.0000	1.0000	1.0000
NC_002483 66089 T	1.0000	0.0000	0.0000	1.0000	1.0000	1.0000	1.0000	1.0000	0.0000	1.0000
NC_002483 83617 C	0.0000	0.0000	0.0000	0.0000	0.0000	0.0000	0.0000	0.0000	0.0000	0.0000
NC_003197 1104985 C	0.0000	0.0000	0.0000	0.0000	0.0000	0.0000	0.0000	0.0000	0.0000	0.0000
NC_003197 1593992 T	0.0000	0.0000	0.0000	0.0000	0.0000	0.0000	0.0000	0.0000	0.0000	0.0000
NC_003197 2058713 NA	0.0000	0.0000	0.0000	0.0000	0.0000	0.0000	0.0000	0.0000	0.0000	0.0000
NC_003197 2358702 G	0.0000	0.0000	0.0000	0.0000	0.0000	0.0000	0.0000	0.0000	0.0000	0.0000
NC_003197 2358706 C	0.0000	0.0000	0.0000	0.0000	0.0000	0.0000	0.0000	0.0000	0.0000	0.0000
NC_003197 2730867 NA	0.0000	0.0000	0.0000	0.0000	0.0000	0.0000	0.0000	0.0000	0.0000	0.0000
NC_003197 2730889 NA	0.0000	0.0000	0.0000	0.0000	0.0000	0.0000	0.0000	0.0000	0.0000	0.0000
NC_003197 2730895 NA	0.0000	0.0000	0.0000	0.0000	0.0000	0.0000	0.0000	0.0000	0.0000	0.0000
NC_003197 2730907 NA	0.0000	0.0000	0.0000	0.0000	0.0000	0.0000	0.0000	0.0000	0.0000	0.0000
NC_003197 2770105 TTAGTTGCAC	0.0000	0.0000	0.0000	0.0000	0.0000	0.0000	0.0000	0.0000	0.0000	0.0000
NC_003197 3676853 A	0.0000	0.0000	0.0000	0.0000	0.0000	0.0000	0.0000	0.0000	0.0000	0.0000
NC_003197 4099877 C	0.0000	0.0000	0.0000	0.0000	0.0000	0.0000	0.0000	0.0000	0.0000	0.0000
NC_003197 4155512 T	0.0000	0.0000	0.0000	0.0000	0.0000	0.0000	0.0000	0.0000	0.0000	0.0000
NC_003197 4155518 A	0.0000	0.0000	0.0000	0.0000	0.0000	0.0000	0.0000	0.0000	0.0000	0.0000
NC_003197 4244681 G	0.0000	0.0000	0.0000	0.0000	0.0000	0.0000	0.0000	0.0000	0.0000	0.0000
NC_003197 4310137 NA	0.0000	0.0000	0.0000	0.0000	0.0000	0.0000	0.0000	0.0000	0.0000	0.0000
NC_003197 4311847 NA	0.0000	0.0000	0.0000	0.0000	0.0000	0.0000	0.0000	0.0000	0.0000	0.0000
NC_003197 4312824 NA	0.0000	0.0000	0.0000	0.0000	0.0000	0.0000	0.0000	0.0000	0.0000	0.0000
NC_003197 4433283 CG	0.0000	0.0000	0.0000	0.0000	0.0000	0.0000	0.0000	0.0000	0.0000	0.0000
NC_003197 4631400 GC	0.0000	0.0000	0.0000	0.0000	0.0000	0.0000	0.0000	0.0000	0.0000	0.0000
NZ_CP009273 1147986 NA	0.0000	1.0000	0.0000	0.0000	0.0000	0.0000	0.0000	0.0000	0.0000	0.0000
NZ_CP009273 1148228 GGCGCA	0.0000	0.0000	0.0000	0.0000	0.0000	0.8102	0.0000	0.0000	0.0000	0.0000
NZ_CP009273 1298631 T	0.0000	0.0000	0.0000	0.0000	0.0000	0.0000	0.0000	0.0000	0.0000	0.0000
NZ_CP009273 1973112 NA	1.0000	0.0000	0.0000	1.0000	1.0000	1.0000	1.0000	1.0000	0.0000	1.0000
NZ_CP009273 2068176 C	0.0000	0.0000	0.0000	0.0000	0.2058	0.1692	0.0000	0.1876	0.0000	0.0000
NZ_CP009273 2107740 NA	0.0000	0.0000	0.0000	0.0000	0.0000	0.0000	0.0000	0.0000	0.0000	0.0000
NZ_CP009273 2133770 NA	0.0000	0.0000	0.0000	0.0000	0.0000	0.0000	0.0000	0.0841	0.5007	0.0000
NZ_CP009273 2278193 NA	0.0000	0.0000	0.0000	0.0000	0.0000	0.0000	0.0000	0.0000	0.0000	0.0000
NZ_CP009273 240327 NA	0.0000	0.0000	0.0000	0.0000	0.0000	0.0000	0.0000	0.0000	0.0000	0.0000
NZ_CP009273 2557859 A	0.0000	0.0000	0.0000	0.0000	0.0000	0.0000	0.0000	0.0000	0.0000	0.0000
NZ_CP009273 2860008 C	0.0000	0.0000	0.0000	0.0000	0.0000	0.0000	0.0000	0.0000	0.0000	0.0000
NZ_CP009273 2860214 NA	0.0000	0.0000	0.0000	0.0000	0.0000	0.0000	0.0000	0.0000	0.0000	0.0000

Supplemental Table S4.2 Evolved Mutations Filtered with N-2 Method (continued)

	Frequency of Mutation									
sample	1a	1b	1c	1d	1e	1f	2a	2b	2c	2d
treatment	E	E	E	E	E	E	E+T7	E+T7	E+T7	E+T7
Mutation (Genome, Basepair Number, New Base)										
NZ_CP009273 2860234 NA	0.0000	0.0000	0.0000	0.0000	0.0000	0.0000	0.0000	0.0000	0.0000	0.0000
NZ_CP009273 2860332 G	0.0000	0.0000	0.0000	0.0000	0.0000	0.0000	0.0000	0.0000	0.0000	0.0000
NZ_CP009273 2860874 NA	0.0000	0.0000	0.0000	0.0000	0.0000	0.0000	0.0000	0.0000	0.0000	0.0000
NZ_CP009273 2904839 NA	0.0000	0.0000	0.0000	0.0000	0.0000	0.0000	0.0000	0.0000	0.0000	0.0000
NZ_CP009273 303915 C	0.0000	0.0000	0.0000	0.0000	0.0000	0.0000	0.0000	0.1730	0.0000	0.0000
NZ_CP009273 3189869 NA	0.0000	0.0000	0.0000	0.0000	0.0000	0.0000	0.0000	0.0000	0.0000	0.0000
NZ_CP009273 3303994 NA	0.0000	0.0000	0.0000	0.0000	0.0000	0.0000	0.0000	0.0000	0.0000	0.0000
NZ_CP009273 3319471 T	0.0000	0.0000	0.0000	0.0000	0.0000	0.0000	0.0000	0.0000	0.0000	0.0000
NZ_CP009273 3336357 NA	0.0000	0.0000	0.0000	0.0000	0.0000	0.0000	0.0000	0.0000	0.0000	0.0000
NZ_CP009273 3386512 NA	0.0000	0.0000	0.0000	0.0000	0.0000	0.0000	0.0000	0.0000	0.0000	1.0000
NZ_CP009273 360927 C	0.0000	0.0000	0.0000	0.0000	0.0000	0.0000	0.0000	0.0000	0.0000	0.0000
NZ_CP009273 361004 A	0.0000	0.0000	0.0000	0.0000	0.0000	0.0000	0.0000	0.0000	0.0000	0.0000
NZ_CP009273 361139 GCCA	0.1624	0.0000	0.0000	0.1765	0.0914	0.0907	0.0000	0.0000	0.0000	0.1764
NZ_CP009273 361140 NA	0.0000	0.0000	0.0000	0.0000	0.0000	0.0000	0.0000	0.0000	0.0000	0.0000
NZ_CP009273 361149 CAGACG	0.0000	0.0000	0.0000	0.0000	0.0000	0.0000	0.0000	0.0000	0.0000	0.0000
NZ_CP009273 361287 A	0.0000	0.0000	0.0000	0.0000	0.0000	0.0000	0.0000	0.0000	0.0000	0.0000
NZ_CP009273 3629231 NA	0.0000	0.0000	0.0000	0.0000	0.0000	0.0000	0.0000	0.0000	1.0000	0.0000
NZ_CP009273 3669214 NA	0.0000	0.0000	0.0000	0.0000	0.0000	0.0000	0.8962	0.0000	0.0000	0.0000
NZ_CP009273 3706292 A	0.0000	0.0000	0.0000	0.0000	0.0000	0.1585	0.0000	0.0000	0.0000	0.0000
NZ_CP009273 3799448 NA	0.0000	0.0000	0.0000	0.0000	0.0000	0.0000	1.0000	0.0000	0.0000	1.0000
NZ_CP009273 3799800 NA	0.0000	0.0000	0.0000	0.0000	0.0000	0.0000	0.0000	0.4284	1.0000	0.0000
NZ_CP009273 3800001 NA	0.0000	0.0000	0.0000	0.0000	0.0000	0.0000	0.0000	0.5772	0.0000	0.0000
NZ_CP009273 3944901 NA	0.0000	1.0000	0.0000	0.0000	0.0000	0.0000	0.0000	0.0000	0.0000	0.0000
NZ_CP009273 3960101 T	0.0000	0.0000	0.0000	0.0000	0.0000	0.0000	0.0000	0.0000	0.0000	0.0000
NZ_CP009273 3960515 T	0.0000	0.0000	0.0000	0.0000	0.0000	0.0000	0.0000	0.0000	0.0000	0.0000
NZ_CP009273 4076055 G	0.0000	0.0000	0.0000	0.0000	0.0000	0.0000	0.0000	0.0000	0.0000	0.0000
NZ_CP009273 4118604 TTCCGGGGATCCGTCGACCT GCAGTTCGAAGTTCCTATTC TCTAGAAAGTATAGGAACTT CGAAGCAGCTCCAGCCTACA	0.0000	1.0000	1.0000	0.0000	0.0000	0.0000	0.0000	0.0000	1.0000	0.0000
NZ_CP009273 4177773 NA	0.0000	0.0000	0.0000	0.0000	0.0000	0.9315	0.0000	0.0000	0.0000	0.0000
NZ_CP009273 4178501 T	0.0000	0.0000	1.0000	0.0000	0.0000	0.0000	0.0000	0.0000	0.0000	0.0000
NZ_CP009273 42141 T	0.0000	0.0000	0.0000	0.0000	0.0000	0.0000	0.0000	0.0000	0.0000	0.0000
NZ_CP009273 4226052 NA	0.0000	0.0000	0.0000	0.0000	0.0000	0.0000	0.0000	0.0000	0.0000	0.0000
NZ_CP009273 4226403 T	0.0000	0.0000	0.0000	0.0000	0.0000	0.0000	0.0000	0.0000	0.0000	0.7953
NZ_CP009273 4226594 NA	0.0000	0.0000	0.0000	0.0000	0.0000	0.0000	0.0000	0.0000	0.0000	0.0000
NZ_CP009273 4227883 NA	0.0000	0.0000	0.0000	0.0000	0.0000	0.0000	0.0000	0.3577	1.0000	0.0000
NZ_CP009273 4228249 NA	0.0000	0.0000	0.0000	0.0000	0.0000	0.0000	0.0000	0.0000	0.0000	0.0000
NZ_CP009273 4228789 T	0.0000	0.0000	0.0000	0.0000	0.0000	0.0000	0.0000	0.0000	0.0000	0.0000
NZ_CP009273 4228998 A	0.0000	0.0000	0.0000	0.0000	0.0000	0.0000	0.0000	0.0000	0.0000	0.0000
NZ_CP009273 4229421 NA	0.0000	0.0000	0.0000	0.0000	0.0000	0.0000	0.0000	0.6332	0.0000	0.0000
NZ_CP009273 4273156 G	0.0000	0.0000	0.0000	0.0000	0.3384	0.1653	0.0000	0.0000	0.0000	0.0000
NZ_CP009273 454246 NA	0.0000	0.0000	0.0000	0.0000	0.0000	0.0000	1.0000	1.0000	1.0000	1.0000
NZ_CP009273 454248 NA	0.0000	0.0000	0.0000	0.0000	0.0000	0.0000	0.0000	0.0000	0.0000	0.0000
NZ_CP009273 513494 T	0.0000	0.0000	0.0000	0.0000	0.0000	0.0000	0.0000	0.0000	0.0000	0.0000
NZ_CP009273 51993 NA	0.0000	0.0000	0.0000	0.0000	0.0000	0.0000	0.0000	0.0000	0.0000	0.8521

Supplemental Table S4.2 Evolved Mutations Filtered with N-2 Method (continued)

	Frequency of Mutation									
sample	1a	1b	1c	1d	1e	1f	2a	2b	2c	2d
treatment	E	E	E	E	E	E	E+T7	E+T7	E+T7	E+T7
Mutation (Genome, Basepair Number, New Base)										
NZ_CP009273 571113 C	0.0000	0.2665	0.0000	0.0000	0.0000	0.0000	0.0000	0.0000	0.0000	0.0000
NZ_CP009273 632236 C	0.5001	0.0000	0.0000	0.0000	0.0000	0.0000	0.0000	0.0000	0.0000	0.0000
NZ_CP009273 733422 NA	0.0000	1.0000	0.0000	0.0000	0.0000	0.0000	0.0000	0.0000	0.0000	0.0000
NZ_CP009273 83868 T	0.5752	0.0000	0.0000	0.0000	0.0000	0.0000	0.0000	0.0000	0.0000	0.0000
NZ_CP009273 83881 T	0.0000	0.0000	0.0000	0.0000	1.0000	0.0000	0.0000	0.0000	0.0000	0.0000
NZ_CP009273 83893 T	0.0000	0.0000	0.0000	0.3492	0.0000	0.0000	0.0000	0.0000	0.0000	0.0000
NZ_CP009273 84227 A	0.0000	0.0000	1.0000	0.0000	0.0000	0.0000	0.0000	0.0000	0.0000	0.0000
NZ_CP009273 84294 A	0.0000	0.0000	0.0000	0.7787	0.0000	0.0000	0.0000	0.0000	0.0000	0.0000
V01146 10203 A	0.0000	0.0000	0.0000	0.0000	0.0000	0.0000	0.0000	0.0000	0.0000	0.0000
V01146 10308 T	0.0000	0.0000	0.0000	0.0000	0.0000	0.0000	0.0000	0.0000	0.0000	0.0000
V01146 10922 A	0.0000	0.0000	0.0000	0.0000	0.0000	0.0000	0.0000	0.0000	0.0000	0.0000
V01146 11197 C	0.0000	0.0000	0.0000	0.0000	0.0000	0.0000	0.0000	0.0000	0.0000	0.0000
V01146 12114 A	0.0000	0.0000	0.0000	0.0000	0.0000	0.0000	0.0000	0.0000	0.0000	0.0000
V01146 1379 NA	0.0000	0.0000	0.0000	0.0000	0.0000	0.0000	0.0000	0.0000	0.0000	0.0000
V01146 16410 A	0.0000	0.0000	0.0000	0.0000	0.0000	0.0000	0.0000	0.0000	0.0000	0.0000
V01146 16795 G	0.0000	0.0000	0.0000	0.0000	0.0000	0.0000	1.0000	0.0000	0.0000	0.0000
V01146 1867 A	0.0000	0.0000	0.0000	0.0000	0.0000	0.0000	1.0000	0.0000	0.0000	0.0000
V01146 19344 C	0.0000	0.0000	0.0000	0.0000	0.0000	0.0000	1.0000	0.0000	0.0000	0.0000
V01146 1936 T	0.0000	0.0000	0.0000	0.0000	0.0000	0.0000	0.0000	0.0000	0.0000	0.0000
V01146 19517 C	0.0000	0.0000	0.0000	0.0000	0.0000	0.0000	0.0000	0.0000	0.0000	0.0000
V01146 19572 T	0.0000	0.0000	0.0000	0.0000	0.0000	0.0000	0.0000	0.0000	0.0000	1.0000
V01146 19584 T	0.0000	0.0000	0.0000	0.0000	0.0000	0.0000	0.0000	0.0000	0.0000	0.0000
V01146 19602 T	0.0000	0.0000	0.0000	0.0000	0.0000	0.0000	0.0000	0.0000	1.0000	0.0000
V01146 19672 NA	0.0000	0.0000	0.0000	0.0000	0.0000	0.0000	0.0000	0.0000	0.0000	0.0000
V01146 19677 C	0.0000	0.0000	0.0000	0.0000	0.0000	0.0000	0.0000	0.0000	0.0000	0.0000
V01146 19728 T	0.0000	0.0000	0.0000	0.0000	0.0000	0.0000	0.0000	0.0000	0.0000	0.0000
V01146 2243 T	0.0000	0.0000	0.0000	0.0000	0.0000	0.0000	0.0000	0.0000	0.0000	0.0000
V01146 23007 T	0.0000	0.0000	0.0000	0.0000	0.0000	0.0000	0.0000	0.0000	0.0000	0.0000
V01146 23230 C	0.0000	0.0000	0.0000	0.0000	0.0000	0.0000	0.0514	0.0000	0.0000	0.0000
V01146 23799 C	0.0000	0.0000	0.0000	0.0000	0.0000	0.0000	0.0000	0.0000	0.0000	0.0000
V01146 23817 T	0.0000	0.0000	0.0000	0.0000	0.0000	0.0000	0.0000	0.0000	0.0000	0.0000
V01146 23991 C	0.0000	0.0000	0.0000	0.0000	0.0000	0.0000	1.0000	0.0000	0.0000	0.0000
V01146 23991 G	0.0000	0.0000	0.0000	0.0000	0.0000	0.0000	0.0000	0.0000	0.0000	1.0000
V01146 24044 C	0.0000	0.0000	0.0000	0.0000	0.0000	0.0000	0.0000	0.0000	0.0000	0.0000
V01146 24046 T	0.0000	0.0000	0.0000	0.0000	0.0000	0.0000	0.0000	0.0000	0.0000	0.0000
V01146 24051 G	0.0000	0.0000	0.0000	0.0000	0.0000	0.0000	0.0000	0.0000	0.0000	0.0000
V01146 24178 A	0.0000	0.0000	0.0000	0.0000	0.0000	0.0000	0.0000	0.0000	0.0000	0.0000
V01146 24204 NA	0.0000	0.0000	0.0000	0.0000	0.0000	0.0000	0.0000	0.0000	0.0000	0.0000
V01146 24273 A	0.0000	0.0000	0.0000	0.0000	0.0000	0.0000	0.0000	0.0000	0.0000	1.0000
V01146 24274 A	0.0000	0.0000	0.0000	0.0000	0.0000	0.0000	0.0000	0.0000	1.0000	0.0000
V01146 24312 A	0.0000	0.0000	0.0000	0.0000	0.0000	0.0000	0.0000	0.0000	0.0000	0.0000
V01146 24346 T	0.0000	0.0000	0.0000	0.0000	0.0000	0.0000	0.0000	0.0000	1.0000	0.0000
V01146 24370 G	0.0000	0.0000	0.0000	0.0000	0.0000	0.0000	0.0000	0.0000	0.0000	0.0000
V01146 24397 A	0.0000	0.0000	0.0000	0.0000	0.0000	0.0000	0.0000	0.0000	0.0000	0.0000
V01146 24498 A	0.0000	0.0000	0.0000	0.0000	0.0000	0.0000	1.0000	0.0000	0.0000	0.0000
V01146 24617 A	0.0000	0.0000	0.0000	0.0000	0.0000	0.0000	1.0000	0.0000	0.0000	0.0000
V01146 24639 G	0.0000	0.0000	0.0000	0.0000	0.0000	0.0000	0.0000	0.0000	0.0000	0.0000

Supplemental Table S4.2 Evolved Mutations Filtered with N-2 Method (continued)

	Frequency of Mutation									
sample	1a	1b	1c	1d	1e	1f	2a	2b	2c	2d
treatment	E	E	E	E	E	E	E+T7	E+T7	E+T7	E+T7
Mutation (Genome, Basepair Number, New Base)										
V01146 24703 C	0.0000	0.0000	0.0000	0.0000	0.0000	0.0000	0.0000	0.0000	0.0000	1.0000
V01146 24725 T	0.0000	0.0000	0.0000	0.0000	0.0000	0.0000	0.0000	0.0000	0.0000	0.0000
V01146 24874 T	0.0000	0.0000	0.0000	0.0000	0.0000	0.0000	0.0000	0.0000	0.0000	0.0000
V01146 24897 A	0.0000	0.0000	0.0000	0.0000	0.0000	0.0000	0.0000	0.0000	0.0000	1.0000
V01146 25295 A	0.0000	0.0000	0.0000	0.0000	0.0000	0.0000	0.0000	0.0000	0.0000	0.0000
V01146 25368 C	0.0000	0.0000	0.0000	0.0000	0.0000	0.0000	0.0000	0.0000	0.0000	0.0000
V01146 25386 A	0.0000	0.0000	0.0000	0.0000	0.0000	0.0000	0.0000	0.0000	0.0000	0.0000
V01146 25392 G	0.0000	0.0000	0.0000	0.0000	0.0000	0.0000	0.0000	0.0000	1.0000	0.0000
V01146 25418 A	0.0000	0.0000	0.0000	0.0000	0.0000	0.0000	0.0000	0.0000	0.0000	0.0000
V01146 25491 T	0.0000	0.0000	0.0000	0.0000	0.0000	0.0000	1.0000	0.0000	0.0000	0.0000
V01146 25775 A	0.0000	0.0000	0.0000	0.0000	0.0000	0.0000	0.0000	0.0000	0.0000	0.0000
V01146 25836 A	0.0000	0.0000	0.0000	0.0000	0.0000	0.0000	0.0000	0.0000	0.0000	0.0000
V01146 25895 C	0.0000	0.0000	0.0000	0.0000	0.0000	0.0000	0.0000	0.0000	0.0000	0.0000
V01146 26114 C	0.0000	0.0000	0.0000	0.0000	0.0000	0.0000	0.0000	0.0000	0.0000	0.0000
V01146 26124 A	0.0000	0.0000	0.0000	0.0000	0.0000	0.0000	0.0000	0.0000	0.0000	0.0000
V01146 26139 T	0.0000	0.0000	0.0000	0.0000	0.0000	0.0000	1.0000	0.0000	0.0000	0.0000
V01146 26227 G	0.0000	0.0000	0.0000	0.0000	0.0000	0.0000	0.0000	0.0000	0.0000	0.0000
V01146 26240 G	0.0000	0.0000	0.0000	0.0000	0.0000	0.0000	0.0000	0.0000	1.0000	0.0000
V01146 26333 T	0.0000	0.0000	0.0000	0.0000	0.0000	0.0000	0.0000	0.0000	0.0000	0.0000
V01146 26335 A	0.0000	0.0000	0.0000	0.0000	0.0000	0.0000	1.0000	0.0000	0.0000	0.0000
V01146 26430 C	0.0000	0.0000	0.0000	0.0000	0.0000	0.0000	0.0000	0.0000	0.0000	0.0000
V01146 26576 T	0.0000	0.0000	0.0000	0.0000	0.0000	0.0000	0.0000	0.0000	0.0000	0.0000
V01146 27119 G	0.0000	0.0000	0.0000	0.0000	0.0000	0.0000	0.0000	0.0000	0.9193	0.0000
V01146 27164 T	0.0000	0.0000	0.0000	0.0000	0.0000	0.0000	0.0000	0.0000	0.0000	0.0000
V01146 29224 T	0.0000	0.0000	0.0000	0.0000	0.0000	0.0000	0.0000	0.0000	0.0000	0.0000
V01146 29244 C	0.0000	0.0000	0.0000	0.0000	0.0000	0.0000	0.0000	0.0000	0.0000	1.0000
V01146 30176 A	0.0000	0.0000	0.0000	0.0000	0.0000	0.0000	0.0000	0.0000	0.0000	0.0000
V01146 30633 G	0.0000	0.0000	0.0000	0.0000	0.0000	0.0000	1.0000	0.0000	0.0000	0.0000
V01146 30649 A	0.0000	0.0000	0.0000	0.0000	0.0000	0.0000	0.0000	0.0000	1.0000	0.0000
V01146 30668 C	0.0000	0.0000	0.0000	0.0000	0.0000	0.0000	0.0000	0.0000	0.0000	0.0000
V01146 30674 T	0.0000	0.0000	0.0000	0.0000	0.0000	0.0000	0.0000	0.0000	0.0000	0.0000
V01146 30721 C	0.0000	0.0000	0.0000	0.0000	0.0000	0.0000	0.0000	0.0000	0.0000	1.0000
V01146 30797 G	0.0000	0.0000	0.0000	0.0000	0.0000	0.0000	0.0000	0.0000	0.0000	0.0000
V01146 30850 A	0.0000	0.0000	0.0000	0.0000	0.0000	0.0000	0.0000	0.0000	0.0000	0.0000
V01146 30853 A	0.0000	0.0000	0.0000	0.0000	0.0000	0.0000	0.0000	0.0000	0.0000	0.0000
V01146 30907 A	0.0000	0.0000	0.0000	0.0000	0.0000	0.0000	0.0000	0.0000	0.0000	0.0000
V01146 30961 C	0.0000	0.0000	0.0000	0.0000	0.0000	0.0000	0.0000	0.0000	0.0000	0.0000
V01146 30974 G	0.0000	0.0000	0.0000	0.0000	0.0000	0.0000	0.0000	0.0000	0.0000	0.0000
V01146 3343 G	0.0000	0.0000	0.0000	0.0000	0.0000	0.0000	1.0000	0.0000	0.0000	0.0000
V01146 33784 A	0.0000	0.0000	0.0000	0.0000	0.0000	0.0000	0.0000	0.0000	1.0000	0.0000
V01146 34 NA	0.0000	0.0000	0.0000	0.0000	0.0000	0.0000	1.0000	0.0000	0.0000	0.0000
V01146 34742 C	0.0000	0.0000	0.0000	0.0000	0.0000	0.0000	0.0000	0.0000	0.0000	0.0000
V01146 34975 G	0.0000	0.0000	0.0000	0.0000	0.0000	0.0000	0.0000	0.0000	1.0000	0.0000
V01146 3522 C	0.0000	0.0000	0.0000	0.0000	0.0000	0.0000	0.0000	0.0000	0.0000	0.0000
V01146 35221 T	0.0000	0.0000	0.0000	0.0000	0.0000	0.0000	0.0000	0.0000	0.0000	0.0000
V01146 35221 TA	0.0000	0.0000	0.0000	0.0000	0.0000	0.0000	0.0000	0.0000	0.0000	0.0000
V01146 35235 T	0.0000	0.0000	0.0000	0.0000	0.0000	0.0000	0.0000	0.0000	0.0000	0.0000

Supplemental Table S4.2 Evolved Mutations Filtered with N-2 Method (continued)

	Frequency of Mutation									
sample	1a	1b	1c	1d	1e	1f	2a	2b	2c	2d
treatment	E	E	E	E	E	E	E+T7	E+T7	E+T7	E+T7
Mutation (Genome, Basepair Number, New Base)										
V01146 35254 C	0.0000	0.0000	0.0000	0.0000	0.0000	0.0000	0.0000	0.0000	0.0000	0.0000
V01146 35257 T	0.0000	0.0000	0.0000	0.0000	0.0000	0.0000	0.0000	0.0000	0.0000	1.0000
V01146 35258 A	0.0000	0.0000	0.0000	0.0000	0.0000	0.0000	0.0000	0.0000	0.0000	0.0000
V01146 35263 C	0.0000	0.0000	0.0000	0.0000	0.0000	0.0000	0.0000	0.0000	1.0000	0.0000
V01146 35263 G	0.0000	0.0000	0.0000	0.0000	0.0000	0.0000	1.0000	0.0000	0.0000	0.0000
V01146 35276 A	0.0000	0.0000	0.0000	0.0000	0.0000	0.0000	0.0000	0.0000	0.0000	0.0000
V01146 35299 G	0.0000	0.0000	0.0000	0.0000	0.0000	0.0000	0.0000	0.0000	0.0000	0.0000
V01146 35833 G	0.0000	0.0000	0.0000	0.0000	0.0000	0.0000	0.0000	0.0000	1.0000	0.0000
V01146 35980 G	0.0000	0.0000	0.0000	0.0000	0.0000	0.0000	0.0000	0.0000	0.0000	1.0000
V01146 36001 T	0.0000	0.0000	0.0000	0.0000	0.0000	0.0000	1.0000	0.0000	0.0000	0.0000
V01146 36184 A	0.0000	0.0000	0.0000	0.0000	0.0000	0.0000	1.0000	0.0000	0.0000	0.0000
V01146 36239 G	0.0000	0.0000	0.0000	0.0000	0.0000	0.0000	0.0000	0.0000	0.0000	1.0000
V01146 36277 G	0.0000	0.0000	0.0000	0.0000	0.0000	0.0000	0.0000	0.0000	0.0000	0.0000
V01146 39557 G	0.0000	0.0000	0.0000	0.0000	0.0000	0.0000	1.0000	0.0000	0.0000	0.0000
V01146 39811 NA	0.0000	0.0000	0.0000	0.0000	0.0000	0.0000	1.0000	0.0000	0.0000	0.0000
V01146 4417 C	0.0000	0.0000	0.0000	0.0000	0.0000	0.0000	0.0000	0.0000	0.0000	1.0000
V01146 4773 T	0.0000	0.0000	0.0000	0.0000	0.0000	0.0000	0.0000	0.0000	0.0000	0.0000
V01146 4843 T	0.0000	0.0000	0.0000	0.0000	0.0000	0.0000	0.0000	0.0000	1.0000	0.0000
V01146 5076 G	0.0000	0.0000	0.0000	0.0000	0.0000	0.0000	0.0000	0.0000	0.0000	0.0000
V01146 5239 A	0.0000	0.0000	0.0000	0.0000	0.0000	0.0000	0.0000	0.0000	0.0000	0.0000
V01146 5329 A	0.0000	0.0000	0.0000	0.0000	0.0000	0.0000	0.0000	0.0000	0.0000	0.0000
V01146 5348 A	0.0000	0.0000	0.0000	0.0000	0.0000	0.0000	0.0000	0.0000	0.0000	0.0000
V01146 8800 G	0.0000	0.0000	0.0000	0.0000	0.0000	0.0000	1.0000	0.0000	0.0000	0.0000
V01146 9919 T	0.0000	0.0000	0.0000	0.0000	0.0000	0.0000	0.0000	0.0000	0.0000	1.0000

Supplemental Table S4.2 Evolved Mutations Filtered with N-2 Method (continued)

	Frequency of Mutation									
sample	2e	2f	3a	3b	3c	3d	3e	3f	4a	4b
treatment	E+T7	E+T7	ES	ES	ES	ES	ES	ES	ES+T7	ES+T7
Mutation (Genome, Basepair Number, New Base)										
NC_002483 52320 A	0.0000	0.7388	0.0000	0.0000	0.0000	0.0000	0.7105	0.0000	0.7529	0.0000
NC_002483 61959 CT	0.0000	1.0000	0.0000	1.0000	1.0000	1.0000	1.0000	1.0000	1.0000	1.0000
NC_002483 61960 T	1.0000	0.0000	0.0000	0.0000	0.0000	0.0000	0.0000	0.0000	0.0000	0.0000
NC_002483 63485 NA	1.0000	1.0000	0.0000	0.0000	1.0000	0.0000	1.0000	1.0000	0.0000	0.0000
NC_002483 63526 C	0.0000	1.0000	0.0000	0.0000	1.0000	0.0000	0.0000	1.0000	1.0000	0.0000
NC_002483 63577 C	0.0000	0.0000	0.0000	0.0000	0.0000	0.0000	0.0000	0.0000	0.0000	0.0000
NC_002483 63655 T	1.0000	1.0000	0.0000	0.0000	1.0000	1.0000	0.0000	1.0000	1.0000	0.0000
NC_002483 63842 A	0.0000	0.0000	0.0000	0.0000	1.0000	0.0000	0.0000	1.0000	0.0000	0.0000
NC_002483 63843 G	0.0000	0.0000	0.0000	0.0000	1.0000	0.0000	0.0000	0.0000	0.0000	0.0000
NC_002483 65446 NA	0.0000	1.0000	0.0000	1.0000	1.0000	1.0000	0.0000	1.0000	1.0000	1.0000
NC_002483 65618 T	1.0000	1.0000	0.0000	1.0000	1.0000	0.0000	1.0000	1.0000	1.0000	1.0000
NC_002483 66089 T	0.0000	1.0000	0.0000	1.0000	1.0000	1.0000	1.0000	1.0000	0.0000	0.0000
NC_002483 83617 C	0.0000	0.0000	0.0000	0.2667	0.0000	0.0000	0.0000	0.0000	0.0000	0.0000
NC_003197 1104985 C	0.0000	0.0000	0.0000	0.0000	0.0000	0.0000	0.0000	0.0000	0.0000	0.0000
NC_003197 1593992 T	0.0000	0.0000	0.0000	0.0000	0.0000	0.0000	0.0000	0.0000	0.0000	0.0000
NC_003197 2058713 NA	0.0000	0.0000	0.0000	0.0000	0.0000	0.0000	0.0000	0.0000	0.0000	0.0000
NC_003197 2358702 G	0.0000	0.0000	0.0000	0.2721	0.0000	0.0000	0.2785	0.2423	0.2564	0.1995
NC_003197 2358706 C	0.0000	0.0000	0.2680	0.3082	0.0000	0.0000	0.2110	0.2046	0.3096	0.0000
NC_003197 2730867 NA	0.0000	0.0000	0.9064	0.0000	0.0000	0.0000	0.0000	0.0000	0.0000	0.0000
NC_003197 2730889 NA	0.0000	0.0000	0.0000	0.0000	0.0000	0.0000	0.0000	0.0000	0.0000	0.1396
NC_003197 2730895 NA	0.0000	0.0000	0.0000	0.0000	0.0000	0.0000	0.0000	0.0000	0.0000	0.4028
NC_003197 2730907 NA	0.0000	0.0000	0.0000	0.0000	0.0000	0.0000	0.0000	0.0000	0.0000	0.2623
NC_003197 2770105 TTAGTTGCAC	0.0000	0.0000	0.0000	0.0000	0.0000	0.0000	0.0000	0.0000	0.0000	1.0000
NC_003197 3676853 A	0.0000	0.0000	0.0000	1.0000	1.0000	0.0000	1.0000	1.0000	0.0000	0.0000
NC_003197 4099877 C	0.0000	0.0000	0.0000	0.0000	0.0000	0.4209	0.0000	0.0000	0.0000	0.0000
NC_003197 4155512 T	0.0000	0.0000	0.0000	0.3532	0.0000	0.0000	0.0000	0.2341	0.0000	0.0000
NC_003197 4155518 A	0.0000	0.0000	0.0000	0.0000	0.0000	0.0000	0.0000	0.0000	0.0000	0.2656
NC_003197 4244681 G	0.0000	0.0000	0.0000	0.0000	0.0000	0.0000	0.0000	0.0000	0.0000	0.0000
NC_003197 4310137 NA	0.0000	0.0000	0.0000	0.0000	0.0000	0.0000	0.0000	0.0000	0.0000	0.0000
NC_003197 4311847 NA	0.0000	0.0000	0.0000	0.0000	0.0000	0.0000	0.0000	0.2191	0.0867	0.0000
NC_003197 4312824 NA	0.0000	0.0000	0.0000	0.0000	0.0000	0.0000	0.0000	0.0000	0.0000	0.0000
NC_003197 4433283 CG	0.0000	0.0000	1.0000	1.0000	0.9467	1.0000	0.9415	1.0000	1.0000	1.0000
NC_003197 4631400 GC	0.0000	0.0000	0.0000	0.0000	0.0000	0.0000	0.0000	0.0000	0.0000	0.0000
NZ_CP009273 1147986 NA	0.0000	0.0000	0.0000	0.0000	0.0000	0.0000	0.0000	0.0000	0.0000	0.0000
NZ_CP009273 1148228 GGCGCA	0.0000	0.0000	0.0000	0.0000	0.0000	0.0000	0.0000	0.0000	0.0000	0.0000
NZ_CP009273 1298631 T	0.0000	0.0000	0.0000	0.0000	0.0000	0.0000	0.0000	0.0000	0.0000	0.7424
NZ_CP009273 1973112 NA	1.0000	1.0000	1.0000	1.0000	1.0000	1.0000	1.0000	1.0000	1.0000	1.0000
NZ_CP009273 2068176 C	0.0000	0.1350	0.2851	0.1549	0.0000	0.0000	0.0000	0.0000	0.1797	0.0000
NZ_CP009273 2107740 NA	0.0000	0.0000	0.0000	0.0000	0.0000	0.0000	0.0000	0.0000	0.0000	0.0000
NZ_CP009273 2133770 NA	0.0000	0.0000	0.0000	0.0000	0.0000	0.0000	0.0000	0.0000	0.0000	0.0000
NZ_CP009273 2278193 NA	0.8535	0.0000	0.0000	0.0000	0.0000	0.0000	0.0000	0.0000	0.0000	0.0000
NZ_CP009273 240327 NA	0.0000	0.0000	0.0000	0.0000	0.0000	0.0000	0.0000	0.0000	0.0000	0.0000
NZ_CP009273 2557859 A	0.0000	0.0000	0.0000	0.0000	0.0000	0.0000	0.0000	0.0000	0.0000	0.0000
NZ_CP009273 2860008 C	0.0000	0.0000	0.0000	0.0000	0.0000	0.0000	0.0000	0.0000	0.0000	0.0000
NZ_CP009273 2860214 NA	0.0000	0.0000	0.0000	0.0000	0.0000	0.0000	0.0000	0.0000	1.0000	0.0000

Supplemental Table S4.2 Evolved Mutations Filtered with N-2 Method (continued)

	Frequency of Mutation									
sample	2e	2f	3a	3b	3c	3d	3e	3f	4a	4b
treatment	E+T7	E+T7	ES	ES	ES	ES	ES	ES	ES+T7	ES+T7
Mutation (Genome, Basepair Number, New Base)										
NZ_CP009273 2860234 NA	0.0000	0.0000	0.0000	0.0000	0.0000	0.0000	0.0000	0.0000	0.0000	0.0000
NZ_CP009273 2860332 G	0.0000	0.0000	0.0000	0.0000	0.0000	0.0000	0.0000	0.0000	0.0000	0.0000
NZ_CP009273 2860874 NA	0.0000	0.0000	0.0000	0.0000	0.0000	0.0000	0.0000	0.0000	0.0000	0.0000
NZ_CP009273 2904839 NA	1.0000	0.0000	0.0000	0.0000	0.0000	0.0000	0.0000	0.0000	0.0000	0.0000
NZ_CP009273 303915 C	0.0000	0.0902	0.0000	0.2587	0.0000	0.0000	0.0000	0.0000	0.0000	0.0000
NZ_CP009273 3189869 NA	0.0000	0.0000	0.0000	0.0000	0.0000	0.0000	0.0000	0.0000	0.0000	1.0000
NZ_CP009273 3303994 NA	0.0000	0.0000	0.0000	0.3038	0.0000	0.0000	0.0000	0.0000	0.0000	0.0000
NZ_CP009273 3319471 T	0.0000	0.0000	0.0000	0.8338	0.0000	0.0000	0.0000	0.0000	0.0000	0.0000
NZ_CP009273 3336357 NA	0.0000	0.0000	0.0000	0.0000	0.0000	0.0000	0.0000	0.0000	0.0000	0.0000
NZ_CP009273 3386512 NA	0.0000	0.0000	0.0000	0.0000	0.0000	0.0000	0.0000	0.0000	0.0000	0.0000
NZ_CP009273 360927 C	0.0000	0.0000	0.0000	0.0000	0.0000	0.0000	0.0000	0.2738	0.0000	0.0000
NZ_CP009273 361004 A	0.0000	0.0000	0.0000	0.0000	0.0000	0.0000	0.0000	0.0000	0.0000	0.2622
NZ_CP009273 361139 GCCA	0.0000	0.0000	0.4161	0.0000	0.2727	0.0000	0.0000	0.3080	0.0000	0.6051
NZ_CP009273 361140 NA	0.0000	0.0000	0.1720	0.0000	0.0000	0.9464	1.0000	0.0000	0.0000	0.0000
NZ_CP009273 361149 CAGACG	0.0000	0.0000	0.0000	0.0000	0.0000	0.0000	0.0000	0.0000	0.0000	0.0000
NZ_CP009273 361287 A	0.0000	0.0000	0.0000	0.0000	0.0000	0.0000	0.0000	0.5364	0.0000	0.0000
NZ_CP009273 3629231 NA	0.0000	0.0000	0.0000	0.0000	0.0000	0.0000	0.0000	0.0000	0.0000	0.0000
NZ_CP009273 3669214 NA	0.0000	0.0000	0.0000	0.0000	0.0000	0.0000	0.0000	0.0000	0.0000	0.0000
NZ_CP009273 3706292 A	0.2577	0.0000	0.0000	0.0000	0.0000	0.0000	0.0000	0.0000	0.0000	0.0000
NZ_CP009273 3799448 NA	0.0000	1.0000	0.0000	0.0000	0.0000	0.0000	0.0000	0.0000	0.0000	0.0000
NZ_CP009273 3799800 NA	1.0000	0.0000	0.0000	0.0000	0.0000	0.0000	0.0000	0.0000	0.0000	0.0000
NZ_CP009273 3800001 NA	0.0000	0.0000	0.0000	0.0000	0.0000	0.0000	0.0000	0.0000	0.0000	0.0000
NZ_CP009273 3944901 NA	0.0000	0.0000	0.0000	0.0000	0.0000	0.0000	0.0000	0.0000	0.0000	0.0000
NZ_CP009273 3960101 T	0.0000	0.0000	0.0000	0.2711	0.0000	0.0000	0.0000	0.0000	0.0000	0.0000
NZ_CP009273 3960515 T	0.0000	0.0000	0.0000	0.0000	0.0000	0.0000	0.0000	0.5015	0.0000	0.0000
NZ_CP009273 4076055 G	0.0000	0.0000	0.0000	0.0000	0.0000	0.0000	0.0000	0.0000	0.0000	0.0000
NZ_CP009273 4118604 TTCCGGGGATCCGTCGACCT GCAGTTCGAAGTTCCTATTCT CTAGAAAGTATAGGAACTTC GAAGCAGCTCCAGCCTACA	0.0000	0.0000	0.0000	0.0000	0.0000	0.0000	0.0000	0.0000	0.0000	0.0000
NZ_CP009273 4177773 NA	0.0000	0.0000	0.0000	0.0000	0.0000	0.0000	0.0000	0.0000	0.0000	0.0000
NZ_CP009273 4178501 T	0.0000	0.0000	0.0000	0.0000	0.0000	0.0000	0.0000	0.0000	0.0000	0.0000
NZ_CP009273 42141 T	0.0000	0.0000	0.0000	0.0000	0.0000	0.0000	1.0000	0.0000	0.0000	0.0000
NZ_CP009273 4226052 NA	0.0000	0.0000	0.0000	0.0000	0.0000	0.0000	0.0000	0.0000	0.0000	0.9110
NZ_CP009273 4226403 T	0.0000	0.0000	0.0000	0.0000	0.0000	0.0000	0.0000	0.0000	0.0000	0.0000
NZ_CP009273 4226594 NA	0.0000	0.0000	0.0000	0.0000	0.0000	0.0000	0.0000	0.0000	0.0000	0.0000
NZ_CP009273 4227883 NA	0.0000	0.0000	0.0000	0.0000	0.0000	0.0000	0.0000	0.0000	0.0000	0.0000
NZ_CP009273 4228249 NA	0.0000	0.0000	0.0000	0.0000	0.0000	0.0000	0.0000	0.0000	0.0000	0.0000
NZ_CP009273 4228789 T	0.0000	0.3438	0.0000	0.0000	0.0000	0.0000	0.0000	0.0000	0.0000	0.0000
NZ_CP009273 4228998 A	0.0000	0.0000	0.0000	0.0000	0.0000	0.0000	0.0000	0.0000	0.0000	0.0000
NZ_CP009273 4229421 NA	0.0000	0.0000	0.0000	0.0000	0.0000	0.0000	0.0000	0.0000	0.0000	0.0000
NZ_CP009273 4273156 G	0.0000	0.0000	0.0000	0.0000	0.2664	0.0000	0.0000	0.0000	0.0000	0.0000
NZ_CP009273 454246 NA	1.0000	1.0000	0.0000	0.0000	0.0000	0.0000	0.0000	0.0000	1.0000	0.0000
NZ_CP009273 454248 NA	0.0000	0.0000	0.0000	0.0000	0.0000	0.0000	0.0000	0.0000	0.0000	0.0000
NZ_CP009273 513494 T	0.0000	0.0000	0.0000	0.0000	0.0000	0.0000	0.0000	0.0000	0.0000	0.0000
NZ_CP009273 51993 NA	0.0000	0.0000	0.0000	0.0000	0.0000	0.0000	0.0000	0.0000	0.0000	0.0000

Supplemental Table S4.2 Evolved Mutations Filtered with N-2 Method (continued)

	Frequency of Mutation									
sample	2e	2f	3a	3b	3c	3d	3e	3f	4a	4b
treatment	E+T7	E+T7	ES	ES	ES	ES	ES	ES	ES+T7	ES+T7
Mutation (Genome, Basepair Number, New Base)										
NZ_CP009273 571113 C	0.0000	0.0000	0.0000	0.0000	0.0000	0.0000	0.0000	0.0000	0.0000	0.0000
NZ_CP009273 632236 C	0.0000	0.0000	0.0000	0.0000	0.0000	0.0000	0.0000	0.0000	0.0000	0.0000
NZ_CP009273 733422 NA	0.0000	0.0000	0.0000	0.0000	0.0000	0.0000	0.0000	0.0000	0.0000	0.0000
NZ_CP009273 83868 T	0.0000	0.0000	0.0000	0.0000	0.0000	0.0000	0.0000	0.0000	0.0000	0.0000
NZ_CP009273 83881 T	0.0000	0.0000	0.0000	0.0000	0.0000	0.0000	0.0000	0.0000	0.0000	0.0000
NZ_CP009273 83893 T	0.0000	0.0000	0.0000	0.0000	0.0000	0.0000	0.0000	0.0000	0.0000	0.0000
NZ_CP009273 84227 A	0.0000	0.0000	0.0000	0.0000	0.0000	0.0000	0.0000	0.0000	0.0000	0.0000
NZ_CP009273 84294 A	0.0000	0.0000	0.0000	0.0000	0.0000	0.0000	0.0000	0.0000	0.0000	0.0000
V01146 10203 A	0.0000	1.0000	0.0000	0.0000	0.0000	0.0000	0.0000	0.0000	0.0000	0.0000
V01146 10308 T	0.4869	0.0000	0.0000	0.0000	0.0000	0.0000	0.0000	0.0000	0.0000	0.0000
V01146 10922 A	0.0000	0.0000	0.0000	0.0000	0.0000	0.0000	0.0000	0.0000	0.0000	0.0000
V01146 11197 C	0.0000	0.0000	0.0000	0.0000	0.0000	0.0000	0.0000	0.0000	0.2734	0.0000
V01146 12114 A	0.2766	0.0000	0.0000	0.0000	0.0000	0.0000	0.0000	0.0000	0.0000	0.0000
V01146 1379 NA	0.0000	1.0000	0.0000	0.0000	0.0000	0.0000	0.0000	0.0000	0.0000	0.0000
V01146 16410 A	0.0000	0.0000	0.0000	0.0000	0.0000	0.0000	0.0000	0.0000	0.0000	0.0000
V01146 16795 G	0.0000	0.0000	0.0000	0.0000	0.0000	0.0000	0.0000	0.0000	0.0000	0.0000
V01146 1867 A	0.0000	0.0000	0.0000	0.0000	0.0000	0.0000	0.0000	0.0000	0.2536	0.0000
V01146 19344 C	0.0000	0.0000	0.0000	0.0000	0.0000	0.0000	0.0000	0.0000	0.0000	0.0000
V01146 1936 T	0.0000	0.0000	0.0000	0.0000	0.0000	0.0000	0.0000	0.0000	0.0000	0.0000
V01146 19517 C	0.0000	0.0000	0.0000	0.0000	0.0000	0.0000	0.0000	0.0000	0.0000	0.0000
V01146 19572 T	0.0000	0.0000	0.0000	0.0000	0.0000	0.0000	0.0000	0.0000	0.0000	0.0000
V01146 19584 T	0.0000	0.0000	0.0000	0.0000	0.0000	0.0000	0.0000	0.0000	0.0000	0.0000
V01146 19602 T	1.0000	0.0000	0.0000	0.0000	0.0000	0.0000	0.0000	0.0000	0.0000	0.0000
V01146 19672 NA	0.0000	0.0000	0.0000	0.0000	0.0000	0.0000	0.0000	0.0000	0.0000	0.0000
V01146 19677 C	0.0000	0.0000	0.0000	0.0000	0.0000	0.0000	0.0000	0.0000	0.0000	0.0000
V01146 19728 T	1.0000	0.0000	0.0000	0.0000	0.0000	0.0000	0.0000	0.0000	0.0000	0.0000
V01146 2243 T	0.0000	0.0000	0.0000	0.0000	0.0000	0.0000	0.0000	0.0000	0.0000	0.0000
V01146 23007 T	0.5823	0.0000	0.0000	0.0000	0.0000	0.0000	0.0000	0.0000	0.0000	0.0000
V01146 23230 C	0.0000	1.0000	0.0000	0.0000	0.0000	0.0000	0.0000	0.0000	0.0000	0.0000
V01146 23799 C	0.0000	0.0000	0.0000	0.0000	0.0000	0.0000	0.0000	0.0000	0.9496	0.0000
V01146 23817 T	0.6061	0.0000	0.0000	0.0000	0.0000	0.0000	0.0000	0.0000	0.0000	0.0000
V01146 23991 C	0.0000	0.0000	0.0000	0.0000	0.0000	0.0000	0.0000	0.0000	0.0000	0.0000
V01146 23991 G	0.0000	0.0000	0.0000	0.0000	0.0000	0.0000	0.0000	0.0000	0.0000	0.0000
V01146 24044 C	0.0000	0.0000	0.0000	0.0000	0.0000	0.0000	0.0000	0.0000	0.0000	0.0000
V01146 24046 T	0.0000	0.0000	0.0000	0.0000	0.0000	0.0000	0.0000	0.0000	1.0000	0.0000
V01146 24051 G	1.0000	0.0000	0.0000	0.0000	0.0000	0.0000	0.0000	0.0000	0.0000	0.0000
V01146 24178 A	0.0000	0.0000	0.0000	0.0000	0.0000	0.0000	0.0000	0.0000	0.0000	0.0000
V01146 24204 NA	0.0000	0.0000	0.0000	0.0000	0.0000	0.0000	0.0000	0.0000	0.0000	1.0000
V01146 24273 A	0.0000	0.0000	0.0000	0.0000	0.0000	0.0000	0.0000	0.0000	0.0000	0.0000
V01146 24274 A	0.0000	0.0000	0.0000	0.0000	0.0000	0.0000	0.0000	0.0000	0.0000	0.0000
V01146 24312 A	1.0000	1.0000	0.0000	0.0000	0.0000	0.0000	0.0000	0.0000	0.0000	0.0000
V01146 24346 T	0.0000	0.0000	0.0000	0.0000	0.0000	0.0000	0.0000	0.0000	0.0000	1.0000
V01146 24370 G	0.0000	0.0000	0.0000	0.0000	0.0000	0.0000	0.0000	0.0000	0.0000	0.0000
V01146 24397 A	0.0000	0.0000	0.0000	0.0000	0.0000	0.0000	0.0000	0.0000	0.0000	0.0000
V01146 24498 A	0.0000	0.0000	0.0000	0.0000	0.0000	0.0000	0.0000	0.0000	0.0000	0.0000
V01146 24617 A	0.0000	0.0000	0.0000	0.0000	0.0000	0.0000	0.0000	0.0000	0.0000	0.0000
V01146 24639 G	0.0000	0.0000	0.0000	0.0000	0.0000	0.0000	0.0000	0.0000	0.0000	0.0000

Supplemental Table S4.2 Evolved Mutations Filtered with N-2 Method (continued)

	Frequency of Mutation									
sample	2e	2f	3a	3b	3c	3d	3e	3f	4a	4b
treatment	E+T7	E+T7	ES	ES	ES	ES	ES	ES	ES+T7	ES+T7
Mutation (Genome, Basepair Number, New Base)										
V01146 24703 C	0.0000	0.0000	0.0000	0.0000	0.0000	0.0000	0.0000	0.0000	0.0000	0.0000
V01146 24725 T	0.0000	0.0000	0.0000	0.0000	0.0000	0.0000	0.0000	0.0000	1.0000	0.0000
V01146 24874 T	0.0000	0.0000	0.0000	0.0000	0.0000	0.0000	0.0000	0.0000	0.0000	1.0000
V01146 24897 A	0.0000	0.0000	0.0000	0.0000	0.0000	0.0000	0.0000	0.0000	0.0000	0.0000
V01146 25295 A	0.0000	0.0000	0.0000	0.0000	0.0000	0.0000	0.0000	0.0000	1.0000	0.0000
V01146 25368 C	0.0000	0.0000	0.0000	0.0000	0.0000	0.0000	0.0000	0.0000	0.0000	0.0000
V01146 25386 A	0.0000	1.0000	0.0000	0.0000	0.0000	0.0000	0.0000	0.0000	0.0000	0.0000
V01146 25392 G	0.0000	0.0000	0.0000	0.0000	0.0000	0.0000	0.0000	0.0000	0.0000	0.0000
V01146 25418 A	0.0000	0.0000	0.0000	0.0000	0.0000	0.0000	0.0000	0.0000	0.0000	1.0000
V01146 25491 T	0.0000	0.0000	0.0000	0.0000	0.0000	0.0000	0.0000	0.0000	0.0000	0.0000
V01146 25775 A	1.0000	0.0000	0.0000	0.0000	0.0000	0.0000	0.0000	0.0000	0.0000	0.0000
V01146 25836 A	0.0000	0.0000	0.0000	0.0000	0.0000	0.0000	0.0000	0.0000	0.0000	1.0000
V01146 25895 C	0.0000	0.0000	0.0000	0.0000	0.0000	0.0000	0.0000	0.0000	0.0000	0.0000
V01146 26114 C	0.0000	0.0000	0.0000	0.0000	0.0000	0.0000	0.0000	0.0000	0.0000	0.0000
V01146 26124 A	0.0000	0.0000	0.0000	0.0000	0.0000	0.0000	0.0000	0.0000	0.0000	0.0000
V01146 26139 T	0.0000	0.0000	0.0000	0.0000	0.0000	0.0000	0.0000	0.0000	0.0000	0.0000
V01146 26227 G	0.0000	0.0000	0.0000	0.0000	0.0000	0.0000	0.0000	0.0000	0.0000	0.0000
V01146 26240 G	0.0000	0.0000	0.0000	0.0000	0.0000	0.0000	0.0000	0.0000	0.0000	0.0000
V01146 26333 T	0.0000	0.0000	0.0000	0.0000	0.0000	0.0000	0.0000	0.0000	0.0000	0.0000
V01146 26335 A	0.0000	0.0000	0.0000	0.0000	0.0000	0.0000	0.0000	0.0000	0.0000	0.0000
V01146 26430 C	0.0000	0.0000	0.0000	0.0000	0.0000	0.0000	0.0000	0.0000	0.0000	0.0000
V01146 26576 T	0.0000	0.0000	0.0000	0.0000	0.0000	0.0000	0.0000	0.0000	0.0000	0.0000
V01146 27119 G	0.0000	0.0000	0.0000	0.0000	0.0000	0.0000	0.0000	0.0000	0.0000	0.0000
V01146 27164 T	0.0000	0.0000	0.0000	0.0000	0.0000	0.0000	0.0000	0.0000	0.0000	0.0000
V01146 29224 T	0.0000	0.0000	0.0000	0.0000	0.0000	0.0000	0.0000	0.0000	0.0000	0.0000
V01146 29244 C	0.0000	0.0000	0.0000	0.0000	0.0000	0.0000	0.0000	0.0000	0.0000	0.0000
V01146 30176 A	0.0000	0.0000	0.0000	0.0000	0.0000	0.0000	0.0000	0.0000	0.0000	0.0000
V01146 30633 G	0.0000	0.0000	0.0000	0.0000	0.0000	0.0000	0.0000	0.0000	0.0000	0.0000
V01146 30649 A	0.0000	0.0000	0.0000	0.0000	0.0000	0.0000	0.0000	0.0000	0.0000	0.0000
V01146 30668 C	0.0000	0.0000	0.0000	0.0000	0.0000	0.0000	0.0000	0.0000	1.0000	0.0000
V01146 30674 T	0.0000	0.0000	0.0000	0.0000	0.0000	0.0000	0.0000	0.0000	0.0000	0.0000
V01146 30721 C	0.0000	0.0000	0.0000	0.0000	0.0000	0.0000	0.0000	0.0000	0.0000	0.0000
V01146 30797 G	0.0000	0.0000	0.0000	0.0000	0.0000	0.0000	0.0000	0.0000	0.0000	0.0000
V01146 30850 A	0.0000	0.0000	0.0000	0.0000	0.0000	0.0000	0.0000	0.0000	0.0000	0.0000
V01146 30853 A	0.0000	0.0000	0.0000	0.0000	0.0000	0.0000	0.0000	0.0000	0.0000	1.0000
V01146 30907 A	0.0000	0.0000	0.0000	0.0000	0.0000	0.0000	0.0000	0.0000	0.0000	0.0000
V01146 30961 C	1.0000	0.0000	0.0000	0.0000	0.0000	0.0000	0.0000	0.0000	0.0000	0.0000
V01146 30974 G	0.0000	1.0000	0.0000	0.0000	0.0000	0.0000	0.0000	0.0000	0.0000	0.0000
V01146 3343 G	0.0000	0.0000	0.0000	0.0000	0.0000	0.0000	0.0000	0.0000	0.0000	0.0000
V01146 33784 A	0.0000	0.0000	0.0000	0.0000	0.0000	0.0000	0.0000	0.0000	0.0000	0.0000
V01146 34 NA	0.0000	0.0000	0.0000	0.0000	0.0000	0.0000	0.0000	0.0000	0.0000	0.0000
V01146 34742 C	0.0000	0.0000	0.0000	0.0000	0.0000	0.0000	0.0000	0.0000	0.0000	0.0000
V01146 34975 G	0.0000	0.0000	0.0000	0.0000	0.0000	0.0000	0.0000	0.0000	0.0000	0.0000
V01146 3522 C	0.0000	1.0000	0.0000	0.0000	0.0000	0.0000	0.0000	0.0000	0.0000	0.0000
V01146 35221 T	0.0000	0.0000	0.0000	0.0000	0.0000	0.0000	0.0000	0.0000	0.0000	0.0000
V01146 35221 TA	1.0000	0.0000	0.0000	0.0000	0.0000	0.0000	0.0000	0.0000	0.0000	0.0000
V01146 35235 T	0.0000	0.0000	0.0000	0.0000	0.0000	0.0000	0.0000	0.0000	0.0000	0.0000

Supplemental Table S4.2 Evolved Mutations Filtered with N-2 Method (continued)

	Frequency of Mutation									
sample	2e	2f	3a	3b	3c	3d	3e	3f	4a	4b
treatment	E+T7	E+T7	ES	ES	ES	ES	ES	ES	ES+T7	ES+T7
Mutation (Genome, Basepair Number, New Base)										
V01146 35254 C	0.0000	1.0000	0.0000	0.0000	0.0000	0.0000	0.0000	0.0000	0.0000	0.0000
V01146 35257 T	0.0000	0.0000	0.0000	0.0000	0.0000	0.0000	0.0000	0.0000	0.0000	0.0000
V01146 35258 A	0.0000	0.0000	0.0000	0.0000	0.0000	0.0000	0.0000	0.0000	1.0000	0.0000
V01146 35263 C	0.0000	0.0000	0.0000	0.0000	0.0000	0.0000	0.0000	0.0000	0.0000	0.0000
V01146 35263 G	0.0000	0.0000	0.0000	0.0000	0.0000	0.0000	0.0000	0.0000	0.0000	1.0000
V01146 35276 A	0.0000	0.0000	0.0000	0.0000	0.0000	0.0000	0.0000	0.0000	0.6301	0.0000
V01146 35299 G	0.6316	0.0000	0.0000	0.0000	0.0000	0.0000	0.0000	0.0000	0.0000	0.0000
V01146 35833 G	0.0000	0.0000	0.0000	0.0000	0.0000	0.0000	0.0000	0.0000	0.0000	0.0000
V01146 35980 G	0.0000	1.0000	0.0000	0.0000	0.0000	0.0000	0.0000	0.0000	0.0000	0.0000
V01146 36001 T	0.0000	0.0000	0.0000	0.0000	0.0000	0.0000	0.0000	0.0000	0.0000	0.0000
V01146 36184 A	0.0000	0.0000	0.0000	0.0000	0.0000	0.0000	0.0000	0.0000	0.0000	0.0000
V01146 36239 G	0.0000	0.0000	0.0000	0.0000	0.0000	0.0000	0.0000	0.0000	0.0000	0.0000
V01146 36277 G	1.0000	0.0000	0.0000	0.0000	0.0000	0.0000	0.0000	0.0000	0.0000	0.0000
V01146 39557 G	0.0000	0.0000	0.0000	0.0000	0.0000	0.0000	0.0000	0.0000	0.0000	0.0000
V01146 39811 NA	0.0000	0.0000	0.0000	0.0000	0.0000	0.0000	0.0000	0.0000	0.0000	0.0000
V01146 4417 C	0.0000	0.0000	0.0000	0.0000	0.0000	0.0000	0.0000	0.0000	0.0000	0.0000
V01146 4773 T	0.0000	0.0000	0.0000	0.0000	0.0000	0.0000	0.0000	0.0000	0.0000	0.0000
V01146 4843 T	1.0000	0.0000	0.0000	0.0000	0.0000	0.0000	0.0000	0.0000	0.0000	0.0000
V01146 5076 G	0.0000	0.0000	0.0000	0.0000	0.0000	0.0000	0.0000	0.0000	1.0000	0.0000
V01146 5239 A	0.0000	0.0000	0.0000	0.0000	0.0000	0.0000	0.0000	0.0000	0.0000	0.0000
V01146 5329 A	0.0000	0.0000	0.0000	0.0000	0.0000	0.0000	0.0000	0.0000	0.8666	0.0000
V01146 5348 A	0.0000	0.0000	0.0000	0.0000	0.0000	0.0000	0.0000	0.0000	0.0000	0.0000
V01146 8800 G	0.0000	0.0000	0.0000	0.0000	0.0000	0.0000	0.0000	0.0000	0.0000	0.0000
V01146 9919 T	0.0000	0.0000	0.0000	0.0000	0.0000	0.0000	0.0000	0.0000	0.0000	0.0000

Supplemental Table S4.2 Evolved Mutations Filtered with N-2 Method (continued)

	Frequency of Mutation					
sample	4d	4e	4f	5a	5b	5c
treatment	ES+T7	ES+T7	ES+T7	S	S	S
Mutation (Genome, Basepair Number, New Base)						
NC_002483 52320 A	0.7183	0.8282	0.0000	0.0000	0.0000	0.0000
NC_002483 61959 CT	0.0000	1.0000	1.0000	0.0000	0.0000	0.0000
NC_002483 61960 T	0.0000	0.0000	0.0000	0.0000	0.0000	0.0000
NC_002483 63485 NA	0.0000	1.0000	1.0000	0.0000	0.0000	0.0000
NC_002483 63526 C	0.0000	0.0000	0.0000	0.0000	0.0000	0.0000
NC_002483 63577 C	0.0000	0.0000	0.0000	0.0000	0.0000	0.0000
NC_002483 63655 T	1.0000	1.0000	1.0000	0.0000	0.0000	0.0000
NC_002483 63842 A	0.0000	0.0000	0.0000	0.0000	0.0000	0.0000
NC_002483 63843 G	0.0000	0.0000	0.0000	0.0000	0.0000	0.0000
NC_002483 65446 NA	1.0000	1.0000	1.0000	0.0000	0.0000	0.0000
NC_002483 65618 T	0.0000	1.0000	0.0000	0.0000	0.0000	0.0000
NC_002483 66089 T	0.0000	1.0000	0.0000	0.0000	0.0000	0.0000
NC_002483 83617 C	0.0000	0.0000	0.0000	0.0000	0.0000	0.0000
NC_003197 1104985 C	0.0000	0.0000	0.0000	0.0000	0.0000	0.0000
NC_003197 1593992 T	0.3045	0.0000	0.0000	0.0000	0.0000	0.0000
NC_003197 2058713 NA	0.0000	0.0000	0.0000	0.2501	0.0000	0.0000
NC_003197 2358702 G	0.2361	0.3098	0.1871	0.0000	0.2638	0.2250
NC_003197 2358706 C	0.0000	0.2346	0.2012	0.0000	0.1936	0.2358
NC_003197 2730867 NA	0.0000	0.0000	0.0000	0.0000	0.0000	0.0000
NC_003197 2730889 NA	0.0000	0.0000	0.0000	0.0000	0.0000	0.0000
NC_003197 2730895 NA	0.0000	0.0000	0.6643	0.0000	0.0000	0.0000
NC_003197 2730907 NA	0.0000	0.0000	0.0000	0.0000	0.0000	0.0000
NC_003197 2770105 TTAGTTGCAC	0.0000	0.0000	0.0000	0.0000	0.0000	0.0000
NC_003197 3676853 A	1.0000	1.0000	0.0000	1.0000	1.0000	1.0000
NC_003197 4099877 C	0.4626	0.0000	0.0000	0.2969	0.0000	0.0000
NC_003197 4155512 T	0.0000	0.0000	0.0000	0.0000	0.0000	0.0000
NC_003197 4155518 A	0.0000	0.0000	0.0000	0.0000	0.0000	0.0000
NC_003197 4244681 G	0.0000	0.0000	0.0000	0.0000	0.2956	0.3082
NC_003197 4310137 NA	0.0000	0.0000	0.0000	0.0000	0.0000	0.0000
NC_003197 4311847 NA	0.2199	0.0000	0.0000	0.0000	0.4228	0.0000
NC_003197 4312824 NA	0.0000	0.0000	0.8562	0.0000	0.0000	0.0000
NC_003197 4433283 CG	1.0000	1.0000	0.9397	0.0000	0.9405	0.9252
NC_003197 4631400 GC	0.0000	0.0000	0.0000	1.0000	0.0000	0.0000
NZ_CP009273 1147986 NA	0.0000	0.0000	0.0000	0.0000	0.0000	0.0000
NZ_CP009273 1148228 GGCGCA	0.0000	0.0000	0.0000	0.0000	0.0000	0.0000
NZ_CP009273 1298631 T	0.0000	0.0000	0.0000	0.0000	0.0000	0.0000
NZ_CP009273 1973112 NA	1.0000	1.0000	1.0000	0.0000	0.0000	0.0000
NZ_CP009273 2068176 C	0.0000	0.0000	0.0000	0.0000	0.0000	0.0000
NZ_CP009273 2107740 NA	0.0000	0.6504	0.0000	0.0000	0.0000	0.0000
NZ_CP009273 2133770 NA	0.0000	0.0000	0.0000	0.0000	0.0000	0.0000
NZ_CP009273 2278193 NA	0.0000	0.0000	0.0000	0.0000	0.0000	0.0000
NZ_CP009273 240327 NA	0.0000	0.0000	0.0000	0.0000	0.0000	0.0000
NZ_CP009273 2557859 A	0.0000	0.0000	0.0000	0.0000	0.0000	0.0000
NZ_CP009273 2860008 C	0.0000	0.0000	0.8113	0.0000	0.0000	0.0000
NZ_CP009273 2860214 NA	0.0000	0.0000	0.0000	0.0000	0.0000	0.0000

Supplemental Table S4.2 Evolved Mutations Filtered with N-2 Method (continued)

	Frequency of Mutation					
sample	4d	4e	4f	5a	5b	5c
treatment	ES+T7	ES+T7	ES+T7	S	S	S
Mutation (Genome, Basepair Number, New Base)						
NZ_CP009273 2860234 NA	0.0000	0.0000	0.0000	0.0000	0.0000	0.0000
NZ_CP009273 2860332 G	0.0000	0.0000	0.0000	0.0000	0.0000	0.0000
NZ_CP009273 2860874 NA	0.8004	0.0000	0.0000	0.0000	0.0000	0.0000
NZ_CP009273 2904839 NA	0.0000	0.0000	0.0000	0.0000	0.0000	0.0000
NZ_CP009273 303915 C	0.0000	0.0000	0.0000	0.0000	0.0000	0.0000
NZ_CP009273 3189869 NA	0.0000	0.0000	0.0000	0.0000	0.0000	0.0000
NZ_CP009273 3303994 NA	0.0000	0.0000	0.0000	0.0000	0.0000	0.0000
NZ_CP009273 3319471 T	0.0000	0.0000	0.0000	0.0000	0.0000	0.0000
NZ_CP009273 3336357 NA	0.0000	0.0000	0.0000	0.0000	0.0000	0.0000
NZ_CP009273 3386512 NA	0.0000	0.0000	0.0000	0.0000	0.0000	0.0000
NZ_CP009273 360927 C	0.0000	0.0000	0.0000	0.0000	0.0000	0.0000
NZ_CP009273 361004 A	0.0000	0.0000	0.0000	0.0000	0.0000	0.0000
NZ_CP009273 361139 GCCA	0.3229	1.0000	0.2010	0.0000	0.0000	0.0000
NZ_CP009273 361140 NA	0.0000	0.0000	0.0000	0.0000	0.0000	0.0000
NZ_CP009273 361149 CAGACG	0.0000	0.0000	0.0000	0.0000	0.0000	0.0000
NZ_CP009273 361287 A	0.0000	0.0000	0.0000	0.0000	0.0000	0.0000
NZ_CP009273 3629231 NA	0.0000	0.0000	0.0000	0.0000	0.0000	0.0000
NZ_CP009273 3669214 NA	0.0000	0.0000	0.0000	0.0000	0.0000	0.0000
NZ_CP009273 3706292 A	0.0000	0.0000	0.0000	0.0000	0.0000	0.0000
NZ_CP009273 3799448 NA	0.0000	0.0000	0.0000	0.0000	0.0000	0.0000
NZ_CP009273 3799800 NA	0.0000	1.0000	0.8790	0.0000	0.0000	0.0000
NZ_CP009273 3800001 NA	0.0000	0.0000	0.0000	0.0000	0.0000	0.0000
NZ_CP009273 3944901 NA	0.0000	0.0000	0.0000	0.0000	0.0000	0.0000
NZ_CP009273 3960101 T	0.0000	0.0000	0.0000	0.0000	0.0000	0.0000
NZ_CP009273 3960515 T	0.0000	0.0000	0.0000	0.0000	0.0000	0.0000
NZ_CP009273 4076055 G	0.3454	0.0000	0.0000	0.0000	0.0000	0.0000
NZ_CP009273 4118604 TTCCGGGGATCCGTCGACCTGCAGTTCGAAGT TCCTATTCTCTAGAAAGTATAGGAACTTCGAAG CAGCTCCAGCCTACA	0.0000	0.0000	0.0000	0.0000	0.0000	0.0000
NZ_CP009273 4177773 NA	0.0000	0.0000	0.0000	0.0000	0.0000	0.0000
NZ_CP009273 4178501 T	0.0000	0.0000	0.0000	0.0000	0.0000	0.0000
NZ_CP009273 42141 T	0.0000	0.0000	0.0000	0.0000	0.0000	0.0000
NZ_CP009273 4226052 NA	0.0000	0.0000	0.0000	0.0000	0.0000	0.0000
NZ_CP009273 4226403 T	0.0000	0.0000	0.0000	0.0000	0.0000	0.0000
NZ_CP009273 4226594 NA	0.0000	0.0000	0.8511	0.0000	0.0000	0.0000
NZ_CP009273 4227883 NA	0.0000	0.0000	0.0000	0.0000	0.0000	0.0000
NZ_CP009273 4228249 NA	1.0000	0.0000	0.0000	0.0000	0.0000	0.0000
NZ_CP009273 4228789 T	0.0000	0.0000	0.0000	0.0000	0.0000	0.0000
NZ_CP009273 4228998 A	0.0000	1.0000	0.0000	0.0000	0.0000	0.0000
NZ_CP009273 4229421 NA	0.0000	0.0000	0.0000	0.0000	0.0000	0.0000
NZ_CP009273 4273156 G	0.0000	0.0000	0.1791	0.0000	0.0000	0.0000
NZ_CP009273 454246 NA	1.0000	1.0000	0.0000	0.0000	0.0000	0.0000
NZ_CP009273 454248 NA	0.0000	0.0000	1.0000	0.0000	0.0000	0.0000
NZ_CP009273 513494 T	0.0000	0.0000	0.0000	0.0000	0.0000	0.0000
NZ_CP009273 51993 NA	0.0000	0.0000	0.0000	0.0000	0.0000	0.0000

Supplemental Table S4.2 Evolved Mutations Filtered with N-2 Method (continued)

	Frequency of Mutation					
sample	4d	4e	4f	5a	5b	5c
treatment	ES+T7	ES+T7	ES+T7	S	S	S
Mutation (Genome, Basepair Number, New Base)						
NZ_CP009273 571113 C	0.0000	0.0000	0.0000	0.0000	0.0000	0.0000
NZ_CP009273 632236 C	0.0000	0.0000	0.0000	0.0000	0.0000	0.0000
NZ_CP009273 733422 NA	0.0000	0.0000	0.0000	0.0000	0.0000	0.0000
NZ_CP009273 83868 T	0.0000	0.0000	0.0000	0.0000	0.0000	0.0000
NZ_CP009273 83881 T	0.0000	0.0000	0.0000	0.0000	0.0000	0.0000
NZ_CP009273 83893 T	0.0000	0.0000	0.0000	0.0000	0.0000	0.0000
NZ_CP009273 84227 A	0.0000	0.0000	0.0000	0.0000	0.0000	0.0000
NZ_CP009273 84294 A	0.0000	0.0000	0.0000	0.0000	0.0000	0.0000
V01146 10203 A	0.0000	0.0000	0.0000	0.0000	0.0000	0.0000
V01146 10308 T	0.0000	0.0000	0.0000	0.0000	0.0000	0.0000
V01146 10922 A	0.6260	0.0000	0.0000	0.0000	0.0000	0.0000
V01146 11197 C	0.0000	0.0000	0.0000	0.0000	0.0000	0.0000
V01146 12114 A	0.0000	0.0000	0.0000	0.0000	0.0000	0.0000
V01146 1379 NA	0.0000	0.0000	0.0000	0.0000	0.0000	0.0000
V01146 16410 A	0.0000	0.0000	0.0000	0.0000	0.0000	0.0000
V01146 16795 G	0.0000	0.0000	0.0000	0.0000	0.0000	0.0000
V01146 1867 A	0.0000	0.0000	0.0000	0.0000	0.0000	0.0000
V01146 19344 C	0.0000	0.0000	0.0000	0.0000	0.0000	0.0000
V01146 1936 T	0.2798	0.0000	0.0000	0.0000	0.0000	0.0000
V01146 19517 C	0.0000	0.0000	1.0000	0.0000	0.0000	0.0000
V01146 19572 T	0.0000	0.0000	0.0000	0.0000	0.0000	0.0000
V01146 19584 T	0.0000	0.0000	0.0000	0.0000	0.0000	0.0000
V01146 19602 T	0.0000	0.0000	0.0000	0.0000	0.0000	0.0000
V01146 19672 NA	1.0000	0.0000	0.0000	0.0000	0.0000	0.0000
V01146 19677 C	0.0000	0.0000	0.0000	0.0000	0.0000	0.0000
V01146 19728 T	0.0000	0.0000	0.0000	0.0000	0.0000	0.0000
V01146 2243 T	0.0000	0.0000	1.0000	0.0000	0.0000	0.0000
V01146 23007 T	0.0000	0.0000	0.0000	0.0000	0.0000	0.0000
V01146 23230 C	0.0000	0.0000	0.0000	0.0000	0.0000	0.0000
V01146 23799 C	0.0000	0.0000	0.0000	0.0000	0.0000	0.0000
V01146 23817 T	0.0000	0.0000	0.0000	0.0000	0.0000	0.0000
V01146 23991 C	0.0000	0.0000	0.0000	0.0000	0.0000	0.0000
V01146 23991 G	0.0000	0.0000	0.0000	0.0000	0.0000	0.0000
V01146 24044 C	1.0000	0.0000	0.0548	0.0000	0.0000	0.0000
V01146 24046 T	0.0000	0.0000	0.0000	0.0000	0.0000	0.0000
V01146 24051 G	0.0000	0.0000	0.0000	0.0000	0.0000	0.0000
V01146 24178 A	0.0000	0.0000	0.0000	0.0000	0.0000	0.0000
V01146 24204 NA	0.0000	0.0000	0.0000	0.0000	0.0000	0.0000
V01146 24273 A	0.0000	0.0000	0.0000	0.0000	0.0000	0.0000
V01146 24274 A	0.0000	0.0000	0.0000	0.0000	0.0000	0.0000
V01146 24312 A	0.0000	0.0000	0.0000	0.0000	0.0000	0.0000
V01146 24346 T	0.0000	0.0000	1.0000	0.0000	0.0000	0.0000
V01146 24370 G	0.0000	0.0000	1.0000	0.0000	0.0000	0.0000
V01146 24397 A	1.0000	0.0000	0.0000	0.0000	0.0000	0.0000
V01146 24498 A	0.0000	0.0000	0.0000	0.0000	0.0000	0.0000
V01146 24617 A	0.0000	0.0000	0.0000	0.0000	0.0000	0.0000
V01146 24639 G	0.0000	0.0000	0.0000	0.0000	0.0000	0.0000

Supplemental Table S4.2 Evolved Mutations Filtered with N-2 Method (continued)

	Frequency of Mutation					
sample	4d	4e	4f	5a	5b	5c
treatment	ES+T7	ES+T7	ES+T7	S	S	S
Mutation (Genome, Basepair Number, New Base)						
V01146 24703 C	0.0000	0.0000	0.0000	0.0000	0.0000	0.0000
V01146 24725 T	0.0000	0.0000	0.0000	0.0000	0.0000	0.0000
V01146 24874 T	0.0000	0.0000	0.0000	0.0000	0.0000	0.0000
V01146 24897 A	0.0000	0.0000	0.0000	0.0000	0.0000	0.0000
V01146 25295 A	0.0000	0.0000	0.0000	0.0000	0.0000	0.0000
V01146 25368 C	1.0000	0.0000	0.0000	0.0000	0.0000	0.0000
V01146 25386 A	0.0000	0.0000	0.0000	0.0000	0.0000	0.0000
V01146 25392 G	0.0000	0.0000	0.0000	0.0000	0.0000	0.0000
V01146 25418 A	0.0000	0.0000	0.0000	0.0000	0.0000	0.0000
V01146 25491 T	0.0000	0.0000	0.0000	0.0000	0.0000	0.0000
V01146 25775 A	0.0000	0.0000	0.0000	0.0000	0.0000	0.0000
V01146 25836 A	0.0000	0.0000	0.0000	0.0000	0.0000	0.0000
V01146 25895 C	0.0000	0.0000	1.0000	0.0000	0.0000	0.0000
V01146 26114 C	1.0000	0.0000	0.0000	0.0000	0.0000	0.0000
V01146 26124 A	0.0000	0.0000	0.0000	0.0000	0.0000	0.0000
V01146 26139 T	0.0000	0.0000	0.0000	0.0000	0.0000	0.0000
V01146 26227 G	0.0000	0.0000	0.0000	0.0000	0.0000	0.0000
V01146 26240 G	0.0000	0.0000	0.0000	0.0000	0.0000	0.0000
V01146 26333 T	0.0000	0.0000	1.0000	0.0000	0.0000	0.0000
V01146 26335 A	0.0000	0.0000	0.0000	0.0000	0.0000	0.0000
V01146 26430 C	0.0000	0.0000	1.0000	0.0000	0.0000	0.0000
V01146 26576 T	0.0000	0.0000	0.0000	0.0000	0.0000	0.0000
V01146 27119 G	0.0000	0.0000	0.0000	0.0000	0.0000	0.0000
V01146 27164 T	0.2792	0.0000	0.0000	0.0000	0.0000	0.0000
V01146 29224 T	1.0000	0.0000	0.0000	0.0000	0.0000	0.0000
V01146 29244 C	0.0000	0.0000	0.0000	0.0000	0.0000	0.0000
V01146 30176 A	0.6430	0.0000	0.0000	0.0000	0.0000	0.0000
V01146 30633 G	0.0000	0.0000	0.0000	0.0000	0.0000	0.0000
V01146 30649 A	0.0000	0.0000	0.0000	0.0000	0.0000	0.0000
V01146 30668 C	0.0000	0.0000	0.0000	0.0000	0.0000	0.0000
V01146 30674 T	0.0000	0.0000	1.0000	0.0000	0.0000	0.0000
V01146 30721 C	0.0000	0.0000	0.0000	0.0000	0.0000	0.0000
V01146 30797 G	1.0000	0.0000	0.0000	0.0000	0.0000	0.0000
V01146 30850 A	0.0000	0.0000	1.0000	0.0000	0.0000	0.0000
V01146 30853 A	0.0000	0.0000	0.0000	0.0000	0.0000	0.0000
V01146 30907 A	0.0000	0.0000	0.0000	0.0000	0.0000	0.0000
V01146 30961 C	0.0000	0.0000	0.0000	0.0000	0.0000	0.0000
V01146 30974 G	0.0000	0.0000	0.0000	0.0000	0.0000	0.0000
V01146 3343 G	0.0000	0.0000	0.0000	0.0000	0.0000	0.0000
V01146 33784 A	0.0000	0.0000	0.0000	0.0000	0.0000	0.0000
V01146 34 NA	0.0000	0.0000	0.0000	0.0000	0.0000	0.0000
V01146 34742 C	0.7595	0.0000	0.0000	0.0000	0.0000	0.0000
V01146 34975 G	0.0000	0.0000	0.0000	0.0000	0.0000	0.0000
V01146 3522 C	0.0000	0.0000	0.0000	0.0000	0.0000	0.0000
V01146 35221 T	0.0000	0.0000	0.0000	0.0000	0.0000	0.0000
V01146 35221 TA	0.0000	0.0000	0.0000	0.0000	0.0000	0.0000
V01146 35235 T	1.0000	0.0000	0.0000	0.0000	0.0000	0.0000

Supplemental Table S4.2 Evolved Mutations Filtered with N-2 Method (end)

	Frequency of Mutation					
sample	4d	4e	4f	5a	5b	5c
treatment	ES+T7	ES+T7	ES+T7	S	S	S
Mutation (Genome, Basepair Number, New Base)						
V01146 35254 C	0.0000	0.0000	0.0000	0.0000	0.0000	0.0000
V01146 35257 T	0.0000	0.0000	0.0000	0.0000	0.0000	0.0000
V01146 35258 A	0.0000	0.0000	1.0000	0.0000	0.0000	0.0000
V01146 35263 C	0.0000	0.0000	0.0000	0.0000	0.0000	0.0000
V01146 35263 G	0.0000	0.0000	0.0000	0.0000	0.0000	0.0000
V01146 35276 A	0.0000	0.0000	0.0000	0.0000	0.0000	0.0000
V01146 35299 G	0.0000	0.0000	0.0000	0.0000	0.0000	0.0000
V01146 35833 G	0.0000	0.0000	0.0000	0.0000	0.0000	0.0000
V01146 35980 G	0.0000	0.0000	0.0000	0.0000	0.0000	0.0000
V01146 36001 T	0.0000	0.0000	0.0000	0.0000	0.0000	0.0000
V01146 36184 A	0.0000	0.0000	0.0000	0.0000	0.0000	0.0000
V01146 36239 G	0.0000	0.0000	0.0000	0.0000	0.0000	0.0000
V01146 36277 G	0.0000	0.0000	0.0000	0.0000	0.0000	0.0000
V01146 39557 G	0.0000	0.0000	0.0000	0.0000	0.0000	0.0000
V01146 39811 NA	0.0000	0.0000	0.0000	0.0000	0.0000	0.0000
V01146 4417 C	0.0000	0.0000	0.0000	0.0000	0.0000	0.0000
V01146 4773 T	0.6820	0.0000	0.0000	0.0000	0.0000	0.0000
V01146 4843 T	0.0000	0.0000	0.0000	0.0000	0.0000	0.0000
V01146 5076 G	0.0000	0.0000	0.0000	0.0000	0.0000	0.0000
V01146 5239 A	0.0000	0.0000	0.9342	0.0000	0.0000	0.0000
V01146 5329 A	0.0000	0.0000	0.0000	0.0000	0.0000	0.0000
V01146 5348 A	0.0000	0.0000	0.0000	0.0000	0.0000	0.0000
V01146 8800 G	0.0000	0.0000	0.0000	0.0000	0.0000	0.0000
V01146 9919 T	0.0000	0.0000	0.0000	0.0000	0.0000	0.0000